M-Pos181 CONFORMATIONAL AND BINDING STUDIES OF PGLa IN PHOSPHOLIPID MEMBRANES. G. Kupcho[1], M. Zasloff[2], and B. A. Wallace[1], [1]Department of Chemistry and Center for Biophysics, Rensselaer Polytechnic Institute, Troy, NY and [2]Div. of Human Genetics and Molecular Biology, Childrens Hosp. of Phila., Univ. of Penn. School of Medicine, Philadelphia, PA.

PGLa is a polypeptide antibiotic isolated from *Xenopus laevis* granular glands, which has been proposed to form channels in lipid membranes. In this study, circular dichroism spectroscopy was used to examine the conformation of this molecule in a variety of environments, as a basis for understanding its structural features. In addition, phospholipid binding studies were used to demonstrate features which permit the association of this polypeptide with membranes.

In the organic solvents methanol and trifluoroethanol, PGLa adopts regular structures that are composed of both helical and sheet-type secondary structures. PGLa also has a substantial solubility in water; but in this environment, it forms an entirely disordered structure.

Ultracentrifugation studies have shown that only small amounts of PGLa are bound to neutral phospholipids, but that the portion of the polypeptide that IS bound undergoes a significant conformational change from that in the aqueous solution. Furthermore, if a small amount of negatively charged phospholipid is present in the vesicles, PGLa binding is significantly enhanced, and this binding induces the polypeptide to undergo a transformation from a completely disordered to an almost entirely helical structure. These studies indicate a possible route for the binding and insertion of this polypeptide into membranes, and suggest that a helical channel may be an appropriate model for the basis of its antimicrobial activity.

M-Pos182 THERMAL BEHAVIOR OF WILD-TYPE AND LPS-MUTANT STRAINS OF *SALMONELLA TYPHIMURIUM* OUTER MEMBRANES AND THE EFFECTS OF POLYMYXIN B AND MAGAININ 2. Fazale Rana and Jack Blazyk, Chemistry Department and College of Osteopathic Medicine, Ohio University, Athens, Ohio 45701.

Several outer membrane mutants of *Salmonella typhimurium* have been characterized which possess lipopolysaccharides (LPS) with deficient polysaccharide structures. The R_a mutant is missing the O-side chain sugars, while the R_b, R_c, R_{d_1}, R_{d_2} and R_e mutants have lost a progressively increasing portion of the core region sugars. These mutants are much more susceptible to antibiotics and antimicrobial peptides than the wild-type organism. The effects of altered polysaccharide structure on the structural characteristics of the LPS in the outer membranes of these organisms have received limited attention and remain poorly understood. We have used FT-IR spectroscopy and differential scanning calorimetery to monitor the order-to-disorder transition of both purified LPS and the intact outer membrane-peptidoglycan complex isolated from a wild-type (smooth) strain (SL 3770) of *S. typhimurium* and six rough LPS mutant strains (SL 3749, SL 3750, SL 3748, SL 3769, SL 3789, and SL 1102) with the respective LPS chemotypes R_a, R_b, R_c, R_{d_1}, R_{d_2} and R_e. The fluidity of the outer membrane-peptidoglycan complex is similar for all strains examined, with a broad phase change centered slightly above growth temperature (37°C); however, the thermally-induced phase behavior varies significantly for the extracted LPS as the length of the polysaccharide chain decreases. While the smooth LPS undergoes a very cooperative phase change at 37°C, both the transition temperature and degree of cooperativity of phase changes for the rough LPS are decreased, with the exception of the R_{d_2} strain. The possibility that changes in the LPS molecule may induce altered structural assemblies, including interdigitated or non-lamellar phases, is discussed. Finally, the effects of polymyxin B and the antimicrobial peptide, magainin 2, on the fluidity and structure of the outer membranes and extracted LPS from these organisms is presented.

M-Pos183 SPIN LABELING OF ACTIVE CENTER SULFHYDRYLS IN 3-HYDROXYBUTYRATE DEHYDROGENASE, A LIPID-REQUIRING MEMBRANE ENZYME. Lauraine A. Dalton, J. Oliver McIntyre and Sidney Fleischer, Department of Molecular Biology, Vanderbilt University, Nashville, TN 37235 USA.

3-Hydroxybutyrate dehydrogenase (BDH) from bovine heart mitochondria is a membrane-inlaid tetrameric enzyme which requires lecithin for optimal function. Each subunit of BDH has two sulfhydryls, SH-1 and SH-2, which have been selectively derivatized with 2,2,6,6-tetramethylmaleimidopiperidinyl-1-oxyl (MSL). We have compared the accessibility of the MSL nitroxide group at SH-1 and SH-2 to water-soluble reducing agent dithiothreitol (DTT) and to hydrated paramagnetic ions. MSL(SH-1)BDH-lipid complex (50 μM) required exposure to 1 mM DTT to effect reduction of the nitroxide ($t_{1/2}$ ~ 2 hr), whereas MSL(SH-2)BDH-MPL was reduced by 0.1 mM DTT more rapidly ($t_{1/2}$ ~ 20 min). These results are consistent with studies of nitroxide interaction with paramagnetic ions. The nitroxide at SH-1 interacts by a dipolar mechanism with Mn^{2+} or Gd^{3+} bound to the lipid vesicle surface. From the dipolar interaction coefficient and MSL size, the distance of SH-1 from the membrane surface was calculated as ≥ 9 Å [Dalton et al., Biochemistry (1987) 26, 2117-2130]. The nitroxide of MSL at SH-2 interacts directly with Mn^{2+} or Gd^{3+} by a Heisenberg spin exchange mechanism, indicating that SH-2 is close to (≤ 5 Å) the surface. SH-1 is in the vicinity of the active center of BDH, since: (1) its alkylation with MSL decreases the affinity for coenzyme and substrate and diminishes enzyme activity (V_{max} reduced ~ 40-fold); and (2) the nitroxide of MSL(SH-1)BDH-lipid is reduced by NADH bound to the enzyme. Alkylation of SH-2 with MSL does not affect the K_m for substrate or NAD^+, although V_{max} is decreased. Hence SH-2 is more distant from the active center.

[Supported in part by NIH grant DK 14632 (SF) and AHA, Tennessee Affiliate (JOM)].

M-Pos184 DOES ACHOLEPLASMA LAIDLAWII B ACCURATELY REGULATE THE BILAYER/NONBILAYER PHASE PREFERENCE OF ITS MEMBRANE LIPIDS? M. Bhakoo, A. Yue, R.N.A.H. Lewis, D. A. Mannock and R. N. McElhaney, Department of Biochemistry, University of Alberta, Edmonton, Alberta, Canada T6G 2H7.

It has been proposed that Acholeplasma laidlawii A accurately regulates the bilayer/nonbilayer phase preference of its membrane lipids by appropriate changes in their polar headgroup distribution. In particular, the proportion of monoglucosyl diacylglycerol (MGDG, the only nonbilayer forming lipid component) appears to decrease with increases in growth temperature, fatty acyl chain unsaturation or cholesterol content, so as to maintain the bilayer/nonbilayer phase transition temperature constant. We have recently investigated the effect of variations in growth temperature, fatty acid composition and cholesterol content on the closely related A. laidlawii B using a much greater range of fatty acid structures and chain lengths and, in each case, we have determined the bilayer/nonbilayer phase transition temperature of the MGDG formed. In contrast to strain A, we find that in A. laidlawii B increases in growth temperature or cholesterol content only reduce MGDG levels in cells enriched in saturated fatty acids, which in any case do not form nonbilayer lipid phases at physiological temperatures. Moreover, we find that there is only a rough relationship between the nonbilayer-forming tendency of a biosynthetically incorporated exogenous fatty acid and its effect on the ratio of nonbilayer to bilayer preferring lipids in the membrane of this organism. In particular, this organism appears to respond in the predicted fashion to branched chain but not to saturated, unsaturated or ω-cyclohexyl fatty acids. We therefore conclude that A. laidlawii B does not posses a biosynthetic mechanism which is capable of accurately regulating the bilayer/nonbilayer phase preference of its membrane lipids. (Supported by the Medical Research Council of Canada and the Alberta Heritage Foundation for Medical Research.)

M-Pos185 KINETICS OF (C-14)CHOLESTEROL EXCHANGE BETWEEN VESICLES PREPARED FROM SYNTHETIC SPHINGOMYELIN ANALOGS. Chu-cheng Kan, Zhong-shi Ruan, and Robert Bittman, Department of Chemistry, Queens College of CUNY, Flushing, NY 11367.

Sphingomyelin (SPM) interacts with cholesterol (chol) more tightly than does PC with similar hydrocarbon chain structure, but the molecular basis for the greater affinity is not fully clear. Increased van der Waals interactions as well as other forces such as hydrogen bonding may contribute to the higher SPM-chol affinity. The hydroxyl group at the 3 position of SPM has been suggested as an additional site at which interaction may occur between SPM and chol. To investigate the influence of the 3-OH group we measured the kinetics of (C-14)chol exchange between SUVs prepared with synthetic SPM analogs bearing substituents at position 3. Donor SUVs contained 10 mol % chol, 75 mol % SPM, and 15 mol % dicetyl phosphate; acceptor SUVs (10-fold excess) contained 10 mol % chol, 90 mol % egg SPM, and (9,10-H-3)-triolein as nonexchangeable marker. Replacement of the 3-OH group by a 3-OMe group gave little change in the half-time for (C-14)chol exchange at 50 C, suggesting that (a) the hydrogen of the 3-OH group does not play an important role as an acceptor in hydrogen bonding with chol, and (b) a moderate increase in steric bulk at this site does not impede SPM-chol interaction. Substitution of the 3-OH group by a 3-O-tetrahydropyranyl group gave a 35-fold enhancement in cholesterol exhange rate, indicating that bulky groups at this position interfere with the molecular packing of chol and SPM in the donor SUVs. The synthesis of 3-substituted SPM analogs and the results of chol exchange rates between SUVs will be presented. Supported by NIH Grant HL-16660.

M-Pos186 ETHANOL INDUCED CHANGES IN SURFACE ORDER OF SYNAPTIC PLASMA MEMBRANES FROM GENETICALLY SELECTED ETHANOL SENSITIVE AND NONSENSITIVE MICE. Harold E. Schueler and George P. Kreishman, Department of Chemistry, University of Cincinnati, Cincinnati, OH 45221, Robert J. Hitzemann, Department of Psychiatry and Behavioral Sciences, SUNY-Stony Brook, Stony Brook, NY 11794 and R. Adron Harris, Department of Pharmacology, University of Colorado Health Sciences Center, Denver, CO 80262.

Ethanol induced changes in the molecular order of the surface and interior domains of synaptic plasma membranes from genetically selected ethanol sensitive and insensitive mice have been measured using delayed Fourier transform ^{1}H-NMR. Ethanol has a disruptive effect in both domains of each strain. The effects are greater in the surface domain for the sensitive strain. From the increase in spectral intensity and a decrease in the apparent linewidth of the choline methyl group, it is postulated that the ethanol causes the average distance between the polar head groups to increase. This is not observed for the insensitive strain. The results will be discussed in relation to the higher monosialoganglioside content in the membranes from the sensitive strain. It is proposed that the basis for the differences in ethanol sensitivity between the two strains arises from the differential ordering at the surface of the neuronal membranes.

M-Pos187 MEMBRANE CHOLESTEROL CONTENT SIGNIFICANTLY AFFECTS THE EQUILIBRIUM LOCATION OF THE 1,4-DIHYDROPYRIDINE, BAY K 8644, IN DIOLEOYLPHOSPHATIDYLCHOLINE LIPID BILAYERS.
R. Preston Mason, Kevin J. Ainger, and Leo G. Herbette. Depts. of Radiology, Medicine, Biochmemistry, and the Biomolecular Structure Analysis Center, Univ. of CT Health Center, Farmington, CT 06032.

Using low angle x-ray diffraction, we examined the time-averaged location of the 1,4-dihydropyridine (DHP) Bay K 8644 in dioleoylphosphatidylcholine (DOPC) multibilayers at 8 A resolution. In the absence of cholesterol, Bay K 8644 is located near the hydrocarbon core/water interface of DOPC membranes. In DOPC membranes with 30 mole percent added cholesterol (the cholesterol concentration previously measured in canine cardiac sarcolemma) the drug's time-averaged location was much closer to the bilayer center. We are currently examining Bay K 8644's location at higher cholesterol concentrations. We also compared this location of Bay K 8644 with its receptor inhibitors, D850 (an analog of verapamil) and amiodarone, in DOPC membranes with 30 mole percent cholesterol, and found that these inhibitors were also near the bilayer center as Bay K 8644. Molecular interactions of DHPs with plasma and intracellular membranes, membranes from cell types of varying cholesterol content, or membranes from individuals suffering from pathological conditions such as hypercholesteremia, may vary substantially due to their different cholesterol contents. From these data we conclude that the membrane cholesterol content can significantly modulate the membrane equilibrium location of DHPs. Supported by HL33026 and RJR Nabisco, Inc. LGH is an Established Investigator of the AHA.

M-Pos188 EVIDENCE FOR BIDIRECTIONAL TRANSVERSE DIFFUSION OF SPIN-LABELED PHOSPHOLIPIDS IN THE PLASMA MEMBRANE OF GUINEA-PIG BLOOD CELLS.
A. Bienvenue, A. Suné, M. Vidal, J. SainteMarie and P. Morin, Intéractions Membranaires (URA 202) and Laboratoire de Biologie Physico-Chimique, F-34060 Montpellier cedex (France). Intr. by Thomas Barman.
The distribution and transverse diffusion kinetics of four spin-labelled phospholipid analogues (PC,PS,PE and sphingomyelin, SM) were studied in the plasma membrane of guinea pig blood cells at 37°C : erythrocytes, reticulocytes and leukemic lymphocytes. In all cells, the distribution equilibrium was reached in less than two hours and the amount left in the external leaflet were in the following order : PS<PE<PC<SM. In the erythrocytes and reticulocytes, the shape change induced by adding phospholipids relaxed partially or completely. All the results were analyzed quantitatively with a simple kinetic model allowing to calculate the rate constants of transverse diffusion.
They varied from $2x10^{-3}$ to $1.2x10^{-1}min^{-1}$ for the flip and from $4x10^{-3}$ to $1.2x10^{-1}min^{-1}$ for the flop, depending on the polar head and the cell type. The relationships between phospholipid distribution, phospholipid transverse kinetics and cell shape were discussed in term of phospholipid translocation and/or phospholipid-cytoskeleton interaction.

M-Pos189 ANALYSIS OF MULTIFREQUENCY FLUORESCENCE ANISOTROPY DECAY IN ARTIFICIAL AND BIOLOGICAL MEMBRANES BY A DOUBLE HINDERED ROTATOR MODEL. Teresa M. Calafut, James A. Dix and A.S. Verkman. Cardiovascular Research Institute, University of California, San Francisco, CA 94143.

Although steady-state anisotropy measurements of phase-sensitive probes provide a qualitative description of the phase behavior of biomembranes, there is little information about the physical state of lipid domains. We have developed a ground-state double hindered rotator (DHR) model for fluorescence anisotropy decay, in which probes possess separate rotational correlation times and r_∞ in each phase. To validate the model, multifrequency differential phase angles (Δ) and modulation amplitudes were measured in a two-compartment cuvette with combinations of POPOP, TMA-DPH, and DPH in isotropic solvents and in DPPC liposomes. Rotational parameters obtained by fitting the DHR model were similar to those of a single hindered rotator model fitted to data obtained separately for each probe. As predicted by the model, negative Δ were obtained when fluorophores in isotropic solvents were paired with fluorophores in DPPC liposomes. The rotational parameters of the phase-sensitive fluorophores cis-parinaric (cPnA) and trans-parinaric (tPnA) acid in DPPC:DMPC (1:1) liposomes were determined at 15-40°C. Two lifetimes (1ns,3ns) were obtained above the phase transition temperature (T_c); >95% of the fluorescence intensity was described by two lifetimes (6ns, 21-32ns) below T_c. Negative Δ were obtained when solid-phase lipid was present. r_∞ varied from 0.26-0.32 below, to 0.11-0.14 above T_c; at intermediate T, where two phases coexist, r_∞ values were ~0.23 and ~0.31. Similar multi-domain data were obtained in red cell ghost membranes. In contrast to previous data using single rotator models, these results indicate very hindered PnA rotation in solid phase lipid. These results establish the utility of ground-state rotational heterogeneity to describe fluorophore rotation in biological membranes.

M-Pos190 STRUCTURE OF POLYMERIZABLE LIPID BILAYERS: WATER PROFILE OF A DIACETYLENIC LIPID BILAYER USING ELASTIC NEUTRON SCATTERING.

S. L. Blechner[1,2], V. Skita[2], and D. G. Rhodes[2]
(1) Department of Physics, University of Connecticut, Storrs, Connecticut 06028, and
(2) Biomolecular Structure Analysis Center, University of Connecticut Health Center, Farmington, Connecticut 06032

Elastic neutron scattering experiments have been used to study the hydration of 1,2-bis(10,12-tricosadiynoyl)-sn-glycero-3-phosphocholine ($DC_{8,9}PC$) multilayers equilabrated with an atmosphere at constant relative humidity. Previously published Fourier-transform infrared (FTIR) spectroscopic data had suggested, based on shifts in the C=O stretch frequencies, that the phosphocholine headgroup in these polymerizable diacetylene bilayers was much less hydrated than that of saturated phosphatidylcholines. Our results demonstrate that the $DC_{8,9}PC$ headgroup at 84% relative humidity is at least as well hydrated as that of a saturated PC, dipalmitoyl phosphatidylcholine, under the same conditions. This result suggests that the shift of the C=O stretch peaks resulted from conformational changes in the phosphocholine headgroup, and not from changes in the hydration of the headgroup. Supported by the Defense Advanced Research Projects Agency (DARPA), U. CONN. Health Center Research Foundation, RJR Nabisco, Inc. and by the State of Conn. Dept. of Higher Education.

M-Pos191 X-RAY STANDING WAVES: A NEW MOLECULAR YARDSTICK FOR BIOLOGICAL MEMBRANES.

M. J. Bedzyk[1], D. H. Bilderback[1], G. M. Bommarito[2], M. Caffrey[3], J. S. Schildkraut[4].

[1]Cornell High Energy Synchrotron Source (CHESS) and School of Applied and Engineering Physics, Cornell University, Ithaca, NY 14853, [2]Department of Chemistry, Cornell University, Ithaca, NY 14853, [3]Department of Chemistry, The Ohio State University, Columbus, OH 43210, [4]Corporate Research Laboratories, Eastman Kodak Company, Rochester, NY 14650.

Structural information with subångstrom resolution has been obtained for a model membrane by means of long-period x-ray standing waves. The Langmuir-Blodgett (LB) trilayer system of zinc and cadmium arachidate (C20:0) was deposited on a layered synthetic microstructure (LSM) consisting of 200 tungsten/silicon layer pairs with a 25Å period. The zinc ion layer, initially located in the LB trilayer at 53Å above the LSM surface, migrated toward this surface some 30Å upon heating above 110°C. The mean position and width of the zinc ion layer was followed during this thermally induced event with a precision of ± 0.3Å. The potential of this method for structurally characterizing peptides and proteins in reconstituted membranes and for profiling ion distribution at the membrane/aqueous interface is under investigation.

M-Pos192 STRUCTURE OF ELECTRIC FIELD-INDUCED MEMBRANE PORES REVEALED BY RAPID-FREEZING ELECTRON MICROSCOPY. D.C. Chang† and T.S. Reese‡. †Department of Physiology and Molecular Biophysics, Baylor College of Medicine, Houston, TX 77030 and ‡NIH, Bethesda, MD 20892.

A large electric field applied externally to a cell can induce transient membrane pores. Very large molecules, such as a gene fragment, can pass through these pores to enter the cell. However, very little is known about the structure of these electric field-induced pores. We have developed a rapid-freezing technique which allows us to examine the ultrastructure of the membrane at various stages of electroporation. Human red blood cells were sandwiched between two thin copper plates which served as electrodes for the applied field. This sandwich was plunged into a liquid propane/ethane mixture by a propelling mechanism. Measurement of specimen capacitance indicated that the cells were frozen within 3 msec. By electronically monitoring the movement of the sample and utilizing a delay circuit, we were able to control the time interval between the application of the pulse and the sample freezing from 1 msec to many minutes. To improve the poration efficiency, we used a radio-frequency pulse (5 kV/cm, 100 kHz, 100 μs wide) instead of a DC pulse. The frozen samples were processed by standard procedures of freeze-fracture electron microscopy. Preliminary results reveal that membrane pores appear almost immediately following application of the electric pulse. The majority of the pores are conical or volcanic in shape. Their diameters range from 25 to 110 nm. We also observed a second type of pore-like structure which is larger in diameter and is less deep. Apparently, one electric pulse can induce many membrane pores in a cell. The pore density varies greatly, and in some cases can be as high as 7 per square micron. The pores appear to gradually reseal on a time scale of seconds.

M-Pos193 INVESTIGATION OF THE MECHANISM OF SYNAPTIC PLASMA MEMBRANE PERTURBATION BY PSYCHOTROPIC DRUGS USING THE FLUORESCENCE PROBE ANS. Mark A. Carfagna,† G. Douglas Ponsler‡ and Barry B. Muhoberac,‡ Department of Pharmacology and Toxicology, Indiana University School of Medicine† and Department of Chemistry, Purdue University School of Science, Indiana University-Purdue University,‡ Indianapolis, IN 46223

The mechanism(s) by which psychotropic drugs alter synaptic plasma membrane structure may be important in elucidating the basis for their CNS-related effects. Amitriptyline increases the F_∞ of the fluorescent membrane probe 1-anilinonaphthalene-8-sulfonic acid (ANS) in a concentration-dependent manner over the range that inhibits (0-95%) synaptic membrane-bound Na^+/K^+-ATPase activity (*The Pharmacologist* A119, 1988). The present study examines the interaction of cationic/hydrophobic drugs versus the ammonium ion with synaptic plasma membranes through changes in ANS fluorescence. ANS titrations with Scatchard-like analyses gave F_∞ and K_{app} values for ANS binding at various concentrations of the drugs or ammonium ion. The concentrations of chlorpromazine, amitriptyline, doxepin and ammonium ion required to produce a 20% increase in F_∞ over control are 10 μM, 30 μM, 75 μM and 100 mM, respectively, with both K_{app} and λ_{max} remaining unchanged for the drugs and the ion. Furthermore, these three drug concentrations correlate ($r=0.99$, $p<0.01$) with their octanol/water partition coefficients. Such results suggest that the increase in F_∞ induced by the psychotropic drugs and the ammonium ion are caused by charge shielding of the anionic portion of phospholipids since all of the compounds studied are cationic at physiological pH. However, these cationic/hydrophobic drugs are approximately four orders of magnitude more potent in increasing F_∞ than the ammonium ion. This difference in potency may be caused by anchoring of the positively charged drug in the biomembrane by the hydrophobic portion of the molecule which results in enhanced charge shielding and/or perturbation of the biomembrane surface creating more binding sites for ANS. [Supported by NIAAA predoctoral fellowship 5285 (MAC) and NIAAA grant 6935 (BBM)]

M-Pos194 FLUORESCENCE STUDY OF STEROL HETEROGENEITY AND EXCHANGE IN SMALL UNILAMELLAR VESICLES (SUV). G. Nemecz*, P. Butko* and F. Schroeder*+ (Intr. by J. Ball) Dept. Pharm. & Med. Chem., Coll. Pharm.*; Pharm. & Cell Biophys., Coll. Med.+, U. Cincinnati, Cincinnati, OH 45267-0004.

Spontaneous sterol exchange between palmitoyloleoyl-phosphatidylcholine (POPC)/sterol SUV was investigated without separation of donor and acceptor vesicles, using a fluorescent cholesterol analogue, dehydroergosterol (DHE) [Biochim. Biophys. Acta 943, 511-521 (1988), Biochemistry in press (1988)]. DHE polarization (T-format) was continously detected during the exchange of sterol between POPC/cholesterol (65:35) acceptor and POPC/DHE (65:35) donor vesicles. The exchange process was also simulated by mixing two populations of SUV (POPC/DHE 65:35 and POPC/cholesterol/DHE 65:32:3) in varying proportions. The relationship between polarization and DHE content in SUV (keeping the total sterol concentration constant) was determined in order to 1) relate polarization changes to the amount of DHE transferred from donor to acceptor SUV, and 2) describe the changes in DHE partitioning between donor and acceptor vesicle populations during the exchange process. Lifetime, polarization, limiting anizotropy and rotational correlation time showed that with increasing proportion of DHE the dehydroergosterol and cholesterol distributed homogeneously within the vesicles up to 30 mol % DHE / 5 mol % cholesterol. In conclusion the quantity of DHE transferred in the polarization exchange assay is proportional to polarization changes. This fluorescence technique allows a high resolution of the exchange process and provides additional information about the asymmetric distribution of sterol domains in the POPC/sterol SUV membrane. (Supported by NIH grant GM31651).

M-Pos195 EFFECT OF MIXED PHOSPHOLIPID HEAD GROUPS ON STEROL EXCHANGE BETWEEN MODEL MEMBRANES. G. Nemecz*, K. Herzog*, Z. Hertelendy*, F. Schroeder*+ (Intr. by Taizer Wang). Dept. Pharm.& Med. Chem., Coll. Pharm.*; Pharm.& Cell Biophys., Coll. Med.+, U.Cincinnati, Cincinnati, OH 45267-004.

The effect of phospholipid head group on spontaneous sterol exchange between small unilamellar vesicles (SUV) using fluorescent sterol, dehydroergosterol (DHE), was investigated. Exchange was monitored by continous detection of polarization (T-format) described earlier [Biochim. Biophys. Acta 943, 511-522] was utilized at 24 °C and 55 °C. Donor vesicles were composed of I) palmitoyloleoylphosphatidylcholine (POPC)/DHE 65:35, II) palmitoyloleoylphosphatidylethanolamine (POPE)/POPC/DHE 33:33:33 and III) sphingomyelin (SP)/POPC/DHE 33:33:33. In the acceptor vesicles DHE was replaced by cholesterol. The polarization curve for SUV (I) best fit a two-exponential function with rate constants k_1=0.0244 min^{-1}, $^1t_{1/2}$= 28.9 min, k_2=0.00385 min^{-1}, $^2t_{1/2}$=180 min at 24 °C. At 55 °C these parameters were k_1=0.469 min^{-1}, $^1t_{1/2}$=1.48 min, k_2=0.1388 min^{-1}, $^2t_{1/2}$=5 min. In cosonicated POPE/POPC/DHE SUV (II) k_1=0.0426 min^{-1}, $^1t_{1/2}$=16.3 min, k_2=0.003485 min^{-1} $^1t_{1/2}$=198 min at 24 °C. In contrast, DHE exchange from cosonicated SP/POPC/DHE vesicles (III) was monoexponential at 24 °C (k_1=0.00197 min^{-1} $t_{1/2}$=352 min) at 55 °C (k_1=0.159 min^{-1} $t_{1/2}$=4.36 min). Arrhenius plots of donor vesicles polarization showed a phase transition in the range of 24 to 31 °C for SP containing vesicles. Transitions for the other vesicles in the temperature range of 13 to 45 °C were not observed. In conclusion, the nature of phospholipid polar head groups in mixed SUV influences exchange properties of sterol pools between membranes. (Supported by NIH grant GM 31651).

M-Pos196 CALCULATION OF THE SURFACE TENSION OF THE LIPID LAYER. Irina Vayl, Ph.D. Brown University, Providence, Rhode Island 02912.

A method for the calculation of the surface tension for a lipid membrane was developed based on the definition of the variation of surface energy due to stretching of the membrane matrix. To calculate the surface energy of the membrane the method of graphs was applied. It allowed to formulate a relatively simple approximation for calculation of the surface energy for homogeneus and heterogeneous structures having unlimited membrane area using the potential energy radial function for any pair of interactable molecules. That approximation allowed to calculate the surface tension for the lipid micelle and vesicle so well as for lipid-channel structures when the atomic surface structure is known.

The calculations in the presence of the water molecules allowed the estimation of the surface pressure and absorption coefficient. The Eötvös law and Ramsay-Shields formula were used to determine the temperature dependence of the surface tension. The series of calculations for the DPPC membrane's surface tension demonstrated its strong dependence on the dielectric constant, the distribution of the partial charges on the lipid head group, the thickness of the surface layer (or density of the lipid layer) and the critical point of temperature.

M-Pos197 TRANSPORT OF FLUORESCENT FREE FATTY ACIDS INTO ADIPOCYTES. A.M. Kleinfeld*, G. Both†, C.P. Lechene†, and J. Storch††. *Medical Biology Institute, La Jolla, CA; †Harvard Medical School, Boston, MA; and ††Harvard School of Public Health, Boston, MA.

Transport of free fatty acids (ffa) from extracellular medium to discrete intracellular triglyceride (TG) drops in 3T3F442A adipocytes was measured using the anthroyloxy ffa (AOffa). Image enhanced fluorescence microscopy was used to determine the fluorescence intensity within the TG drops as a function of time, following addition of AOffa to the external medium. Cells were observed as confluent monolayers at 37°C, in the absence of serum. Addition of a short chain, 11 carbon analog (11AU), resulted in rapid, seconds to minutes, labeling of intracellular TG droplets. Transport of 18 carbon analogs (12AS or 12AO), were >2 orders of magnitude slower. The observed rate of fluorescence increase is due to transport of ffa since chromatographic analysis of extracted lipids reveals that >90% of all AOffa remain unesterified during the time course of the measurements. Addition of the AOffa to dispersed TG droplets, under the same conditions as for cells, results in immediate (~1 s) labeling of TG by both long and short chain AOffa, with similar intensities. If cells are permeabilized with digitionin, a 2 to 4 fold increase is seen in TG associated fluorescence of 12AO. On the other hand, treatment of cells with the stilbene compound DIDS reduces the already low rate of long chain AOffa transport by >50%. We conclude that ffa transport in adipocytes cannot be accounted for by rapid diffusion through the lipid phase of the membrane, and, in agreement with Abumrad *et al.*, (*JBC 259*:8945, 1984) and Schwieterman *et al.* (*PNAS 85*:359, 1988), that a significant component of transport is protein mediated. (Supported by grants from AHA and NIH).

M-Pos198 **MIXTURES OF LONG-CHAIN DIACETYLENIC AND SHORT-CHAIN SATURATED PHOSPHATIDYLCHOLINES - STRUCTURE AND CHEMICAL BEHAVIOR** - David G. Rhodes[1] and Alok Singh[2] - (1) U. of Conn. Health Center, Biomolecular Structure Analysis Center, Dept. of Radiology, Farmington, CT 06032 and (2) Naval Research Laboratories, Bio/Molecular Engineering Branch, Washington, DC 20375-5000

Polymerization of 1,2-bis(10,12-tricosadiynoyl)-sn-glycero-3-phosphocholine (DC8,9PC) was enhanced by addition of 1,2-dinonoyl-3-phosphocholine (DNPC). This effect could be due either to increased crystallinity in the region of the diacetylene, resulting in improved orientation of successive diacetylene monomers or to less stringent conformational constraints in the distal methylene region of the DC8,9PC acyl chains, which could more easily accomodate the conformational changes of polymer formation. Low angle x-ray diffraction studies were carried out to determine whether the distal methylene segments were interdigitated with those of the opposing monolayer (more ordered) or "melted" by the presence of DNPC. These studies do not support the interdigiated chain model, but do indicate that the two lipid species may be phase separated. Low angle x-ray diffraction studies of an analogous one-molecule structure, 1-(10,12-tricosadiynoyl), 2-nonoyl-sn-glycero-3-phosphocholine, indicated that bilayers of this lipid were interdigitated, such that the terminal methyl group of the tricosadiynoyl chain on each lipid in the bilayer was adjacent to the diacetylenic moiety of a lipid on the opposing monolayer. Bilayers of this lipid did not polymerize. Implications of these findings pertinent to identifing significant factors in polymerization of diacetylenic phospholipid bilayers will be discussed. **Supported by the Defense Advanced Research Projects Agency (DARPA) and the State of Connecticut Dept. of Higher Education.**

M-Pos199 APPROACHES TO COMPUTER GRAPHICS OF LIPID STRUCTURES.

W.R. Light, C.R. Vinayaka, and B.P. Gaber (Intr. by Richard Thompson). Bio/Molecular Engineering Branch, Code 6190, Naval Research Laboratory, Washington, D.C., 20375.

Molecular graphics of phospholipid assemblies has been complicated by the difficulty in obtaining crystal structures, and the absence of software optimized for the visualization of lipids. From the fourteen known lipid crystal structures, a library of fragments has been constructed to aid in the computer construction of novel lipids. Monolayers and bilayers are formed by the propagation of the lipids using crystallographic symmetry operations. We are in the process of writing display software (NanoVision™) for the Macintosh™ and are developing a hierarchal nomenclature for lipid structure. Using these techniques and tools, we will present bilayer models of several different lipids and our taxonomy scheme.

This work was supported by the Office of Naval Research.

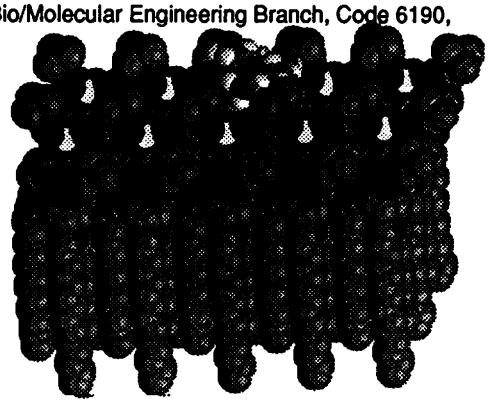

A monolayer of dimyristoylphosphatidylcholine with a trehalose molecule.

M-Pos200 AMPHIPATH-MEDIATED PLATELET SHAPE CHANGES OCCUR WITHOUT DIRECT INVOLVEMENT OF THE CELLULAR CYTOSKELETON. L. S. Brunauer, S. I. Waters, M. J. Stevenson, and W. H. Huestis, Stanford University, Stanford, CA.

Amphipathic molecules induce platelet morphological alterations in a manner consistent with the bilayer couple hypothesis of Sheetz and Singer. Anionic amphipaths (e.g. dilaurylphosphatidylcholine (DLPC)) induce spiculation at low concentrations and shedding or vesiculation of membrane at high concentration, while cationic amphipaths (e.g. chlorpromazine (CPZ)) induce sphering. The involvement of the cytoskeleton in amphipath-induced shape changes was investigated by examining the effects of cytoskeletal disrupting agents on amphiphile-induced shape changes and the effects of amphiphile treatment on the actin polymerization state. Human platelets were incubated with amphiphile and/or cytoskeletal agents at 37°C. In some cases cells were subsequently stimulated with thrombin. Cells were then fixed with glutaraldehyde and examined by phase microscopy or scanning electron microscopy, or were thin-sectioned and examined by transmission electron microscopy (TEM). Platelet cytoskeletons were prepared for examination by TEM by a simultaneous fixation and extraction procedure. The extent of actin polymerization in treated cells was determined by DNaseI inhibition assay. In contrast to cytoskeletons isolated from thrombin stimulated cells, cytoskeletons extracted from DLPC spiculated cells displayed a peripheral microtubule ring and organellar distribution similar to those of resting cells. TEM analysis of thin-sectioned cells showed that, while the gross morphology of DLPC-spiculated cells is similar to that of thrombin-stimulated cells, the internal organization of DLPC-spiculated cells resembles control rather than thrombin-stimulated cells. Treatment of platelets with cytoskeletal disrupting agents (cytochalasin E, phalloidin, or colchicine) prior to incubation with amphipaths (e.g. DLPC, CPZ) did not alter amphipath-induced shape changes. Amphipath pretreatment had no significant reproducible effect upon the state of actin polymerization in either resting or thrombin-stimulated cells. These observations suggest that amphipath-induced platelet morphological changes result from amphipath intercalation into the lipid bilayer and not from interaction with the cellular cytoskeleton.

M-Pos201 NEW DATA ON CELL MEMBRANES PROPERTIES

V. Vasilescu
Department of Biophysics, Faculty of Medicine, Bucharest, Romania 76241

During the last 10 years an increasing experimental support for the hypothesis of the involvement of the cell membrane alterations in the pathogenesis of the essential hypertension has been evidentiated.

Four key factors have been revealed as involved in the generation of sodium-dependent hypertension: 1) genetic or acquired defect in renal sodium excretion; 2) dietary sodium intake; 3) natriuretic hormone as sodium pump inhibitor; 4) Na^+-Ca^{2+} exchange in smooth muscle and plasma membranes (Blaustein, 1984). Taking them into account, a comparative study of erythrocyte shape modifications between control and hypertensive human subjects is presented. The shapes of cells were investigated by an inverted light microscope after their sedimentation on glass cover-slips. The computer analysis of images revealed a significant difference ($p < 0.01$) between the control and hypertensive subjects as concern the echinocytes/total cells ratios, concluding that a shape modification of erythrocytes is occured in case of essential hypertension.

The high rate of transformation of the biconcave disks into echinocytes found in case of hypertension is correlated with ATP pool decreasing that we have previously observed at the same disease.

The results are discussed in terms of molecular membrane properties of the mammalian erythrocytes and their structure proteins organization. A model of cell shape transformation upon ATP pool control is presented for the hypertensive disease.

M-Pos202 DIRECT PHASE DETERMINATION FOR THE MOLECULAR ENVELOPE OF TRYPTOPHANYL-tRNA SYNTHETASE FROM *BACILLUS STEAROTHERMOPHILUS* BY SOLVENT DENSITY CONTRAST VARIATION C. W. Carter, Jr., K. V. Crumley, and F. Hage, Department of Biochemistry, CB# 7260 University of North Carolina at Chapel Hill, Chapel Hill, NC 27599-7260, USA and G. Bricogne, Batiment 209D, LURE/CNRS Campus d'Orsay, 91405 Orsay, France.

Monoclinic crystals of *Bacillus stearothermophilus* tryptophanyl-tRNA synthetase grown in the presence of substrate tryptophan (space group $P2_1$) display evidence of a low resolution trigonal space group (P321). The origin and averaging transformations for the local 32 point group of this unusually clear, six-fold non-crystallographic symmetry may be inferred without prior estimation of the electron density. We have expoited this local symmetry in conjunction with solvent density contrast variation to determine the shape of the molecular envelope. X-ray intensities measured from crystals equilibrated in mother liquors of three different electron densities were used to estimate three parameters for each reflection: the modulus of the envelope transform, $|G_h|$; and components, X_h and Y_h, relative to G_h, of the structure factor vector for the transform of intramolecular density fluctuations. The moduli $\{|G_h|\}$ behave somewhat like structure factor amplitudes from small molecule crystals, and estimation of their phases was successfully carried out by statistical direct methods. Reflections to 18 Å resolution, which obey the symmetry of space group P321, were merged to produce an asymmetric unit in that space group. $|G_h|$ values for the 34 strongest of these were phased using the small molecule direct methods package MITHRIL (Gilmore, C.J., 1984, *J. Appl Cryst.*17:42-46). The best phase set was expanded back to the $P2_1$ lattice and negative density was truncated to generate initial phases for all reflections to 18 Å resolution. Imposition of the local 32 symmetry produced an envelope with convincing features consistent with known properties of the enzyme. Phase extension for $\{|G_h|\}$ and estimation of phases for $\{|F_{obs}|\}$ values using Bayesian statistical methods (Bricogne, 1988, *Acta Cryst* A44:517-545) are in progress, and will be described.

The current envelope implies that the tryptophanyl-tRNA synthetase dimer is an elongated structure with an axial ratio of about 4:1, in which the monomers have two distinct domains of unequal size. The smaller of these occurs at the dimer interface, and resembles the nucleotide binding portion of the tyrosyl-tRNA synthetase structure. On this basis it is proposed that this domain contains amino terminal sequences identified previously to be those involved in a nucleotide-binding domain of the tryptophanyl enzyme. (Supported by NIGMS RO1-26203)

M-Pos203 REACTION OF EOSIN-6-ISOTHIOCYANATE (E-6-SCN) WITH THE HUMAN RED BLOOD CELL ANION TRANSPORT PROTEIN: EVIDENCE FOR HALF-OF-THE-SITES REACTION? Si-qiong Liu. Dept. of Biophysics, University of Rochester School of Medicine, Rochester, NY 14642.

Cells reacted with 300 μM E-6-SCN at 37°C and pH 6.75 in 150 mM Cl^- medium exhibit a progressive loss of Cl^- exchange capacity over the first 1-2 hours. After this time the rate of inhibition slows and reaches a plateau at about 50%. (At higher pH, the inhibition progresses to over 90%.) The observed plateau in inhibition at pH 6.75 could mean that under these conditions E-6-SCN inhibits each band 3 molecule by 50% or that E-6-SCN reacts with only half of the band 3 molecules. In the latter case, only 50% of the band 3 molecules would be available for reaction with DIDS (4,4'-diisothiocyano-stilbene-2,2'-disulfonate), another irreversible inhibitor of anion exchange (if E-6-SCN and DIDS compete with each other). To test this, both control and E-6-SCN pretreated cells were treated with different concentrations of DIDS at 37°C for 1 hour, and then Cl^- efflux was measured at 0°C. For both control and E-6-SCN pretreated cells, the Cl^- exchange rate constant of each DIDS treated sample divided by the control rate constant was plotted against the DIDS concentration. From the intersection point of each line with x axis, the number of DIDS binding sites per cell is 1.28×10^6 for control cells and 0.6×10^6 for E-6-SCN pretreated cells. This indicates that E-6-SCN reacts with only half of the band 3 molecules. After E-6-SCN pretreatment, however, E-6-SCN still reversibly inhibits Cl^- exchange at 0°C. This suggests that E-6-SCN reaction with some band 3 molecules does not prevent **binding** of E-6-SCN to other sites, but rather inhibits the covalent **reaction** with band 3, possibly due to monomer-monomer interactions within a band 3 dimer. (Supported by NIH grant DK27495.)

M-Pos204 CHARACTERIZATION OF INHIBITORY SH GROUP(S) IN THE THIOL ACTIVATED K:CL COTRANSPORTER OF LOW K (LK) SHEEP RED BLOOD CELLS. K.H. Ryu and P.K. Lauf. Dept. of Physiology & Biophysics, Wright State University School of Medicine, Dayton, OHIO 45401-0927.

The thiol reagents N-ethylmaleimide (NEM) and methylmethane thiosulfonate (MMTS) stimulate ouabain resistant (OR) K:Cl transport in LK sheep red cells at low but not at high concentrations. The stimulatory NEM effect on K:Cl flux at pH 7.4 is highest when the NEM treatment is carried out around pH 6 and decreases as pH increases (Bauer and Lauf, J. Memb. Biol. 73:257, 1983). In contrast diamide only stimulates OR K:Cl flux (Lauf J. Memb. Biol. 101:179, 1988). Hence NEM or MMTS may react with additional but inhibitory thiol groups of the already thiol-activated K:Cl cotransporter. To test this hypothesis we activated first K:Cl transport with diamide and then exposed the cells to various concentrations of NEM or MMTS and studied the effect of these compounds as function of pH. As the concentration of NEM or MMTS increased, the diamide activated K:Cl cotransport was steadily decreased toward the control value of before diamide stimulation. This inhibitory effect was also dependent on the compound's exposure time. When the pH of NEM treatment was varied from 6 to 8, inhibition of OR K:Cl flux increased. These results are in agreement with our hypothesis of the presence in the K:Cl cotransport protein complex of two types of SH groups, i.e. activating and inhibitory with two different pK_a values, respectively. Thus high concentrations of NEM and MMTS exert their inhibitory effects through SH groups different from those whose oxidation to disulfide by diamide results in activation of OR K:Cl cotransport. (Supported by NIH Grant DK 37,160)

M-Pos205 INTERACTION AMONG ANION, CATION AND GLUCOSE TRANSPORT PROTEINS IN THE HUMAN RED CELL. A. Janoshazi and A. K. Solomon, Biophysical Laboratory, Harvard Medical School, Boston, MA 02115.(Sponsored by C. Lechene)

We have previously used the reaction time constant, τ_{DBDS}, of fluorescence enhancement, following binding of the specific stilbene anion exchange inhibitor, DBDS (4,4'-dibenzamido-2,2'-stilbene disulfonate), to red cell band 3 to report on the conformational state of band 3. We have now validated this method by showing that the K_I (0.3 ± 0.1 uM) for H_2-DIDS (4,4'-diisothiocyano-2,2'-dihydrostilbene disulfonate) modulation of τ_{DBDS} is essentially the same as the K_I (0.47 ± 0.04 uM) for Cl^- exchange inhibition. Cytochalasin B, which binds specifically to the glucose transport protein when the cytoskeletal binding sites have been blocked by cytochalasin E, decreases τ_{DBDS}^{-1} in the native red cell from 8.0 sec^{-1} to 5.0 sec^{-1}. 10 uM ouabain affects Cl^- flux in the native red cell, significantly increasing $\tau_{Cl^-}^{-1}$ from 1.4 ± 0.1 sec^{-1} to 2.5 ± 0.3 sec^{-1}. These experiments show that both the glucose transport protein and the Na^+,K^+-ATPase are either contiguous to band 3 or related to it by a link through which conformational information can flow. It is significant that these linkages are absent in white ghosts, which shows that the constraints present in the native red cell are important for preservation of the native interactions among membrane proteins. (Supported in part by the Amer. Heart Assoc., Mass. affiliate and the Amer. Cancer Soc., Mass. Div.)

M-Pos206 SOLUTE/MEMBRANE INTERACTIONS OF HYDROPHILIC ALCOHOLS AND THEIR EFFECT ON TRANSPORT PARAMETERS IN THE HUMAN RED CELL. Michael R. Toon and A. K. Solomon, Biophysical Laboratory, Harvard Medical School, Boston, MA 02115.

Simultaneous determination of the permeability coefficient of a solute, ω_i, and its reflection coefficient, σ_i, makes it possible to compute f_{sm}, the frictional coefficient between the solute and the membrane. We have made a systematic study of f_{sm}, which dominates the interactions of short-chain di- and tri- hydroxylic alkanols with red cell membranes. The importance of hydrogen bonding is shown by the observations that i) addition of a single -OH group increases f_{sm} by a large factor; and ii) replacement of intermolecular H-bonds with intramolecular ones decreases f_{sm} significantly. In general, steric factors, either alone as shown by addition of $-CH_2$, or together with H-bonding, as shown by addition of $-CH_2OH$, markedly increase f_{sm}. 29 measurements of σ_i for seven diols/triols give values significantly less than 1.0, providing thermodynamic evidence that these solutes cross a significant stretch of the membrane through an aqueous channel. Ethylene glycol reversibly inhibits osmotic red cell water permeability by about 60% or more with K_I in the range of 500 mM, showing that ethylene glycol interacts with an accessible membrane element which modulates water passage through the aqueous channel, consistent with passage of ethylene glycol and water through a common pathway. (Supported in part by the Amer Cancer Soc, Mass Division, and the Squibb Research Institute)

M-Pos207 PREPARATION AND CHARACTERIZATION OF AN ANTIBODY AGAINST THE ANION EXCHANGE INHIBITOR, H_2DIDS. Joseph R. Casey and Reinhart A.F. Reithmeier, MRC Group in Membrane Biology, Department of Medicine and Department of Biochemistry, University of Toronto, Toronto, Ontario, Canada M5S 1A8.

Anion exchange in human erythrocytes is irreversibly inhibited by covalent attachment of 1,2-(2,2'-disulfo-4 ,4'diisothiocyano)diphenylethane (H_2DIDS) to a lysine residue in Band 3. Antibodies against H_2DIDS were raised in rabbits injected with Keyhole Limpet hemocyanin, labeled with H_2DIDS. The antibody was affinity purified using H_2DIDS-labeled bovine serum albumin coupled to Sepharose. The antibody was characterized and was used to identify and purify H_2DIDS-labeled Band 3 peptides. Competitive ELISA assays and Western blots showed that the antibody reacts with H_2DIDS, 4,4'-diisothiocyanostilbene-2,2'-disulfonate (DIDS) and 4-acetamido-4'isothiocyanostilbene-2,2'-disulfonate (SITS). On Western blots of red cell ghost membrane proteins, the antibody binds specifically to H_2DIDS-labeled Band 3 and proteolytic fragments of Band 3 labeled with H_2DIDS. Following denaturation in sodium dodecyl sulfate, H_2DIDS-labeled Band 3 and labeled proteolytic fragments of Band 3 can be immunoprecipitated by the antibody. The purified antibody will be coupled to Sepharose and this resin will be used to purify H_2DIDS-labeled peptides. The peptides will be sequenced to identify the site of attachment of H_2DIDS. (Supported by the Medical Research Council of Canada).

M-Pos208 **MORPHOLOGICAL STUDIES OF SICKLE ERYTHROCYTES (SS CELLS) BY IMAGE ANALYSIS:** Kazumi Horiuchi, Jun Ohata, Yasuyuki Hirano, and Toshio Asakura, The Children's Hospital of Philadelphia, Dept. of Pediatrics and Depts. of Biochem. & Biophys., Univ. of Penna. School of Med., Philadelphia, PA.

Recently we found a close relationship between the degree of sickling of SS cells and the formation of dense cells and irreversibly sickled cells (ISCs) (Blood 71:46, 1988). To further characterize the morphology of sickle cells, an automated image analysis system (Vidas, Zeiss) was used to analyze shape differences in SS cells under oxygenated or deoxygenated conditions. Images of SS cells observed by light microscopy were transferred to the image analysis system via CCD camera and enhanced by threshold values of light intensity, processed to binary (black and white) images, and then analyzed by circular shape factor (CSF) and elliptical shape factor (ESF). We found that the shape of SS cells under deoxygenated conditions could be classified into several groups by differences in CSF and ESF (Table). This system was also applied to study morphological changes of SS cells exposed to deoxygenation-oxygenation cycles between PO_2=100 and 0 mm Hg (one cycle; 12 min) at pH 6.9 and pH 7.4. At both pHs, morphology of sickled cells after the first deoxygenation was predominantly maple leaf- or star-shaped. The number of elongated sickled cells increased as the number of d-o cycles increased. Sickled cells desickled at oxygenation phase more easily at pH 7.4 than at pH 6.9. The advantage of automated image analysis over the classic visual method is that it can provide an accurate numerical expression of the degree of sickling and shape of sickle cells. (NIH HL 20750 and Sickle Center Grant HL38632).

Table		CSF	ESF
SS Cells	rounded	0.89+0.05	0.75+0.11
	maple leaf-shape	0.61+0.14	0.68+0.13
	elongated	0.41+0.12	0.34+0.12
AA Cells		0.96+0.02	0.89+0.06

Less dense discocyte-rich fraction of SS cells was deoxygenated and separated into 3 groups by shape.

M-Pos209 POTASSIUM CHANNEL IN SICKLE CELL ANEMIA ERYTHROCYTES HAS A DIMINISHED CALCIUM SENSITIVITY, R. Grygorczyk and C. Grygorczyk, Department of Physiology and MRC Group in Periodontal Physiology, University of Toronto, Toronto, Ont. Canada, M5S 1A8.

Sickle cell anemia erythrocytes, like normal cells, possess a Ca^{2+}-activated, quinine-inhibitable K^+ channel. Earlier tracer flux studies have implicated a lower calcium sensitivity of the channel which could be modulated by calcium ionophore A23187. We have employed the patch-clamp technique to study properties of single, Ca^{2+}-activated K^+ channels in excised membrane patches from sickle cell anemia red cells. Experiments were performed at room temperature on homozygous SS cells which assumed the classic sickled shape. Single-channel conductance was very close to that observed in normal red cells but susceptibility of the channel to activation by intracellular calcium was significantly reduced in SS cells. The calcium concentration corresponding to half-maximal channel activation was about 15 μM in sickled cells as compared to about 2.1 μM in normal cells. Analysis of open and closed time histograms indicates that significant reduction of the probability of the channel being open in SS cells results mainly from prolonged dwell times of the channel in a long lasting (desensitized) closed state. This study directly demonstrates a diminished calcium sensitivity of the Ca^{2+}-activated K^+ channel in sickled red cells and that this property is preserved in isolated membrane patches.

M-Pos210 LIPID SPIN LABEL STUDIES OF SICKLE CELLS Leslie Wo-Mei Fung, Yin Zhang, Cheryl L. Nehme and Gang Li, Department of Chemistry, Loyola University of Chicago, Chicago, IL 60626.

We have used fatty acid spin labels and phospholipid spin labels to investigate sickle cell membrane abnormalities. Phospholipid spin labels are introduced into the cells to monitor the lipid mobilities in sickle and normal erythrocytes. The introduction of fatty acid spin labels into erythrocyte membranes in intact cells allows us to compare the reduction of the radicals on the spin labels by cytoplasmic components in normal and sickle cells, and differences were found between these two types of cells. Sickle cells separated by density gradients also show different reduction rates. The reductions are also different depending on hemoglobin molecule ligands. The reduction is independent of intracellular glutathione contents. Glutathione peroxidase activities and EM data of these cells were also obtained. The spin label results were correlated with the enzyme activity and EM data to reveal some of the membrane abnormalities in sickle cells.

(Supported in part by a grant from NIH)

M-Pos211 PASSIVE Ca^{2+} FLUXES ACROSS THE ERYTHROCYTE MEMBRANE SUGGEST A CARRIER MODEL. S.A. Desai, P.H. Schlesinger and D.J. Krogstad. Intr. by P. De Weer. Washington Univ, St. Louis, MO.

Ca^{2+} movement across the human red blood cell membrane consists of at least two components: a well-characterized ATP-requiring extrusion mechanism, the Ca^{2+} pump, and a poorly understood passive flux. We used $^{45}Ca^{2+}$ to examine the kinetics of ATP-independent Ca^{2+} transport. Unidirectional influx rates in erythrocytes pretreated with iodoacetamide (to deplete ATP and thus inhibit the Ca^{2+} pump) and loaded with Benz 2 (a Ca^{2+} chelator) are adequately described by a first order saturable process with Michaelis-Menten parameters V_{max} = 20 nmol/ml RBC·hr and K_m = 750 μM in 60 mM NaCl, 80 mM KCl and 20 mM HEPES at pH = 7.4 and 37°C. Unidirectional Ca^{2+} efflux is also a first order saturable process with V_{max} = 7.3 nmol/ml RBC·hr and K_m = 36 μM in the same medium (plus 1 mM EGTA) as determined by fitting the time course of passive Ca^{2+} efflux to the integrated form of the Henri-Michaelis-Menten equation by the nonlinear least squares method. Furthermore, the unidirectional passive flux rates in both directions were increased by trans unlabeled Ca^{2+}. This phenomenon (trans acceleration) is difficult to explain with simple pore and channel models; it is highly suggestive of a simple carrier which presents its Ca^{2+} binding site to one side of the membrane at a time. Nevertheless, our data fail to satisfy the thermodynamic constraint on the simple carrier model requiring that the V_{max}/K_m ratios for influx and efflux of Ca^{2+} obey the equation:

$$(V_{max}/K_m)\text{efflux}/(V_{max}/K_m)\text{influx} = \exp(2FV_m/RT).$$

Possible explanations include residual Ca^{2+} pump activity, alteration of kinetic parameters by changes in membrane potential, or the need for co- or countersubstrates.

(Supported by grants TG AI07172 and 5 T32 GMO 7200).

M-Pos212 RECONSTITUTION OF ERYTHROCYTE CYTOSKELETON AT THE PHOSPHOLIPID-WATER INTERFACE: STUDIES OF BINDING AND MECHANICAL PROPERTIES. K.Takeshita, B.M.Abraham, R.C.MacDonald and N.K. Subbarao, Dept. Biochemistry, Molecular and Cell Biology, Northwestern Univ., Evanston, IL 60208.

To gain insight into the molecular origin of the mechanical properties of the cytoskeletal network of erythrocyte membranes, we have begun the reconstitution of the cytoskeletal network at the phospholipid-water interface. With isolated components, we found that spectrin binds to phosphatidylserine (PS) liposomes and that its binding is markedly enhanced by band 4.1. We have also examined binding of unfractionated cytoskeletal proteins. The solution prepared from "Triton shells" by dissociation with 1M Tris/HCl (pH 7.2) was incubated with PS liposomes for 1h at 25°C in reconstitution buffer (physiological pH and ionic strength). Spectrin, band 4.1, actin and ankyrin all bound to the PS liposomes. In contrast, only trace amounts of proteins bound to phosphatidylcholine (PC) liposomes. These observations suggest that a cytoskeletal network was reconstituted specifically on PS membranes, although not necessarily with a structure identical to that of the native cytoskeleton. The cytoskeletal solution was also injected into reconstitution buffer under a preformed PS or PC monolayer at the air-water interface in a surface shear apparatus. The complex shear modulus (the elasticity and viscosity) were then measured directly. After incubation for 3h at 25°C (not final equilibrium), the elastic modulus and the surface viscosity at a protein concentration of 0.4mg/ml were 0.66 dyne/cm and 0.020 dyne-sec/cm, respectively, for the PS monolayer. Much smaller values for the elastic modulus, but similar values for the viscosity were obtained for the PC monolayer, indicating a strong preference of the cytoskeletal proteins for PS monolayer. These observations suggest that the cytoskeletal proteins had formed an extended network at the PS-water interface. Supported by NIH Grant DK36634. Introduced by I.M. Klotz

M-Pos213 CALMODULIN STIMULATED CALCIUM ATPASE OF HUMAN ERYTHROCYTE MEMBRANES IN MUSCULAR DYSTROPHY AND IN PSYCHIATRIC PATIENTS WITH BIPOLAR ILLNESS. Y.ZHANG (1), R.W.KULA (2), S.A.SHAFIQ (2) AND H.L.MELTZER (1). (1), Dept. of Molecular Psychopharmacol., NYS Psychiatric Institute, NY, NY 10032; (2), Dept. of Neurology, SUNY-HSCB, Brooklyn, NY 11203

Membrane abnormalities are suspected in the etiology of bipolar illness and muscular dystrophies. For a kinetic study of calmodulin-stimulated Calcium ATPase (Calm-CaATPase), erythrocyte ghosts were prepared from blood collected in acid-citrate- dextrose solution. An extended study was completed with 21 normal control subjects who were compared with 28 psychiatric outpatients with bipolar illness (BP). In addition, preliminary results are available for 7 subjects with unipolar depression, 6 subjects with Duchenne muscular dystrophy (DMD) and 6 subjects with myotonic dystrophy (MD). Three parameters of Calm-CaATPase, namely, Km, Vmax and total enzyme concentration in the membrane (Et) were determined in unmodified plasma membranes as well as following brief treatment with trypsin. Remaining CaATPase activity was measured in the presence of a saturating concentration of calmodulin. Et of the erythrocyte membranes was found to be higher in BP patients than in normal controls or those with unipolar depression. Of the dystrophic patients those with DMD had Et in the normal range whereas those with MD showed lower activity than the controls. Trypsin treatment of the membranes lead to loss of calmodulin stimulation in all subjects. BP and MD patients (who also had abnormal Et) showed inter-individual variability in the amount of trypsin required for maximal effect. The abnormal Et and variability in trypsin sensitivity may reflect specific changes in microenvironment of calcium ATPase in patients with BP and MD which could be of pathogenetic significance.

M-Pos214 LOCAL ALTERATION OF ERYTHROCYTE SHAPE DUE TO THRUST OF HbS MACROFIBER AGAINST MEMBRANE. Sunday O. Fadulu and H. Richard Leuchtag, Department of Biology, Texas Southern University, Houston, TX 77004.

The shape assumed by an erythrocyte in equilibrium has been shown to minimize the membrane potential energy (Elgsaeter et al., Science 234:1217, 1986). This principle should also apply to a membrane skeleton constrained by contact with an internal structure of crystallized HbS fibers. Near the point of macrofiber contact, the membrane of a cell in echinocyte or sickle-cell configuration takes on a tent-like shape. Equilibrium at a transverse plane implies a force balance between differential pressure P, tangential membrane tension T and fiber thrust F. Axial symmetry about the spicule simplifies the problem, yielding for the tension

$$T = (F + \pi R^2 P)/2\pi R \sin \Theta$$

where Θ is the angle between the membrane normal and the fiber, and R the radius, at the plane.

Supported by DRR/NIH RCMI award RR-0345.

M-Pos215 FLUORESCENCE ENERGY TRANSFER BETWEEN ERYTHROCYTE PROTEIN 4.1 AND THE MEMBRANE BILAYER. Z. Shahrokh, A.S. Verkman, S.B. Shohet. U.C., San Francisco.

To assess the molecular architecture of erythrocyte skeletal proteins at the bilayer interface, we have begun to measure distances between selected protein sites and bilayer lipids using fluorescence energy transfer. Inside-out vesicles (IOVs) were prepared by spectrin depletion of ghosts. The inner leaflet was labelled with diOC14(3) or N-tetramethylrhodamine-PE (TMR-PE) to be used as energy acceptors. The SH groups of band 4.1 were labelled with 1,5-IAEDANS and fluorescein-5-iodoacetamide, which served as donors to diOC14(3) (pair 1) and TMR-PE (pair 2), respectively. To prevent 4.1 aggregation and also to protect the 30 Kd N-terminal glycophorin binding domain during labelling, labelling was done in situ on intact IOVs. In view of the protease-resistance of this 30 Kd SH-containing domain, we suggest that only the three most accessible SH groups found within the first 31 amino acids were labelled. Steady state fluorescence studies showed quenching of the donor emission in the presence of acceptor (14%, pair 1; 20%, pair 2). Similar transfer efficiencies were calculated from sensitized emission. About 15% of the bound label was found in band 4.1 (65% on band 2.1, 10% on band 3). To exclude possible contribution of proteins other than 4.1, labelled 4.1 was purified from labelled IOVs and incorporated into freshly prepared IOVs. Energy transfer was again observed and confirmed by comparison of the spectra from the doubly-labelled IOVs with the spectra of a mixture of IOVs labelled separately with equivalent concentrations of donor and acceptor. Addition of triton X-100 to disrupt the geometric relationship between the donor and the acceptor also abolished the donor quenching and sensitized emission. Energy transfer was further validated by finding reductions in donor lifetime parallel to donor quenching. Using $K^2 = 2/3$, $n = 1.4$, and $Q_D = 0.5$, an overlap integral of 3.58×10^{-13} cm^3M^{-1} ($R_O = 57$Å) was calculated for pair 1. From this an average distance of 53Å between the labelled sulfhydryl(s) on band 4.1 and the plane of the bilayer was calculated. These results provide direct physical evidence for the close apposition of the 30 Kd N-terminal domain of protein 4.1 and the inner leaflet of the bilayer of the erythrocyte membrane.

M-Pos216 MECHANISM OF PHLORETIN INHIBITION OF ERYTHROCYTE ANION EXCHANGE. O.Fröhlich and S. Mayer. Dept. Physiol., Emory University School of Medicine, Atlanta, GA 30322.

Phloretin is a noncompetitive or mixed inhibitor of chloride exchange in human erythrocytes, with an inhibitory potency of about 2 µM at neutral pH. At 0°C, it crosses the lipid bilayer at a sufficiently slow rate to permit studies of the sidedness of its action. We found that the high-affinity inhibition of phoretin was mediated by extracellular phloretin, but an additional, lower-affinity site also exists intracellularly. At pH_o=7.0, Dixon plots were linear up to at least $10 \times ID_{50}$, suggesting only one extracellular binding site under these conditions.

The inhibitory potency of phloretin strongly depended on pH_o, reflecting the known titration of phloretin with a pK of about 7.4. ID_{50} ranged from 1.3 µM at pH_o<6.5 to 30 µM at pH_o=10.0, with twice the minimal value at pH 7.6-7.8. ID_{50} did not rise as steeply with incresing pH_o as expected for a simple titration. This suggests that the anionic form also inhibited, but with a lesser affinity. In addition, superlinear Dixon plots revealed the existence of at least one more phloretin binding site with an affinity in the range of 50-100 µM.

The inhibition of phloretin depended on the membrane potential: the potency decreased with more negative V_m. Lowering pH_o below 7.0 abolished this voltage dependence, and raising pH_o enhanced it. This suggests that the negative charge on phloretin migrates into the low-dielectric region of the protein on its way to the phloretin binding site.

M-Pos217 EFFECTS OF INTRACELLULAR FREE Ca AND THE RATE OF Ca INFLUX ON THE Ca PUMP. Y.C. Yang and D.R. Yingst, Dept. of Physiology, Wayne State University, Detroit, MI 48201.

The activity of the Ca pump of human red cells was studied in resealed ghosts as a function of intracellular free Ca (FCa_i) and the rate of FCa_i accumulation. Resealed ghosts were made by the agarose column method to contain, in addition to other constituents, less than 0.1 uM FCa_i, 100 uM arsenazo III, and either 1 mM ATP plus an ATP regenerating system (active ghosts) or less than 1 uM ATP and no regenerating system (passive ghosts). The rate of Ca influx into these ghosts was manipulated by suspending them in solutions containing various combinations of free Ca (1 to 30 uM) and the Ca ionophore A23187 (0.1 to 0.7uM). Entering Ca increased the FCa_i and activated the pump in active ghosts. In passive ghosts all the Ca movement could be described by a single rate constant. The activity of the Ca pump was calculated from the rate of net Ca uptake in active ghosts using the rate constant for passive Ca movement as determined in the passive ghosts. FCa_i and the rates of Ca transport in both active and passive ghosts were calculated from the absorbance of the entrapped arsenazo III. In general, increasing FCa_i from 1 to 10 µM activated the pump, whereas higher FCa_i progressively inhibited. The major new finding is that the rate of active transport at a given FCa_i between 1 and 10 uM varied with the rate of FCa_i accumulation. For example, at 3 uM FCa_i the pumping rate went form 25 to 75 uMoles/liter ghosts per min when the rate of net FCa_i accumulation was increased by a factor of four. These results show that the activity of the Ca pump is not a unique function of the FCa_i - they suggest that the rate of FCa_i accumulation could play a role in determining the activity of the Ca pump at a given FCa_i.
(Supported by NIH grant GM 32223, RCDA AM 01253, and by the American Heart of Michigan.)

M-Pos218 SOME NEW TRANSMEMBRANE SEQUENCES OF THE HUMAN ANION TRANSPORT PROTEIN AND A MODEL OF THEIR ARRANGEMENT. K.J. Kanes, N.J. Vogelaar and S.I. Chan, Division of Chemistry and Chemical Engineering, California Institute of Technology, Pasadena, CA 91125

To effectively model the architecture of the anion transport protein (band 3) and predict the amino acids critical for anion transport, one must obtain the putative amphiphilic helices transversing the membrane. We have extensively proteolyzed erythrocyte ghosts using the relatively non-specific protease papain in order to isolate peptides with boundaries close to that of the membrane edge. An HPLC technique was developed to separate the tightly membrane-associated segments of the anion transport protein, and other less abundant proteins found in human erythrocyte ghosts. The N-terminal 40 residues of the purest band 3 peptide were determined by amino acid sequencing to be: (V or A)WIGFWILILLVVLVVAFEGSFLVRFISNYTQEIFSFLIVLI with the first amino acid corresponding to number 51● of the murine band 3 protein. A second less pure but major peptide has the following sequence: GPLPNTALLSLVVMAGTFQGAMMLR(KF)KN with the beginning amino acid corresponding to position 583 of the mouse sequence. This peptide has also been sequenced elsewhere for human band 3, but the boundary of that sequence was at murine band 3 position 577. As expected, the humantransmembrane sequences are mainly but not completely conserved with respect to the mouse sequences. In addition to the above sequences, several smaller sequences have been obtained. These results tend to support the idea that positively charged amino acids, especially arginines, prolines and glycines are located near the edge of the membrane spanning sections in the anion transport protein. However, there are also some glycines and prolines within the helices. Finally, it appears that hydropathy plots do not predict the edges of membrane helices very effectively.

M-Pos219 WATER TRANSPORT THROUGH A SINGLE-FILE PORE: A KINETIC APPROACH. Julio A. Hernandez[#], Jorge Fischbarg[+@] and Larry S. Liebovitch[@,#], Dep. de Biofisica, Fac. de Human. y Ciencias, Univ. de la Republica, Montevideo, Uruguay[#], and Depts. of Physiol. & Cell. Biophys.[+], and Ophthal.[@], Coll. of P.& S., Columbia Univ., NYC 10032.

We have formulated a description of water transport across a single-file pore based on chemical kinetics. In it, the water molecule migrations between adjacent sites are expressed as chemical reactions. The advantage of the use of a kinetic model is that the migrations can have different rate constants along the pore, and thus yield a model for a non-homogeneous pore. Current models for single-file pores usually assume that the frictional resistance to the movement of water molecules remains constant along the pore, namely, that the pore is homogeneous. For such a homogeneous pore, the ratio between the osmotic and diffusional permeabilities (P_f/P_d) equals the number of water molecules inside the pore. Under homogeneous conditions, our kinetic model reproduces this result. However, using the kinetic model, we find that in a non-homogeneous pore, P_f/P_d may not equal the number of water molecules inside it.

Supported by NIH Grants EY06178 (JF) and EY06234 (LSL), Amer. Heart Assoc. and Whittaker Found. (LSL), and Res. Prevent. Blindness (JAH).

M-Pos220 EXPRESSION OF MOUSE ERYTHROID BAND 3 IN CULTURED CELLS AND XENOPUS OOCYTES. R. B. Gunn and R. Kopito, Emory University School of Medicine, Atlanta, GA 30322 and Stanford University, Stanford, CA 94305.

An expression vector was constructed containing the promoter-enhancer from the cytomegalovirus intermediate early gene. The cDNA for murine band 3 or either of two deletion mutants of band 3 were inserted between the promoter and polyadenylation sequence and co-transfected into a human embryonic kidney cell line (293 cells). G418-resistant clones were selected and screened for band 3 expression by immunofluorescence microscopy. Several positive clones were identified, which were subsequently shown to express the band 3 and mutant polypeptides by immunoblotting with a band 3 antiserum. The same band 3 expression plasmid was injected into nuclei of Xenopus oocytes. Baseline oocyte chloride-36 efflux was 0.4-0.5 nmoles/(oocyte•hr) at 22°C and was increased 10-fold in some oocytes 40 hours after this nucleus was injected with the full-length band 3 construct. Most injected oocytes had no enhancement or were leaky as judged by the loss of chloride-36 during the one-minute wash. If the inserted band 3 behave like native red cell band 3 molecules then there are 10^8 band 3 inserted per oocyte with a surface concentration of 33 band 3 per μ^2 while a red cell has 7,000 band 3 per μ^2. Supported in part by USPHS grant HL28674.

M-Pos221 IS PHOSPHATIDYLSERINE A DETERMINANT FOR RETICULOENDOTHELIAL RECOGNITION OF SCENESCENT ERYTHROCYTES? Allen, T.M., Williamson, R.A. and Schlegel, R.A. Dept. of Pharmacology, University of Alberta, Edmonton, AB; Dept. of Biology, Amherst College, Amherst, MA; Dept. of Molecular and Cell Biology, Pennsylvania State University, University Park, PA.

The removal of scenescent erythrocytes from circulation by uptake into the reticuloendothelial (RE) system has been postulated to be a consequence of abolition of the asymmetric distribution of phospholipids in the erythrocyte membrane. Shuffling of external and internal leaflet lipids results in two alterations of the membrane surface, each of which might provide a signal for recognition: a) the appearance of phosphatidylserine (PS) and phosphatidylethanolamine (PE) on the exterior of the cell and b) a looser packing of the phospholipids in the exterior leaflet. Liposomes formulated to resemble the outer leaflet of the erythrocyte membrane were used as a model system in which to study this problem. These liposomes substantially avoid recognition and clearance by the RE system. When these models of the erythrocyte surface were modified by the incorporation of > 2 mol% PS, but not other negatively-charged phospholipid or PE, their ability to remain in circulation was greatly reduced. A new method using the fluorescent dye merocyanine 540 was used to assess packing of external phospholipids. No significant difference in overall lipid packing of external phospholipids was detected between liposomes which showed dramatic differences RE uptake. We conclude that alterations in phospholipid packing are not contributing to RE recognition of liposome models of the erythrocyte surface. PS at a threshold concentration of 2 mol% is therefore implicated directly in the recognition of erythrocyte surface models by the RE system, and by analogy in the recognition of scenescent erythrocytes.

M-Pos222 FREQUENCY DOMAIN STUDIES OF IMPEDANCE CHARACTERISTICS OF BIOLOGICAL CELLS USING THE MICROPIPET TECHNIQUE. By K.Asami, Y.Takahashi and S.Takashima, Department of Bioengineering, University of Pennsylvania, Philadelphia, PA 19104-6392.

The purpose of this study is the measurement of the membrane capacity and conductivity of small biological cells using the micropipet technique. The use of AC signals as an input voltage enables the magnitude and phase angle of membrane impedance to be measured at various frequencies. The measurements were performed using a computer operated system between 1Hz and 1KHz. In addition, the suspension method was used in attempts to supplement the new method with the one which has been in use for many years.

The membrane capacitance of human erythrocyte was found to be 1.05uF/cm^2 at low frequencies. This value, however, gradually decreases as the frequency of input signal increases and reaches a value of 0.75uF/cm^2 at high frequencies. The decrease in capacitance is, however, so broad that we could not detect a well defined frequency dispersion of membrane capacitance. On the other hand, the conductance of erythrocyte membrane is found to be less than 5uS/cm^2. Based on this observation, we conclude that the membrane of human red blood cells behaves nearly as an insulator. This conclusion is in agreement with those reached by previous investigators using different methods. The membrane capacitance of mouse lymphocytes was found to be 1.02uF/cm^2 at low frequencies. The membrane conductance of lymphocyte is, on the other hand, of the order of 10-15 uS/cm^2 at resting state. This value is considerably larger than that of erythrocyte. This research is partially supported by a grant from Olympus Optical Company, Tokyo, Japan.

M-Pos223 SINGLE-HIT VERSUS MULTI-HIT HEMOLYSIS: pH EFFECTS ON A SCHISTOSOME LYTIC AGENT. M.R. Kasschau and M.P. Byam-Smith. Programs in Biological and Allied Health Sciences, University of Houston-Clear Lake, Houston, TX 77058.

The human blood parasite, Schistosma mansoni, has been reported to have an active membrane-bound hemolytic agent. The hemolysin has been shown to have an acid pH optimum and requires a lag phase prior to rapid hemolysis (Kasschau & Dresden, Exp. Parasitol. 61:201). Assays at the pH optimum yielded 80-90% hemolysis in 2 hours; at pH 7.5, less than 10% lysis occurred in 6-8 hours. However, rapid efflux of K^+ ions was observed at both pH's. We recently found that 2X or 3X the amount of lytic agent at pH 7.5 will give significant hemolysis with no lag phase; whereas at pH 5.1, these concentrations only decrease the lag phase observed at 1X by 30%. Thus, hemolysis at pH 7.5 is much more concentration dependent than at pH 5.1. By varying the concentration of RBCs per assay from 0.25% to 16% and holding the lytic agent concentration constant, we found that two different mechanisms of hemolysis are indicated at pH 5.1 and pH 7.5. With RBC suspensions from 4-16%, at pH 5.1, the same number of cells were lysed indicating that a single-hit mechanism of hemolysis is involved. In contrast, at pH 7.5 minimal hemolysis occurred in a 2% RBC suspension after 8 hours. This suggests that the lytic agent requires a multi-hit process of lysis at neutral pH. We therefore propose that at pH 5.1, hemolysis is caused by a single-hit mechanism resulting in osmotic lysis as suggested by the presence of the lag phase. While at pH 7.5, a multiple number of lytic agents (2-3) is necessary to form a pore large enough for direct hemoglobin release. Funded by NSF grant DCB-8517512.

M-Pos224 BIOTIN-CONJUGATED REAGENTS AS SITE SPECIFIC PROBES OF MEMBRANE PROTEIN STRUCTURE: APPLICATION TO THE STUDY OF THE HUMAN ERYTHROCYTE GLUCOSE TRANSPORTER. Mark R. Deziel and Meredith M. Mau. Department of Medicine, Division of Endocrinology, State University of New York at Buffalo School of Medicine, Erie County Medical Center, Buffalo, NY 14215.

A novel labelling procedure using biotin-conjugated protein-modifying reagents has been employed to study of the structure and function of the human erythrocyte glucose transporter. The carbohydrate moiety of isolated, membrane reconstituted transporter was labelled using galactose oxidase/biotin-hydrazide. Cysteine residues, which are essential for transporter function, were tagged with biotin-maleimide. Initial localization of biotinylated sites was undertaken by tryptic cleavage of labelled transporter into two membrane domains. Transporter reacted with galactose oxidase/biotin hydrazide was labelled on the broadly migrating 25 kDa glycosylated tryptic fragment, but not on the carbohydrate-free 19 kDa peptide. Cysteine residues labelled with biotin-maleimide were located on both peptides. The transporter polypeptide was also fragmented using S. aureus V8 protease. Limited digestion produced a broad band migrating from 30-50 kDa and sharper bands of 23 and 21 kDa. More extensive digestion resulted in the disappearance of the 23 kDa peptide and the appearance of sharp bands of 20, 19, 17, 12, 8, 5, and 3 kDa. Biotin label introduced with galactose oxidase/biotin hydrazide was found only on the broad 30 kDa band, confirming its identity as a glycopeptide. The broadly migrating glycopeptide and all of the sharp bands weighing more than 8 kDa contained cysteine residues labelled with biotin maleimide. These results demonstrate the potential usefulness of biotin-conjugated reagents as site specific probes of membrane protein structure. Supported by American Heart Association, New York State Affiliate, grant 87-100G.

M-Pos225 REGULATION OF SWELLING-STIMULATED K TRANSPORT BY PHOSPHORYLATION-DEPHOSPHORYLATION. Michael L. Jennings and Nayef S. Al-Rohil. Department of Physiology and Biophysics, University of Texas Medical Branch, Galveston, TX 77550

We showed recently that rabbit erythrocytes have a swelling-activated, anion-dependent, ouabain-resistant K transport system that is very similar to that in other species of red cell. The mechanism by which cell volume affects K transport was examined by measuring the kinetics of activation (by swelling) and inactivation (by shrinkage). Hypotonic swelling activates K transport with a characteristic time lag of about 6 minutes. Sudden shrinkage of pre-swollen cells causes a very abrupt inactivation of the K flux; the time lag for inactivation is less than 2 minutes. A minimal model for the transport regulation postulates that there are two states of the transport protein; the "Active" state has a high transport rate and the "Inactive" state has a low or even zero transport rate. The proportions of the two states depend on cell volume. The ratio k_{12}/k_{21} is increased by cell swelling, and the rate of approach to a new steady state is given by $k_{12} + k_{21}$. The fact that the time course of activation in hypotonic medium is slower than that for inactivation in isotonic medium indicates that activation involves an inhibition of k_{21} rather than an acceleration of k_{12}. Phosphatase inhibitors (F, VO_4, HPO_4) were found to inhibit activation of the transport by cell swelling; the same agents do not inhibit inactivation by sudden shrinkage. ATP depletion slows inactivation by cell shrinkage. The data suggest that swelling-activation of transport involves a dephosphorylation that decreases k_{21}; inactivation of the transport involves a phosphorylation that increases k_{21}. Supported by NIH Grant HL37479.

$$\text{Inactive} \underset{k_{21}}{\overset{k_{12}}{\rightleftharpoons}} \text{Active}$$

M-Pos226 AN ANALYSIS OF THE DIFFERENCES BETWEEN THE SOLUTION AND THE CRYSTAL STRUCTURES OF ALPHA-BUNGAROTOXIN WITH THE USE OF MOLECULAR DYNAMICS REFINEMENT

C.A. Schiffer, V.J. Basus*, W.F. van Gunsteren**, and R.M. Stroud***
Biophysics Program, *Department of Pharmaceutical Chemistry,***Department of Biochemistry, University of California, San Francisco, CA 94143, **Laboratory of Physical Chemistry, University of Groningen, 9747 AG Groningen, The Netherlands

Alpha-bungarotoxin is a snake neurotoxin which is one of the major components in the venom of Bungarus multicintus. The x-ray crystal structure (R.A. Love and R.M. Stroud, Protein Engineering, 1, 37 (1986)) and the NMR solution structure (V.J. Basus et. al. Biochemistry, 27, 2763 (1988)) differ significantly in two distinct regions. With the use of molecular dynamicswe are trying to better characterize these differences. Molecular dynamics combined with distance geometry efficiently samples many 3D structures so as to find structures that have reasonable internal energies as well as satisfying the NMR data set (J. de Vlieg et. al. Proteins, 3, 2090 (1988)). Molecular dynamics in x-ray refinement has a much larger radius of convergence than tradional x-ray refinement techniques (A.T. Brunger et. al., Science, 235, 458 (1987)). The initial molecular dynamics/x-ray refinements of alpha-bungarotoxin are very encouraging; the 2.5A structure without water was refined from an R-factor of 31% to an R-factor of 24.8%, thus making the electron density maps much more interpretable.

M-Pos227 **BINDING-INDUCED CONFORMATIONAL CHANGES REVEALED BY NMR STUDIES OF THE INTERACTION BETWEEN α-BUNGAROTOXIN AND PEPTIDE MODELS OF THE LIGAND BINDING SITE ON THE NICOTINIC ACETYLCHOLINE RECEPTOR.**

Guo-qiang Song, Ian Armitage*, and Edward Hawrot, Depts. of Pharmacology, *Molecular Biophysics and Biochemistry, and *Diagnostic Radiology, Yale Univ. Sch. of Med., New Haven, CT 06510

NMR studies reveal that significant conformational changes occur upon the binding of the snake neurotoxin, α-bungarotoxin (BGTX), to either of two synthetic peptides derived from the primary sequence of a portion of the binding domain located on the α subunit of the nicotinic acetylcholine receptor. One synthetic peptide, a 12mer corresponds to residues 185-196, and the other, an overlapping 18mer, extends from 181-198 of the α subunit. In both cases, upon formation of the complex the C4 proton resonance from His-4 of BGTX is converted to two resonances of equal intensity, in apparent slow exchange with each other. With the 18mer, the two peaks can be immediately observed, whereas with the 12mer, a longer time of incubation is required to resolve the two peaks, although other resonance changes in the 12mer are observed immediately upon mixing. The interpretation that the two resonances represent chemical exchange between two conformers of the bound complex is supported by variable temperature studies, by varying the ratio of components, as well as by saturation transfer and selective inversion experiments. Perturbations in other aromatic resonances show similar evidence for multiple conformers. Upon complex formation, a number of new resonances appear in the downfield region possibly corresponding to the C2 protons of the three histidines in the complex. Preliminary studies suggest that some of these peaks also are modulated by chemical exchange. In a control study, BGTX was added to a 14mer comprised of an unrelated peptide sequence. No perturbations were observed in any of the resonances in the aromatic region of the spectrum suggesting that the changes observed with the 12mer and the 18mer were due to "specific" binding interactions. All proton resonances of the 12mer have been assigned using various techniques including COSY and homonuclear decoupling. These assignments will be valuable in further studies aimed at elucidating the binding interaction. Supported by the Amer. Heart Assoc., NIH grants GM32629, DK18778 and instrumentation grants from NIH (RR03475), NSF (DMB-8610557), the Amer. Cancer Society (RD259) and Yale University School of Medicine.

M-Pos228 **ANALYSIS OF MEMBRANE PENETRATION DEPTH OF TRYPTOPHAN RESIDUES IN THE NICOTINIC ACETYLCHOLINE RECEPTOR IN RECONSTITUTED SYSTEMS USING FLUORESCENCE QUENCHING BY SPIN-LABELED PHOSPHOLIPIDS.**

Amitabha Chattopadhyay and Mark G. McNamee; Department of Biochemistry & Biophysics, University of California, Davis, California 95616.

The nicotinic acetylcholine receptor (nAChR) is a transmembrane glycoprotein found postsynaptically at the vertebrate neuromuscular junction and at the synapses of certain electric fish. It is an essential component in cholinergic synaptic transmission. Although a low resolution molecular model of the receptor is emerging, there is not total agreement about the molecular structure of nAChR. The purified receptor from electric tissue of Torpedo californica is reconstituted into membrane bilayers containing a mixture of dioleoylphosphatidylcholine (DOPC) and a spin-labeled phospholipid at low lipid to protein mole ratios (< 1000:1) by a cholate dialysis procedure. The spin-labeled lipid serves as the quenching lipid. From the fluorescence quenching obtained by using two different spin-labeled phospholipids in which the position (or depth) of the carbon atom to which the spin-labels are attached is different, the average depth of the tryptophan residues can be determined [Chattopadhyay, A., and London, E. (1987) Biochemistry **26**, 39-45]. We have used phospholipids carrying a nitroxide spin-label on the 5, 10, and 12 carbon atoms of one of the acyl chains as quenchers. Such measurements indicate that the tryptophan residues on the average are probably at a shallow location in the membrane. In addition, low levels of quenching obtained from these experiments imply that the majority of tryptophan residues are located in the putative extramembranous region of the nAChR and this is consistent with the proposed models for the nAChR. These measurements are relevant to ongoing analysis of the overall conformation and orientation of the nAChR in the membrane. (Supported by N.I.H. grant NS13050)

M-Pos229 THE ROLE OF pH IN MODULATION OF CALMODULIN STRUCTURE AND FUNCTION.
Christopher Weis, Charles Suhayda, Shixing Yuan and Alfred Haug. Dept. of Physiology, Microbiology, Pesticide Research Center and Center for Environmental Toxicology, Michigan State University, East Lansing, MI. 48824

Calmodulin is now known to be involved as an intracellular mediator of the calcium transient in such wide ranging physiological processes as the initiation of development in Xenopus oocytes, calcium accumulation and release from sarcoplasmic reticulum, and adrenergic stimulation. Many such processes occur coincident with or are profoundly altered by physiologically relevant changes in pH.

As indicated by the fluorescence anisotropy of mastoparan's single tryptophan residue, this small peptide associates with calmodulin in a pH dependent manner. The rotational correlation time of spinich calmodulin indicates a more compact conformation at pH 7.5 than pH 6.5 as judged by the molecular parameters of a bimane fluorescence probe attached to the single cysteinyl residue. This is consistent with circular dichroic data suggesting reduced helix induction at pH 6.5 as compared with that at pH 7.5. The hydrophobic surface probe 8-anilino naphthalene sulfonate indicates an increase in hydrophobicity of calmodulin with decreasing pH while calmodulin stimulated phosphodiesterase activity is 2.5 fold higher at pH 7.4 than pH 6.5. Cooperative interaction of calcium with calmodulin is minimally affected by pH at physiological ionic strength, yet the association constant varies over an order of magnitude between pH 5.5 and pH 7.5 as judged by intrinsic tyrosine fluorescence of bovine brain calmodulin. [NSF-PCM-8314662]

M-Pos230 ANTIGEN BINDING CAUSES CALCIUM-DEPENDENT CYTOPLASMIC ACIDIFICATION OF RBL-2H3 CELLS.
Michael A. McCloskey, Dept. of Physiology and Biophysics, University of California, Irvine, California 92717. (Intr. by James Hall)

Cross-linkage of IgE receptors on rat basophilic leukemia (RBL-2H3) cells initiates several biochemical events associated with the secretion of allergic mediators. These events include a rise in ionized cytosolic calcium, $[Ca^{2+}]_i$, or, in the absence of external Ca^{2+}, uptake of extracellular sodium. To test the possible mediation of Na^+ uptake by a Na^+/H^+ exchanger, which should cause cytosolic alkalinization, I monitored changes of intracellular pH following antigenic stimulation (500-1500 ng/ml of DNP-IgG) of anti-DNP IgE sensitized RBL-2H3 monolayers. Changes in pH were followed with two pH-sensitive fluorescent dyes, BCECF and DAPN, which respond with opposite changes in fluorescence intensity to a given change in pH. Contrary to the prediction, a slight drop in pH occurred in the absence of extracellular Ca^{2+}. Moreover, in the presence of 1 mM external Ca^{2+} both dyes reported a substantial antigen-induced acidification (0.20 $\pm$0.08 pH units). This occurred with a half-time of ~110 sec at 31°C, and it stabilized within ~7 min. Further evidence that acidification may depend upon the antigen-triggered rise in $[Ca^{2+}]_i$ is that, in the presence of external Ca^{2+}, addition of the Ca^{2+} ionophore ionomycin replicated the antigen-induced decline in pH. Acidification apparently was not a consequence of exocytosis, as 1 mM colchicine blocked by $\geq$50% the secretion of the granule enzyme, B-hexosaminidase, without affecting acidification. Although BCECF was partially sequestered by various organelles, the pH change probably occurred in the cytosol, as DAPN was uniformly distributed and it too reported an acidification. The source of the extra protons is unclear, but it does not appear to be acidic intracellular compartments. Thus, antigen binding to cells bearing the fluorescent base quinacrine in their acidic organelles caused no redistribution of the dye to the cytosol, whereas collapse of the pH gradient with nigericin released the trapped base. In summary, i) antigen-induced Na^+ uptake probably is not due to activation of a Na^+/H^+ counter-transporter, and ii) antigen-binding to RBL-2H3 cells triggers cytosolic acidification apparently as a secondary consequence of the $[Ca^{2+}]_i$ signal, by an as yet unresolved mechanism. [Supported by NIH grant GM-35901 and a Medical Research and Education Society award].

M-Pos231 ACTIVATION OF A Cl^-/ANION EXCHANGE PATHWAY BY CYTOPLASMIC ALKALINIZATION AND THE ROLE OF THIS EXCHANGER IN REGULATION OF FIBROBLAST pH.
P.Lin, M.Ahluwalia, and E.Gruenstein, Department of Molecular Genetics, Biochemistry, and Microbiology, Univeristy of Cincinnati Medical School, Cincinnati, OH 45267

In previous studies we have identified three types of Cl^- transport pathways in human fibroblasts: (i)an electroneutral Cl^-/anion exchanger, (ii) an electroneutral Cl^-/cation cotransporter, and (iii) an electrically conductive Cl^- channel. In addition there are two other Cl^- channels, one regulated by cAMP and the other regulated by Ca^{++}. We report here on the regulation of a Cl^- transport pathway by intracellular pH. Using both spectrofluorimetry and video imaging microscopy with the fluorescent pH indicator BCECF, we have found that cytoplasmic alkalinization activates a Cl^- efflux which is inhibited either by DIDS or by removal of Cl^- from the extracellular medium. These data indicate that this is an anion exchange pathway, a conclusion that is further strengthened by the insensitivity of the pathway to the Cl^-/cation cotransport inhibitor bumetanide. Following alkalinization of the cytoplasm, recovery of the pH to neutrality is impaired by DIDS or by removal of HCO_3^- from the extracellular medium. Recovery is unaffected by the Na^+/H^+ exchange inhibitor amiloride. These results indicate that this Cl^-/anion exchange pathway functions to restore intracellular pH to its homeostatic set point after alkalinization of the cytoplasm.

M-Pos232 INTRACELLULAR Ca IN SQUID GIANT AXONS AS MEASURED BY FURA 2 AND AEQUORIN. J. Requena, J. Whittembury, A. Scarpa and L. J. Mullins. IDEA, Centro de Biociencias, Caracas 1015-A, Venezuela, Case Western Reserve University, Cleveland, Ohio and University of Maryland, Baltimore, MD 21201.

Squid Giant Axons have been injected simultaneously with Fura 2 (a fluorescent Ca indicator) and with aequorin. Fura fluorescence was calibrated in situ by measuring its maximum and minimum values. These were obtained by letting Ca enter the axon with prolonged depolarization in the presence of CN and by injecting Ethyleneglycol-bis-(β-aminoethly ether)-N,N,N',N'-tetraacetic (EGTA) at the end of the experiment. Average intracellular Ca obtained with Fura was 170 (+15) nM (n = 27). A comparison of aequorin light signal with Fura fluorescence allows one to demonstrate that light output by aequorin is linear with intracellular Ca up to values of 500 nM and then changes to a square law relationship. The technique employed allows one to observe Na-free Ca entry and that Ca entry that follows depolarization of the axon with high K concentrations in seawater. The sensitivity of Fura 2 to intracellular Ca is at least as great as that of aequorin, thus permitting its use in squid giant axon. However, it was found that voltage clamp techniques, requiring an internal current electrode, are not possible to employ since current flow in the axoplasm destroys the fluorescence produced by Fura.

Supported by CONICIT S1-1147 (Caracas).

M-Pos233 THREE-DIMENSIONAL RECONSTRUCTION OF THE INTERCALATED DISC OF NORMAL ADULT HUMAN MYOCARDIUM. S. J. Sutterfield[1], J. C. Kinnamon[2], M. E. Billingham[3], and N. B. Ingels, Jr.[1], [1]Research Institute, Palo Alto Medical Foundation, Palo Alto, CA, 94301; [2]University of Colorado, Boulder, CO, 80309; and [3]Stanford University, Stanford, CA, 94305.

The intercalated disc is the complex region of membrane specialization which contains gap junctions in heart. The intercalated disc has been described from two-dimensional studies as a step-like interdigitating structure. Its three-dimensional nature, however, has not been fully elucidated by reconstructions from serial sections. An understanding of the three-dimensional geometry of this region is important for developing models of intercellular communication as well as models of cardiac development and dynamics. To reconstruct this structure in human heart, normal adult human cardiac tissue was obtained through the heart transplant program at Stanford in the form of a needle biopsy taken from the right ventricular endocardium of the donor heart just prior to transplantation. The biopsy was fixed and embedded in epon, sectioned serially in a transverse plane into 80nm sections, and mounted and stained for transmission electron microscopy. A capillary was used as a landmark to follow a population of cells through these serial sections, and micrographs (3425x) were taken from each section. Using an IBM PC-based three-dimensional reconstruction software package, five regions of intercalated disc that were completely represented in these micrographs were digitized and reconstructed. Their volumes were approximately: 34μm^3, 41μm^3, 48μm^3, 81μm^3, and 130μm^3. To our knowledge, these are the first calculations of human intercalated disc volume, and the first three-dimensional reconstructions of the intercalated disc region from normal adult human endomyocardial tissue. They show that the intercalated disc is a geometrically complex structure. We find it to be a more sloping, twisting structure than can be easily reconciled with its definition as a step-like planar system.

M-Pos234 *CHANGES IN Ca^{++}, H^+ AND JUNCTIONAL RESISTANCE IN CRAYFISH AXONS UNCOUPLED BY ACIDIFICATION.* C. Peracchia, Department of Physiology, University of Rochester Medical Center, Rochester, NY 14642.

It has been shown that gap junction channel permeability is affected by changes in $[H^+]_i$ but still unclear is whether or not the channels are gated directly by this ion. Recently, we have studied the relationship between junctional electrical resistance and $[Ca^{++}]_i$ or $[H^+]_i$ in crayfish septate axons uncoupled by lowered intracellular pH (Na-acetate substituting for NaCl). Four microelectrodes were inserted into axon pairs, two on each side of the septum, for measuring junctional (R_j) and non-junctional (R_m) membrane resistances, and an ion selective microelectrode was inserted into one of the two axons for simultaneously measuring changes in $[Ca^{++}]_i$ or $[H^+]_i$. Intracellular pH decreases with 3 min exposure to acetate from 7.3 to 6.2 but the peak of acidification precedes the peak of maximum increase in R_j by 40-90 seconds. In addition, the shape of both pH_i and $[H^+]$ curves differs markedly from that of the R_j curve and fast pH_i changes obtained by doubling the superfusion flow rate cause changes in R_j 60-70% smaller than those following slow pH_i changes of the same magnitude. $[Ca^{++}]_i$ increases with acidification from 0.1-0.3 to 2-5 uM, but in contrast to the pH_i curve the peak of the Ca^{++} curve matches in time the peak of the R_j curve. In addition, both pCa and $[Ca^{++}]$ curves are similar in shape to the R_j curve. In fact, $[Ca^{++}]$ and R_j curves are virtually superimposed. These curves show that R_j is affected by Ca^{++} in the nanomolar range; however, preliminary experiments in which $[Ca^{++}]_i$ was increased at normal pH_i show that R_j is affected by 1 uM or greater $[Ca^{++}]$. This suggests that cytoplasmic acidification may have two effects on coupling, one mediated by an increase in $[Ca^{++}]_i$ and the other by an increase in channel sensitivity to Ca^{++}. The latter could follow activation of phosphatases and channel protein dephosphorylation. Evidence for increase in junctional conductance with cAMP could fit this scheme as cAMP-induced phosphorylation could reduce the channel sensitivity to Ca^{++}.

Supported by NIH Grant GM20113.

M-Pos235 RECORDING OF JUNCTIONAL CURRENT FROM ISOLATED FROG LENS EPITHELIAL CELL PAIRS. K.E. Cooper and J.L. Rae, Depts. of Physiology and Biophysics and Ophthalmology, Mayo Foundation, Rochester, MN.

Epithelial sheets were removed from whole frog lenses using a standard decapsulation procedure. The cells were dissociated from the capsule using a low Ca++, trypsin solution and gentle trituration. This procedure yielded primarily individual cells but also yielded the cell pairs that were used for the studies reported here. Each cell of a pair was independently voltage clamped by a separate patch clamp amplifier. With the voltage in one cell held constant, voltage steps or ramps were applied to the second cell. The change in current recorded from the first cell in response to the change in voltage in the second cell then gave a direct measurement of the current flowing through the junctions. The current-voltage relationships thus obtained were linear. The likely explanation for this result is that the junctional channels have gating which is independent of the transjunctional voltage. Initial junctional resistances ranged from 20 MΩ to 600 MΩ. This compares to a single cell input resistance of approximately 2 GΩ for cells from this same population. Supported by NIH grants EY03282 and EY06005.

M-Pos236 VOLTAGE-DEPENDENT GATING OF EMBRYONIC CARDIAC GAP JUNCTION CHANNELS. By Richard D. Veenstra, Dept. of Pharmacology, SUNY/Health Science Center, Syracuse, NY 13210.

The dependence of macroscopic gap junctional conductance ($G_j = I_j/V_j$) on trans-junctional voltage ($V_j = V_2 - V_1$) was examined in paired myocytes, isolated from 7-day old embryonic chick ventricles and cultured for one day in vitro. The membrane voltage of both cells (V_1 and V_2) was independently controlled by separate patch-clamp circuits in the whole-cell configuration. Instantaneous and steady-state G_j measurements were taken from the beginning and end of a 1 sec step in V_j ranging from 0 to ±90 mV. Instantaneous G_j remained linear over the entire voltage range examined, while the steady-state G_j declined when V_j exceeded ±30 mV. Exponential time constants for the decay of junctional current (I_j) became faster with increasing voltage, averaging 162 ± 70 msec (N = 6), while the recovery time constant was 7 times slower, requiring 1.1 sec at V_j = 80 mV. The normalized steady-state G_j-V_j curve could be defined by a two-state Boltzmann distribution, assuming an effective gating charge of 1.78 electrons, a half inactivation voltage of 56 mV, and a residual voltage-insensitive G_j of 35% of maximum. Single channel recordings revealed the closure of several gap junction channels with each V_j step to 80 mV and the ensemble average of 5 such records produced an exponential decay of I_j with a time constant of 184 msec. The single channel conductance remained linear at 145 pS over the entire V_j range. The results support the hypothesis that a population of 145 pS gap junction channels are gated closed when V_j exceeds ±30 mV. This mechanism may play a functional role in reducing electrical communication between differentiated heart cells and non-myocardial or injured myocardial cells with low resting potentials. This work was supported by a research grant from the National Heart, Lung and Blood Institute (#HL38536).

M-Pos237 **CARDIAC GAP JUNCTION CHANNELS SHIFT TO LOWER CONDUCTANCE STATES WHEN TEMPERATURE IS REDUCED.** **Yan-hua Chen and Robert L. DeHaan, Dept. of Anatomy and Cell Biology, Woodruff Health Sciences Center, Emory University, Atlanta GA 30322**

Pairs of ventricular cells, isolated from the hearts of 7-day chick embryos, were voltage clamped with two patch-electrodes in whole-cell clamp mode. Mean junctional current (I_j) and single-channel currents (i_j) of 5-20 pA were measured above a background current noise of 1-2 pA (Veenstra and DeHaan, AJP:Hrt 254:H170-H180, 1988), while slowly changing bath temperature from 26°C to 14°C. With pipette solution buffered to 4 μM free Ca^{2+} with 10 mM EGTA, junctional conductance ($G_j = I_j/V_j$) averaged 2.7 nS at 26°C (16 cell pairs). G_j fell more than ten-fold with slow bath cooling to 0.20 nS at 14°C. At 20-26° we measured single-channel events with three sub-conductance levels near 80, 160 and 240 pS. As the temperature was decreased, 240 pS events diminished in frequency, and disappeared below about 21°. The 80 pS and 160 pS subconductance events continued to 16°, at which 160 pS activity stopped; 80 pS events ceased at 15°. Between 18° and 14°, junctional current noise quieted to less than 1 pA, and 40 pS events could be recorded. We conclude that the reduction in G_j with decreased temperature results both from a decrease in open-state probability of each conductance state, and from a shift from high-conductance to low-conductance states. (Supported by NIH HL-27385 to RLD).

M-Pos238 INTRACELLULAR Ph MODULATES THE EFFECT OF *V-SRC* ON CELL-TO-CELL COMMUNICATION VIA GAP JUNCTIONS. Hyrc, K. and Rose, B., Dept. Physiology and Biophysics, University of Miami School of Medicine, P.O. Box 016430, Miami, Fl 33101

Gap junctional communication is known to be reduced by the viral *src* gene product (*v-src*), a membrane-bound protein tyrosine kinase. We worked with cells containing a temperature-sensitive *v-src* mutant with low kinase activity at 40°C and high activity at 34°C. Upon a temperature shift from 40°C to 34°C, these cells switch within 10-30 min from a state of high junctional permeability to low permeability (measured by cell-cell transfer of a fluorescent tracer, Lucifer Yellow). We show that this permeability response is prevented when the intracellular pH (pH_i) is lowered from the usual 7.2 to 6.8 (by dropping the extracellular pH (pH_e) from 7.5 to 6.6) before the temperature downshift. (pH_i was measured by means of the fluorescent indicator BCECF, using the video image ratio technique). Moreover, at 34°C, the high permeability state is restored in these cells over a period of 2-3 hr when pH_i is lowered to 6.8. Upon subsequent pH_i shift to 7.2, permeability drops within 15-30 min. In cells kept at 40°C, junctional tracer transfer was little affected by pH_i. This also was so for the uninfected parent cells at either temperature. Cells infected with the wild-type *v-src* on the other hand, showed the same pH_i dependency of junctional permeability as did the temperature sensitive mutant-infected cells. The block by pH_i of the *v-src* effect on junctional permeability could be due to a block of the *v-src* kinase activity by lowered pH_i or due to a pH-sensitive intermediary. TMB-8 which we had shown to block the *v-src* effect on junction, does not much affect pH_i. Its mechanism of interfering with the action of *v-src* on the junction therefore lies elsewhere, not via pH_i. This work was supported by research grant CA14464 from the National Cancer Institute, National Institutes of Health.

M-Pos239 THE ROLE OF ATP-SENSITIVE K^+ CHANNELS ON CLUSTERS OF PANCREATIC β-CELLS. T.R. Chay, J.R. Kim, and M.H. Lambert, Department of Biological Sciences, University of Pittsburgh, Pittsburgh, PA 15260.

The inhibition of ATP-sensitive K^+ channels in pancreatic β-cells by metabolites of glucose is believed to give rise to many of the cellular activities including insulin release. We demonstrate by a mathematical model how the burst electrical activity is initiated and $[Ca^{2+}]_i$ level rises as the K-ATP channels are inhibited by a small rise in the cellular [ATP]. We also deomonstrate how the opening and closing of K-ATP channels influence the membrane noise in isolated single β-cells. With brief current stimuli, we show that the plateau duration is controlled by the intercellular electrical coupling and K-ATP stochastic noise.

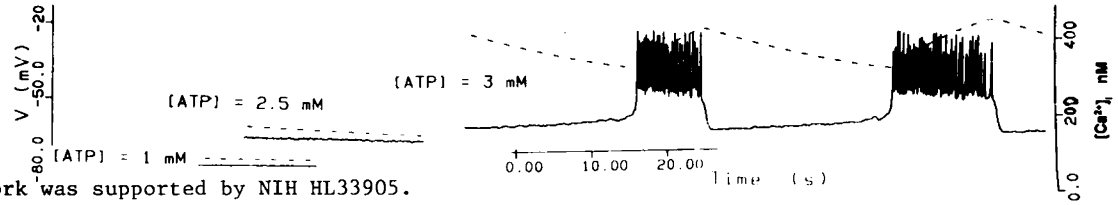

This work was supported by NIH HL33905.

M-Pos240 EFFECTS OF GLUCOSE AND BICARBONATE ON THE PH OF THE INTERCELLULAR SPACE IN MOUSE ISLETS OF LANGERHANS. Moura, A.S., Riquelme, G., Rojas, E. and Atwater, I. LCBG, NIDDK, NIH, Bethesda, MD.

Mouse islets of Langerhans consist mainly of tightly packed B-cells which secrete insulin in response to glucose; the intercellular space (excluding capillary space) represents less than 1% of the islet volume. B-cells are electrically synchronous, and during the burst pattern of electrical activity, K is accumulated and Ca is depleted in the intercellular space. Glucose sensitivity of the B-cell is controlled by K permeability; two of the K-channels described have been reported to show pH sensitivity. Although glucose metabolism may be expected to acidify the cytosol, and thus transiently acidify the intercellular space, measurements of cytosolic pH in B-cells are conflicting. Single microdissected mouse islets (0.5 mm minimum diameter) were continuously perifused while measuring the intercellular pH with a liquid H-sensitive micro-electrode. The intercellular space at the center of the islet was slightly more acidic than the bath solution; addition of 22 mM glucose induced a slight alkalinization. Reducing the NaHCO3 concentration from 25 to 5 mM and the CO2 from 5% to 1% decreased the buffering capacity of the solution without changing the pH from 7.4; this decreased the intercellular pH to 6.6 (22 mM glucose) or 6.3 (glucose). The results indicate that a large buffering capacity in the bath medium may be required to prevent excessive acidification of the restricted intercellular space. The apparent glucose induced alkalinization of the intercellular space is difficult to reconcile with the expected increased production of H during metabolism, but may be due to a change in the fixed charge of the islet matrix upon exposure to glucose or may reflect co-secretion of buffer molecules with insulin.

M-Pos241 THE CATALYTIC SUBUNIT OF cAMP-DEPENDENT PROTEIN KINASE MIMICS THE EFFECT OF ISOPROTERENOL ON JUNCTIONAL CONDUCTANCE IN HEART. W. C. De Mello, Department of Pharmacology, Medical Sciences Campus, GPO Box 5067, San Juan, P. R. 00936.

It is known that the intracellular injection of cAMP increases the electrical coupling of heart cells within 30 sec. (De Mello, 1984). The quick action of the nucleotide on gj might be due to activation of protein Kinase and consequent phosphorylation of junctional proteins (De Mello, 1983). In order to investigate this hypothesis the catalytic subunit of cAMP-dependent protein Kinase was dialyzed into pairs of ventricular cells isolated with collagenase from rat's heart. Giga-ohms sealing was achieved in each cell and their cell membrane broken and whole cell clamp was produced. The catalytic subunit from Sigma (30-35 picomolar units per mg protein) was added (35 ug/ml) to solution used to fill the micropipettes. Time = 0 of dialysis was taken at the moment cell membranes were broken. Holding potential for both cells was - 40 mV and only cell 1 was pulsed to - 20 mV for 100 ms. Measurements of I2 and V1 indicated an increase in gj within 140 sec. of rupture of cell membrane. The average increase in gj was 90% (S.E. ± 2.5) (n = 10) measured 6 min. after dialysis was started. The finding that the intracellular dialysis of cAMP-d-protein Kinase inhibitor blocks the effect of isoproterenol on gj (De Mello, 1988) as was as the present results represent a strong support to the phosphorylation hypothesis. (Supported by Grant No. HL-34148 from NIH.)

M-Pos242 **CYTOKINE MODULATION OF ADHESION AND MOTILITY DURING TUMOR CELL-LYMPHOCYTE INTERACTIONS. Beverly S. Packard. DCB, CBER, FDA. Bethesda, MD 20892**

Enhancement of the interactions between tumor cells and lymphocytes is integral to the success of adoptive immunotherapy; recently identified and cloned cytokines represent potentially powerful tools for this approach to cancer treatment. In the present study human tumor cell lines of neural crest origin were established and assayed for the ability to interact with cultured lymphocytes of autologous, allogeneic, and xenogeneic origin. Cotreatment of tumor cells with the cytokines interferon-γ (6.7 nM) and tumor necrosis factor-α (5.3 nM) for three days induced an increase in surface area in contact with the substratum, a decrease in extent of the actin filament network, and diminished motile capability. Both autologous and allogeneic but not xenogeneic lymphocytes adhered to treated as well as to control tumor cells and maintained extensive motility on the surfaces of both. Introduction of human lymphocytes to cytokine-treated tumor cells induced the latter to detach from the substratum whereas coculture of lymphocytes and untreated tumor cells did not affect the latter's adhesion or motility. The biophysical basis of these observations will be discussed.

M-Pos243 FUSION OF ERYTHROCYTES TO FIBROBLASTS MEDIATED BY A VIRAL FUSION PROTEIN: A PATCH CLAMP STUDY. A.E. Spruce, J.M. White[1] and W. Almers, Dept. Physiology & Biophysics, U. Washington, Seattle, WA, and [1]Dept. Pharmacology, U. California, San Francisco, CA.

We used 3T3-HA-b fibroblasts (FBs) expressing the influenza virus fusion protein (HA) on the cell surface (Doxsey et al, J Cell Biol 101:19). FBs were made fusion-competent by mild trypsinization and decorated with human erythrocyte (RBC) ghosts loaded with Lucifer Yellow (LY). When HA was activated by dropping pH from 7.2 to 4.8 LY fluorescence spread from RBC to FBs within 5 min, indicating fusion. In whole-cell recordings, fusion competent FBs decorated with 1-2 fresh RBCs had a conductance (G) of 0.8±0.3 nS and a capacitance (C) of 18±4 pF (±SEM, n=8). When pH=4.8, the conductance began to increase within 13±3 s (n=5), reached a peak of 3.3±1.1 nS above baseline within 31±5 s and then declined again to near-baseline levels. The increase in G was often accompanied by a small increase in C (up to 0.7 pF per RBC). In FBs without RBCs, pH=4.8 caused instead a decline in conductance (by 0.3±0.1 nS, n=5). RBCs decorating FBs had G=136±38 pS and C=850±47 fF (n=11, whole cell). In one experiment, pH=4.8 increased C to 11 pF, indicating fusion; G increased by 8 nS. In 6 other experiments, some with untrypsinized FBs, pH 4.8 increased C by <100 fF, indicating that no fusion took place; g decreased by 27±14 pS. Conclusion: 1) When FBs and RBCs fuse G increases strongly, 2) the increase is much larger than the conductance of the fusion partner, 3) the increase is directly related to fusion because it does not occur when FBs are fusion-incompetent or when the fusion partner is missing, hence 4) the fusion contact formed by HA is leaky, not only connecting the fusing cells, but also causing a transient permeability pathway between cytosol and cell exterior. This leaky fusion with RBCs contrasts with the tight membrane fusion during exocytosis, or the tight cell-cell connection formed by gap junctions. Supported by GM-39520.

M-Pos244 MONOVALENT ION SELECTIVE CHANNELS DERIVED FROM RED BEET ENDOPLASMIC RETICULUM.

E. Rousseau and D.P. Briskin*. Department of Physiology and Biophysics, Faculty of Medicine, University of Sherbrooke, Sherbrooke, Quebec, Canada. J1H 5N4. *Department of Agronomy, University of Illinois, Urbana, Il. 618 01, U.S.A.

Endoplasmic Reticulum (ER) microsomal membrane from Red Beet were fused into Planar Lipid Bilayers (PLB). Vesicles were isolated by differential and sucrose gradient centrifugations, frozen under liquid N_2, transported on dry ice and stored at -80°C. Experiments were performed at room temperature. PLB were made of a lipid mixture of Diphytanoylphosphatidylcholine and Phosphatidylserine. An asymmetric fusion Buffer was used: 250 mM KCl, 10 mM K-HEPES, 5 mM $CaCl_2$, pH 7.2 cis/50 mM KCl, 10 mM K-HEPES, 5 mM $CaCl_2$, pH 7.2 trans. K^+ channels of 50-55 pS in 250 mM/50 mM KCl were consistently observed. Their selectivity was assessed using different cis/trans KCl ratios and after perfusion with K-Acetate. Perfusion of both chambers with a Choline-Cl Buffer (100 mM cis/100 mM trans) revealed the presence of a low conducting Cl^- selective channel (10 pS). Following the detection of K^+ channels the cis chamber (cytoplasmic face) was perfused with a 1 μM Ca^{2+} 250 mM HEPES/125 mM Tris pH 7.2 solution and the trans with a 50 mM $Ca(OH)_2$, 250 mM HEPES pH 7.2. A similar gradient has been previously used to observe Sarcoplasmic Reticulum Ca^{2+} release channel. However, we failed to record any divalent cation selective channel even after addition of IP_3 (up to 50 μM) and ATP (up to 4 mM). Consequently experimental conditions revealing the presence of a putative ER Ca^{2+} release channel remain to be work-out. E.R. is a scholar of the Canadian Heart Foundation.

M-Pos245 DO CALCIUM IONS MEDIATE THE VOLTAGE DEPENDENT INHIBITION OF SPERM ENTRY IN SEA URCHIN EGGS? David H. McCulloh, Pedro I. Ivonnet and Edward L. Chambers. Dept. Physiol. & Biophys., University of Miami School of Medicine, Miami, FL 33101. (Intr. by David S. Weiss.)

Sperm enter eggs of the sea urchin, Lytechinus variegatus, depolarized to 0 mV but are blocked when the egg's membrane potential is held near its resting value (-70 mV). Whether this voltage dependence is mediated by charges/dipoles within the membrane or by an ion flux is not clear. We have asked whether substitution of $[Na^+]_o$ or $[Ca^{++}]_o$ affects the voltage dependence of sperm entry. Eggs voltage clamped at various membrane potentials were inseminated. The probability of sperm entry at each membrane potential was estimated from the number of sperm which entered eggs divided by the number of sperm which caused electrophysiological responses following attachment to the egg's surface. The Boltzmann equation which best fitted the data obtained in normal seawater indicated that the probability of entry increased at more positive membrane potentials attaining a probability of 0.5 at -31 mV (V_{50}). Displacement of the equivalent of 3.2 electronic charges through the membrane field can account for the voltage dependence. Substitution of choline or N-methyl glucamine for Na had no effect on the voltage dependence of sperm entry. Increasing $[Ca^{++}]$ from 10mM (normal seawater) to 31.6 or 100 mM (by isosmotic decrease of $[Na^+]$) shifted V_{50} to more positive values. Decreasing $[Ca^{++}]$ to 1 mM shifted V_{50} to a more negative value. V_{50} shifted 52 mV for a ten-fold change of calcium activity, indicating that roughly 1.8 calcium ions are involved in shifting the voltage dependence. Calcium ions either act as voltage sensors or affect the local field for the voltage sensor which regulates sperm entry. (Supported by NIH #HD 19126 and NSF #DCB-8711787 to E.L.C.)

M-Pos246 Scanning Tunneling Microscopy of Metal Coated T7 and fd Bacteriophages

D. Keller and C. Bustamante Department of Chemistry, University of New Mexico, Albuquerque, NM 87131

We report a method for reliably and reproducibly imaging virus particles and other biological samples with the Scanning Tunneling Microscope (STM). The chief problems encountered in STM imaging of biological samples are: a) the low conductivity of biological material, and b) finding a reliable method of depositing the sample on an atomically flat, conducting substrate. We have solved the first problem by coating our samples with platinum carbon. The deposition problem has been solved by 1) the use of atomically flat gold surfaces that can be easily made by melting and resolidifying a gold droplet, and 2) the use of a dosing device which holds the gold substrate and keeps it continually immersed during the deposition and washing steps. Images of several different viruses are shown. This method allows STM imaging of thick, insulating biological samples, which may be difficult to image reliably without coating.

M-Pos247 X-RAY FIBER DIFFRACTION STUDIES OF THE U2 STRAIN OF TOBACCO MOSAIC VIRUS

Rekha Pattanayek and Gerald Stubbs, intr. by John H. Venable
Dept. of Molecular Biology, Vanderbilt University, Nashville, TN 37235

U2 is a strain of tobacco mosaic virus (TMV), the type member of the tobamovirus group of plant viruses. There is 73% amino acid sequence homology between the coat proteins of U2 and TMV vulgare, but the viruses differ in physical, chemical and biological properties. Tobamoviruses are rod-shaped helical viruses, 3000Å long and 180Å in diameter, with 49 coat protein subunits (MW 17,500) in three turns of the viral helix. A single RNA strand follows the helix at a radius of 40Å, with three nucleotides bound to each protein subunit. The radial electron density distributions of TMV and U2 at low resolution show significant differences near the inner viral surface, where the homology is only about 50%. This region of the viruses is of particular interest, as it includes the binding site for a calcium ion that is important in electrostatic control of viral assembly and disassembly.

X-ray fiber diffraction data to 3.6Å resolution have been collected from native U2. An initial model of U2 based on the TMV vulgare structure has an R-factor of 0.23. However, molecular replacement methods are much less powerful in fiber diffraction than they are in conventional crystallography, and R-factors are inherently lower. It is therefore not yet known whether this model can be refined. A combination of molecular replacement and multi-dimensional isomorphous replacement may be a more effective strategy, and data have been collected from three heavy-atom derivatives. Further work using both approaches is in progress.

M-Pos248 COMPARATIVE SELF-ASSEMBLY PROPERTIES OF RECOMBINANT AND NATIVE COAT PROTEINS OF TOBACCO MOSAIC VIRUS: EFFESCTS OF N-TERMINAL ACETYLATION.

K. Raghavendra, G. MacDonald and T. M. Schuster, Molecular & Cell Biology, U-125, University of Connecticut, Storrs, CT 06268, S.J. Shire, D.W. Leung, G.J. Cachianes, E. Jackson, W.I. Wood and P. McKay, Genentech, Inc., California 94080.

Coat protein of Tobacco Mosaic Virus obtained by recombinant method (rTMVP) has its N-terminus free unlike its acetylation in the wild type (vulgare) (wTMVP). Preliminary studies on the self-assembly behavior of rTMVP indicated that the assembly follows the familiar endothermic polymerization process but there are subtle differences when compared to that of wTMVP (Shire et al. Biophys. J. 1987, 51, 91a). We have investigated the pH dependence of the aggregation behavior of rTMVP, by using sedimentation velocity, electron microscopy and CD spectral measurements, and found that there are similarities and differences when compared to that of wTMVP: (i) under protein crystallization conditions, rTMVP forms dimers of bilayer disk aggregates (4 layers of subunits) like wTMVP; (ii) under virus assembly conditions, rTMVP seems to display a mixture of dimers of disks and helical aggregates, but only the latter species is observed with wTMVP and (iii) at pH 5.5, long helical aggregates appear to coexist with dimers of disks unlike wTMVP. We conclude that the absence of N-terminal acetylation and the consequent introduction of an extra amino group in rTMVP seems to retard the formation of the helical aggregates unlike wTMVP. Finally the influence of free N-terminus on in-vitro virus assembly is discussed. (Supported by the NIH grant AI-11573 to TMS).

M-Pos249 STRUCTURAL STUDIES OF THE CONTRACTED FORMS OF THE FILAMENTOUS PHAGE FD
Linda M. Roberts and A. Keith Dunker Biochemistry/Biophysics Program Washington State University Pullman, WA. 99164-4660

The filamentous bacteriophage fd consists of a circular molecule of single-stranded DNA surrounded by 2700 copies of a major coat protein, with a few copies of minor coat proteins located at each end of the virus. The fd phage (900 x 5 nm) contracts into spherical shaped particles which are 40 nm in diameter upon exposure to a $CHCl_3/H_2O$ interface at room temperature. If the temperature of the interface is lowered to less than 15°C, the filaments contract into rod-shaped particles (250 x 15 nm) called I-forms. Both spheroids and I-forms are more labile to detergents than is the intact phage. The structures of the contracted particles have been studied in detail using fluorescence, absorbance and circular dichroism spectroscopy. Our results show that contraction of fd to spheroids or I-forms results in a substantial decrease in the fluorescence of the single tryptophan residue of the major coat protein. The decrease in fluorescence is accompanied by an increase in UV absorbance at 260 nm, indicating that the viral DNA has become unstacked. Extinction coefficients of the contracted forms were determined and used to calculated concentrations of the CD samples. CD spectra indicate that contraction to spheroids and I-forms involves a significant loss in helical structure of the major coat protein as previously reported (Manning *et al* 1983 Biochem. and Biophys. Res. Comm. **112**:349-355). However, our data suggest that the conformations of the coat protein in I-forms and spheroids are very similar to each other which is in disagreement with the previous results.

M-Pos250 ANTISECRETORY PEPTIDE ISOLATED FROM PORCINE HEART INHIBITS INTESTINAL Cl SECRETION. Scott M. O'Grady and Paul J. Wolters, Department of Veterinary Biology, 295 Animal Science/ Veterinary Medicine Building, University of Minnesota, St. Paul, MN 55108.

A heat stable, low molecular weight peptide was isolated from porcine heart that inhibited vasoactive intestinal polypeptide (VIP) and ionomycin (a Ca ionophore) stimulated Cl secretion across the rat ileum. Tetrodotoxin (TTX), a neuronal conduction blocker, had no effect on the ability of the peptide to inhibit Cl secretion suggesting that submucosal nerves were not involved in mediating the antisecretory activity of this peptide. Activity was found in extracts of the right and left atria and in the ventricles of the heart. The antisecretory effect of the peptide was not mimicked by atrial natriuretic factor (ANF) or by putative antisecretory factors (neuropeptide-Y, somatostatin, enkephalin and norepinephrine) suggesting that cardiac antisecretory peptide (CAP) is a unique antisecretory peptide. These results suggest that through the release of CAP, the heart may potentially regulate intestinal fluid secretion and consequently the volume and composition of the extracellular fluid.

M-Pos251 METABOLISM AND TRANSPORT OF FLUORESCENTLY-LABELLED PHOSPHOLIPIDS IN CULTURED HUMAN COLON CARCINOMA CELLS (CACO-2). Celestia L. Pryor and Ronald T. Borchardt, Pharmaceutical Chemistry Dept., Univ. of Kansas, Lawrence, KS.

Human colon carcinoma cells (Caco-2) become polarized with distinct apical and basolateral membranes when grown in culture on transwells (Raub et al, FASEB J. 2, 2539, 1988). This system is presented as a reasonable 'in vitro' model for the intestinal epithielium. In this study we follow the uptake and subsequent fate of a related series of fluorescent 6 and 12 carbon (C_6 and C_{12}) sn-2 acyl chain 4-nitrobenzo-2-oxa-1,3-diazol (NBD) phospholipid analogues. These compounds are presented to the apical membrane as 20 mol% in dioleoylphosphatidylcholine (DOPC) liposomes and the metabolic products are monitored by a fluoresent HPLC assay (Martin and Pagano, Anal. Biochem. 159, 101, 1986). C_6-NBD-phosphatidic acid (PA) taken up by the Caco-2 cells is metabolised to C_6-NBD-diglyceride, -triglyceride (TG), and -phosphatidylcholine (PC). The newly synthesized phospholipid is not transported out of the cell while some of the other products (including TG)do appear on the basolateral side. C_{12}-NBD-PA gives the same C_{12}-labelled products. The C_6- and C12-NBD-fatty acids, respectively, are formed by phospholipase A_2 cleavage of the sn-2 acyl chain. When C_6-NBD-fatty acid is complexed to BSA and fed to the apical membrane, the transport to the basolateral side is markedly reduced by lowering the temperature, perhaps indicating an endocytotic pathway. C_6- and C_{12}-NBD-phosphatidylethanolamine (PE) and -PC are also incorporated into the cells where the labelled TG and fatty acid are produced. Based on these results, this system appears to be a useful model for lipid transport and metabolism. (Supported by a grant from The Upjohn Company).

M-Pos252 REAL-TIME MEASUREMENT OF OSMOTIC AND DIFFUSIONAL WATER TRANSPORT IN THE VASOPRESSIN-SENSITIVE KIDNEY COLLECTING TUBULE MEASURED BY QUANTITATIVE RATIO IMAGING. K. Fushimi, James A. Dix and A.S. Verkman. Cardiovascular Research Inst., Univ. of Calif., San Francisco.

Regulation of water transport in the mammalian collecting tubule by vasopressin involves a cycling of intracellular membranes containing water channels to and from the apical surface. Isolated perfused cortical collecting tubules from rabbit were perfused at 5-50 nl/min with buffers containing impermeant fluorophores; fluorescence along the tubule lumen was monitored by quantitative imaging using a SIT camera. For measurement of osmotic water permeability (P_f), tubules were perfused with volume-sensitive and insensitive fluorophores (fluorescein sulfonate and rhodamine-dextran) having different fluorescence spectra. P_f was determined in response to a 120 mOsm bath-to-lumen osmotic gradient from tubule geometry, lumen perfusion rate and the dissipation of osmotic gradient along the tubule given by the ratio image of the two fluorophores. For measurement of diffusional water permeability (P_d), tubules were perfused with H_2O/D_2O-sensitive and insensitive fluorophores (aminonapthalenetrisulfonic acid and rhodamine-dextran) in D_2O and bathed in an isosmotic H_2O buffer. P_d was determined from tubule geometry, lumen perfusion rate and the dissipation of the diffusional water gradient along the tubule given by the ratio image. P_f and P_d were fitted by non-linear regression assuming axial homogeneity. P_f increased from 15 x 10^{-4} cm/s to 280 x 10^{-4} cm/s with vasopressin (250 μU/ml); P_d increased from 7 x 10^{-4} cm/s to 23 x 10^{-4} cm/s with vasopressin (37°C). These results are in agreement with values reported by radioactive tracer methods. This new method provides a real-time approach for measurement of water permeability in perfused tubules with improved accuracy over previous methods because the full spatial profile of osmotic or diffusional gradient is measured.

M-Pos253 EXTREMELY HIGH WATER PERMEABILITY IN VASOPRESSIN-INDUCED ENDOCYTIC VESICLES FROM TOAD URINARY BLADDER. Lan-Bo Shi and A.S. Verkman (Intro. P.-Y. Chen). CVRI, UCSF, CA 94143.

The regulation of transepithelial water permeability in toad urinary bladder is believed to involve a cycling of endocytic vesicles containing water transporters between an intracellular compartment and the cell luminal membrane. Endocytic vesicles from luminal membrane were labelled in the intact toad bladder with the impermeant marker 6-carboxyfluorescein (6CF). A microsomal preparation containing labelled endocytic vesicles was prepared by cell scraping, homogenization and differential centrifugation. Osmotic water permeability (P_f) was measured by a stopped-flow fluorescence technique in which microsomes were subject to an inward sucrose gradient; the time course of endosome volume was inferred from the time course of 6CF fluorescence self-quenching. Endocytic vesicles were prepared from toad bladders with hypoosmotic lumen solution containing 6CF treated with serosal vasopressin at 23°C (group A) and 2°C (group B), and bladders handled identically but without vasopressin (group C). Stopped-flow results in all 3 groups showed a slow rate of CF fluorescence decrease (exponential time constants 1.0-1.7 s) indicating a component of non-endocytic 6CF entrapment into sealed vesicles. However in vesicles from group A, there was a very rapid 6CF fluorescence decrease (time constant 10.2±0.1 ms, 60 mOsm gradient, SEM, 14 preparations) with P_f >0.1 cm/s (18°C, for small osmotic gradients) and activation energy of 3.9±0.8 kcal/mole. The rapid fluorescence decrease was absent in vesicles in groups B and C. These results demonstrate the presence of functional water transporters in vasopressin-induced endocytic vesicles from toad bladder, supporting the hypothesis that water channels are cycled to and from the luminal membrane. P_f in the vasopressin-induced endocytic vesicles is the highest P_f reported for any biological or artificial membrane.

M-Pos254 MEMBRANE FLUIDITY MODULATES THE Cl CONDUCTANCE IN PANCREATIC ZYMOGEN GRANULES. K Gasser and U Hopfer. Dept. Physiol & Biophys, CWRU, Cleveland, OH.

Pancreatic zymogen granule membranes contain transport pathways for Cl/anion exchange, Cl conductance, and K conductance. These pathways are responsible for the primary fluid production associated with exocytotic macromolecular secretion. The mechanisms employed for their regulation are not completely understood; however, one factor may be the modulation of granule membrane fluidity. In particular, the Cl conductance was found to be highly sensitive to benzyl alcohol promoted changes in membrane order. Transport measurements are based on the half-time for lysis of suspended granules after addition of the electrogenic K ionophore valinomycin. Chloride conductance measured by this method displays a dose-response increase in transport rate, reaching a 12-fold increase with 40 mM benzyl alcohol. This transport retains anion selectivity with a sequence of SCN~I > Br > acetate > Cl > isethionate > SO_4 >> gluconate. In addition, benzyl alcohol had no effect on granules suspended in nonionic solutions. Decreasing the temperature from 37°C to 17°C reverses the benzyl alcohol induced increase in transport, causing a 10-fold reduction in the transport rate; however, the selectivity sequence remains the same. Furthermore, cholesterol loading causes a decrease in fluidity and is associated with a 3-fold rate reduction. These results suggest that fluidity could have a physiologically relevant role in the control of granule ionic permeability. (Support: NIH DK25170; Cystic Fibrosis Foundation Z0298).

M-Pos255 COLD INHIBITS FAST SODIUM-CURRENT OVERSHOOT IN R.PIPIENS SKIN.
T. Hoshiko, R. Ambigapathy and S. Machlup. Dept. of Physiology & Biophysics and Dept. of Physics, Case Western Reserve University, Cleveland, OH 44106.

Relaxation of sodium-current overshoot upon sudden exposure of apical surface to high [Na] is thought to be due to self-inhibition of amiloride-sensitive Na-selective channels. This hypothesis was tested by examining the effect of low temperatures on transient and steady-state current following sudden increase in apical [Na] from 0.1 to 120 mM. The basolateral surface was bathed in sulfate Ringer's (in mM: 118 Na, 2 K, 0.5 Ca, 5 tris, pH 8). K was replaced with Na in the apical solution and tris was used to substitute for Na. The fast solution changes were made manually using a syringe and were completed in less than 0.05 sec. At 19 C, peak current was 70% greater than the steady-state value, whereas with temperatures below 4 degrees C the peak was less than 10% greater than the steady-state value. The rate of current relaxation from the peak was greatly slowed in the cold. The stimulatory effect of BIU (benzimidazolyl-urea) on short-circuit current, which at room temperature acts within seconds, was delayed to minutes. Our study shows that the peak overshoot current is much more sensitive to reduced temperature than the steady-state current, indicating that the rate-limiting step governing the overshoot cannot be identical to that governing the steady-state current.

M-Pos256 Luminal Responses to Bradykinin on the Canine Tracheal Epithelium: Effects of BK Antagonists. P. K. Rangachari, B. Donoff, R. J. Vavrek and J. M. Stewart. Intestinal Diseases Research Unit, Dept. of Medicine, McMaster Univ. Hamilton Ont. Canada and Dept. of Biochemistry, Univ. of Colorado Health Sciences Center, Denver, Colorado 80262, U.S.A.

Rapid responses are elicited on the open-circuited canine tracheal epithelium by the luminal addition of tachykinins and bradykinin (BK). Particularly dramatic is the rapid decrease in transmucosal P.D. (the "DIP"), which reflects a selective, transient increase in anion conductance (1). That specific receptors were involved was suggested on the basis of agonist potencies and cross-tachyphylaxis (2). We have now used a variety of BK antagonists to alter the responses to BK. All experiments were done using the open-circuited tracheal preparation. "DIPS" were obtained using 10^{-7} M concentrations of BK, lysine Bradykinin (lys-BK) and Substance P (SP).

Of the antagonists tested, $DPhe^{1,7},Thi^{5,8}$ BK (B4158), $DPhe^{2,7}$ BK (B4404), $DPhe^{7},Hyp^{8}$ BK (B5092) were ineffective. However, $DArg^{0},Hyp^{3},Thi^{5,8},DPhe^{7}$ BK (B5630) produced reversible dose dependent inhibition of "DIPS" elicited in response to BK and lys-BK. The estimated IC_{50} was 2.82×10^{-8} M. This compound had no agonist activity even at the highest concentrations tested, nor did it affect the responses to SP. We have shown earlier that $Des\text{-}Arg^{9}$ BK (BK_1 agonist) produces no responses on the tracheal epithelium(3). The studies shown here, suggest that receptors involved are of the BK_2 variety.

1. Rangachari, M^{c}Wade (1986) B.B.A. 863, 305 2. Rangachari et al (1987) Reg. Peptides 18, 101 3. Rangachari et al (1988) Reg. Peptides 21, 237

M-Pos257 THE REGULATION OF A CHLORIDE CHANNEL IN A DISTAL NEPHRON CELL LINE. Y. Marunaka & D. C. Eaton, Dept. of Physiol., Emory Univ. Med. Sch., Atlanta, Georgia. To examine the regulation of a renal chloride channel, we studied the effects of varying the cytosolic Ca concentration and, separately, the effect of cyclic AMP on single chloride channels. The chloride channels were characterized by a small unit conductance (3pS) and were originally observed in cell-attached patches from the apical membrane of the distal nephron cell line, A6, which had been cultured on permeable supports. The I-V relationship for channels from cell-attached patches or inside-out patches with low concentrations of Ca (10^{-6}M) in the bath strongly rectified with no inward current at potentials more negative than E_{Cl} but with increasing outward current above E_{Cl}. However, when inside-out patches were exposed to higher concentrations of Ca on the cytosolic surface the rectification was decreased until at high cytosolic Ca (8×10^{-4}M) the I-V relationship was linear. Another effect of increasing cytosolic Ca was to increase the open probability of the channel by reducing the closing rate of the channel at all potentials. The effect of cytosolic Ca on the opening rate was more complex. An increase in cytosolic Ca decreased the opening rate at patch potentials of -70 mV but increased the opening rate at +70 mV. When dibutyryl-c-AMP is applied to cells on which cell-attached patches have been made, the open probability of Cl^- channels within the patch increases. Also, c-AMP increases the steepness of the open probability vs voltage relationship of the Cl^- channels. The c-AMP-induced alterations in open probability are attributable to an increase in the opening rate without any change in the closing rate. On the other hand, c-AMP does not affect the single channel conductance or the shape of the I-V relationship.

M-Pos258 DIFFERENT TYPES OF CHLORIDE CHANNELS IN A DISTAL NEPHRON CELL LINE. Y. Marunaka & D. C. Eaton (Sponsored by R. F. Abercrombie), Dept. of Physiol., Emory Univ. Med. Sch., Atlanta, Georgia. We used single channel recording methods to examine the conductive pathways in the apical membrane of a distal nephron cell line (A6). In patches formed on the apical membrane there are two different types of single channel events which can be attributed to Cl^- channels. In cell-attaced patches, one of these has a single channel conductance of 3 pS, while the other has a single channel conductance of 8 pS. The smaller conductance channel (3 pS) has a relatively high selectivity to Cl^- ($P_{Cl}/P_{Na} = 11$), while the larger conductance channel (8 pS) has a lower selectivity to Cl^- ($P_{Cl}/P_{Na} = 6$). In cell-attached patches, the current from the 3 pS Cl^- channel outwardly rectifies, while the 8 pS Cl^- channel has a linear I-V relationship. The 3 pS Cl^- channel has one open state and one closed state, while the 8 pS Cl^- channel has one open state and two closed states. The open probability of the 3 pS Cl^- channel was very low (always less than 0.1) and voltage-dependent (increasing with depolarization from close to zero with no applied potential to less than 0.1 at +140mV), while the open probability of the 8 pS Cl^- channel was large (about 0.8) and not voltage-dependent. The closing and opening rates of the 3 pS Cl^- channel were decreased and increased respectively in response to depolarization. On the other hand, the closing rate of the 8 pS Cl^- channel was decreased when the membrane was depolarized, but the opening rates were unchanged.

M-Pos259 **PLANAR BILAYER RECORDING OF CHLORIDE CHANNELS FROM SKELETAL MUSCLE AND AIRWAY EPITHELIAL CELLS: SIMILARITIES AND DIFFERENCES.** Hector H. Valdivia, William P. Dubinsky and Roberto Coronado. (Intr. by H. Strauss). Department of Physiology and Molecular Biophysics, Baylor College of Medicine; and Department of Physiology and Cell Biology, The University of Texas Health Science Center at Houston, Houston, Texas 77030.

Membranes vesicles from T-tubules of rabbit skeletal muscle and apical-membranes from bovine trachea were reconstituted into planar lipid bilayers. Based upon frequency of presentation, anion channels of 50 pS and 71 pS in symmetrical 150 mM NaCl appear to be the major contributors of Cl^- current in skeletal muscle and airway epithelium, respectively. Spontaneous openings could be elicited in both preparations, but phosphorylation with the catalytic subunit of the cAMP-dependent protein kinase plus ATP was required to avoid rundown of epithelial channels. Channel activity following phosphorylation can be conveniently used to test putative blockers, toxins, or modulators of chloride secretion. The stilbene disulfonate derivative DIDS (25 μM added to the external side) decreased mean open current and channel lifetime in the skeletal channel and completely blocked currents in the epithelial channel. In both tissues, channels displayed a strong voltage-dependence, increasing open probability (Po) at negative voltages. In skeletal muscle, DIDS shifted the Po vs voltage curve by approximately 120 mV towards positive potentials. Neither channel is Nernst selective for Cl^- over Na^+ (P_{Cl}/P_{Na}<15) nor sensitive to [Ca^{++}]. Supported by NIH, AHA, and MDA.

M-Pos260 **HYPOSMOTIC STIMULATION OF Cl^- EFFLUX AND ACID SECRETION BY ISOLATED GASTRIC PARIETAL CELLS OF THE RABBIT.** T.J. Sernka, Dept. of Physiology and Biophysics, Wright State University, Dayton, OH 45435.

A hyposmotic medium of 200 mOsm/kg has been found to stimulate acid secretion by isolated gastric glands of the rabbit (FASEB J. 2:A1276, 1988). Since the glands contain both parietal cells that secrete acid and non-parietal cells that can release histamine, a potent secretagogue, the cellular mechanism of hyposmotic acid stimulation could not be resolved using glands. Therefore, gastric cells were prepared from gastric glands by successive incubations in pronase and collagenase to test the responses of isolated cells to hyposmolality. As determined by the accumulation of the weak base, ^{14}C-aminopyrine, corrected for extracellular ^{14}C-inulin space, acid secretion by the mixed gastric cells incubated in hyposmotic medium, 200 mOsm/kg, was more than twice that of paired cells incubated in isosmotic medium. The hyposmotic response of gastric cells peaked at 15 min, as was found for gastric glands. The response of cells to 250 mOsm/kg medium was intermediate. The hyposmotic stimulation was sustained by either glucose or pyruvate as substrate and was abolished by substitution of N_2 for O_2 gas. These results with mixed gastric cells indicate that hyposmolality stimulates the parietal cell to secrete acid by a direct action rather than by histamine mediation. This direct action may involve an increase in apical Cl^- conductance. Parietal cells of about 90% purity were prepared by the Nycodenz density gradient method and equilibrated with ^{36}Cl for 1 hr prior to addition of fresh isosmotic or hyposmotic medium. ^{36}Cl efflux from hyposmotically incubated parietal cells was nearly 50% greater than that of paired cells bathed by isosmotic medium of the same Cl^- concentration during 1 to 5 min incubations.

M-Pos261 **PATCH-CLAMP STUDIES OF K^+ AND Cl^- CHANNELS AT THE APICAL MEMBRANE OF KIDNEY PROXIMAL TUBULE CELLS IN PRIMARY CULTURE.** L. Parent, L. Dubé, G. Roy, and R. Sauvé. Groupe de Recherche en Transport Membranaire. Université de Montréal. Montréal, Qué. H3C 3J7.

Patch-clamp experiments were performed in kidney proximal tubule cells in primary culture. In a separate study, kidney proximal nature of the cell culture was asserted by i) the specific enzymatic activities of alkaline phosphatase; gamma glutamyl transpeptidase; and leucine amino peptidase; and ii) the specific binding of the antibody of enkephalinase (Blais and Berteloot, 1987). Two channels (K^+ channel and anionic channel) were characterized at the apical membrane of semi confluent cells. The K^+ channel is a calcium-and voltage-activated K^+ channel, K(Ca). Its single-channel I/V curve is linear with a slope conductance of 195 pS (SD=10, n=5) in symmetrical 150 mM KCl. Channel activity increases as a function of internal calcium (0.1-10 μM) and membrane potential in a bell-shape manner. For 10 μM <Cai> 2 μM, channel activity first increases between -100 to 0 mV and then decreases between 0 to 100 mV. Under physiological conditions, the K^+ channel is likely to be closed at the resting potential. In contrast, the anionic channel behaves as an outward rectifier in symmetrical 150 mM KCl. Slope conductance is 41 pS (SD=3, n=3) as measured between 40 and 100 mV. Anionic channel activity is slightly more important at negative potentials. The role of these two channels in cell volume regulation was investigated. Cell-attached experiments were performed where the external medium was perfused with a hypo-osmotic medium. K(Ca) and the anionic channel are clearly sequentially activated as the cells undergo volume regulation. L. Parent and L. Dubé are beneficiary of fellowships from the Medical Research Council of Canada.

M-Pos262 INTERACTION OF CALMODULIN WITH Ca^{2+}-ATPase.

T. Bzdega*, K. Nemcek+, J.D. Johnson+, and Kosk-Kosicka.* University of Maryland, School of Medicine, Baltimore, Md,* and State Ohio University, Physiological Chemistry, Columbus, OH.+.

The fluorescent spinach calmodulin derivative, MIANS-CaM (2-4-maleimidoanilino)-naphthalene-6-sulfonic acid-calmodulin) was used to investigate calmodulin interaction with the purified, $C_{12}E_8$ solubilized erythrocyte Ca^{2+}-ATPase. Previous studies showed that the Ca^{2+}-ATPase exists in equilibria between monomeric and oligomeric forms; we report here that MIANS-CaM binds to both enzyme forms, with a ~50% fluorescence enhancement. These findings confirm our previous observation that the oligomers retain their ability to bind calmodulin, even though they are fully activated in the absence of calmodulin. Activation of monomers is half-maximal at 5 nM MIANS-CaM. The interaction of MIANS-CaM with the enzyme is Ca^{2+}-dependent, and the $K_{1/2}$ values are 0.75 and 0.2 μM Ca^{2+} for the monomeric and oligomeric enzyme, respectively. The difference in Ca^{2+} affinities suggests that calmodulin conformation is different depending upon which Ca^{2+}-ATPase form it is bound to. Stoichiometry measurements of monomers versus oligomers using MIANS-CaM are in progress.
Supported by NIH GM 37143* & AHA 880832* and AM 33727+.

M-Pos263 TB^{3+} LUMINESCENCE AND DIFFUSION-ENHANCED ENERGY TRANSFER IN DOC PURIFIED SARCOPLASMIC RETICULUM VESICLES C. D. Sprowl and D. D. Thomas Dept. of Biochemistry, Univ. of Minnesota Medical School, Mpls., MN 55455 Intro. by E. Ackerman

We have observed the fluorescence lifetime characteristics of Tb^{3+} in the presence of deoxycholate (DOC)-purified skeletal sarcoplasmic reticulum (DOCSR) vesicles. In the absence of DOCSR, Tb^{3+} exhibits a monoexponential fluorescence decay with a lifetime of ~400 us. In the presence of DOCSR at ratios of Tb^{3+}:HA-Ca-BS (high-affinity Ca^{2+}- binding sites) over the range of 0.1:1 to 4:1, Tb^{3+} exhibits a triexponential decay. The lifetimes and their associated amplitudes are approximately: 90us (5%), 710us (65%), and 1200us (30%). None of the these lifetimes is the same as that of Tb^{3+} free in solution. The amplitudes (mole fractions) and lifetimes are constant over this ratio range. This suggests that Tb^{3+} is bound in three environments. This was an unexpected finding, since our original assumption was that Tb^{3+} would behave as a Ca^{2+} analogue, as it does in some small water-soluble Ca^{2+}-binding proteins, and thus bind specifically to the two high-affinity Ca^{2+}-binding sites. Therefore we expected to observe two bound Tb^{3+} populations at ratios <1:1 and an additional free population at ratios >1:1. Also, each lifetime is sensitive to the presence of the resonance energy acceptor Co(III)EDTA. These data indicate the presence of at least three bound populations of Tb^{3+}, all accessible to a small negatively charged acceptor. Furthermore, these data suggest that Tb^{3+} does not behave as a Ca^{2+} analogue in that it may bind to more than two sites on the vesicles even at ratios well below 1:1. The results of our study of non-specific Tb^{3+} binding will be presented in an oral report.

M-Pos264 THE EFFECT OF Li^+ ON Na-Ca EXCHANGE ACTIVITY, KINETICS, AND STOICHIOMETRY MEASUREMENTS IN CARDIAC SARCOLEMMAL VESICLES. Rebecca S. Keller and Calvin C. Hale, Dept. of Biomedical Sciences and the John M. Dalton Research Center, Univ. of Missouri-Columbia, Columbia, MO 65211.

We have examined the effects of Li^+ on Na-Ca exchange in cardiac sarcolemmal (SL) vesicles. Li^+ inhibited Na-dependent Ca^{2+} uptake in SL vesicles in a dose dependent manner (Ca_o=12 μM). External Li^+ (160 mM) maximally inhibited the initial rate of exchange by 49.8% ± 2.9% (S.E.) (n = 6) compared to K^+ or choline$^+$ (Ca_o=12 μM). In other experiments, Na-dependent Ca^{2+} uptake was inhibited 18.3% (n=2) by external Li^+ compared to uptake in the presence of external K^+ or choline$^+$ (Ca_o=100 μM). Neither internal Li^+ or K^+ were capable of substituting for Na^+ in driving Ca^{2+} uptake in SL vesicles. Na-dependent Ca^{2+} efflux (Ca_i=100 μM) was not inhibited by 160 μM internal Li^+. Kinetic determinations for Na-dependent Ca^{2+} uptake indicated that external Li^+ increased Km for Ca^{2+} (96.3 μM) compared to K^+ and choline$^+$ (25.5 and 22.9 μM respectively) while Vmax (1.4, 1.2, and 1.1 nM/mg protein/sec respectively) remained unchanged suggesting Li^+ may have acted as a competitive inhibitor of the exchange process. Using a previously described thermodynamic approach (JBC 259:7733-7739, 1984) it was concluded that the inhibitory effect of Li^+ (Ca_i=Ca_o=100μM) did not alter the experimentally derived exchange value of $3Na^+$ for 1 Ca^{2+}. In those experiments, since Li^+ did not affect the Na^+ equilibrium potential required to offset potential driven Ca^{2+} movements, it is likely that Li^+ did not substitute for transported Na^+ in the exchange process. (supported by NSF DCB-8602234 and Am Heart Assoc-MO Affiliate)

M-Pos265 THE EFFECT OF THE BASIC POLYPEPTIDE MELITTIN ON ENZYMATIC ACTIVITY AND PROTEIN DYNAMICS OF THE Ca-ATPase IN SKELETAL SR. Woubalem Birmachu, Franz L. Nisswandt, and David D. Thomas. Department of Biochemistry, University of Minnesota, Minneapolis, MN, 55455.

We have studied the effect of the small basic peptide, melittin, on enzymatic activity and protein dynamics of the Ca-ATPase in skeletal SR using time-resolved phosphorescence. Melittin decreases the Ca-ATPase activity with 50% inhibition occurring at a total concentration of 0.32 mg melittin/mg SR protein. The time-resolved phosphorescence anisotropy decay of the Ca-ATPase labeled with erythrosin-5-isothiocyanate indicates that protein mobility becomes more restricted in the presence of melittin. At 4°C, in the absence of melittin, the phosphorescence anisotropy is characterized by three correlation times: ϕ_1 and ϕ_2 with values of 7 and 70 μs resulting from the rotational motion of ATPase monomers and a third correlation time ϕ_3 of approximately 280μs, that is more characteristic of the motion of an ATPase oligomer. The amplitude corresponding to ϕ_2 decreases with increasing melittin concentration, while the values of ϕ_1 and ϕ_2 remain constant. The amplitude of ϕ_1 remains constant, indicating that this correlation time is most likely due to protein segmental motion. ϕ_3 increases in value and decreases in amplitude while the residual anisotropy increases, indicating the progressive formation of higher oligomers. The effect of melittin on protein dynamics correlates with the inhibition of ATPase activity consistent, with previous reports that protein aggregation inhibits Ca-ATPase activity.

M-Pos266 PROTEIN AND LIPID DYNAMICS IN CARDIAC AND SKELETAL SR STUDIED BY TIME-RESOLVED FLUORESCENCE AND PHOSPHORESCENCE. Woubalem Birmachu and David D. Thomas. Department of Biochemistry, University of Minnesota, Minneapolis, MN, 55455.

Unlike the skeletal ATPase, the activity of the cardiac enzyme is regulated through the phosphorylation of an endogenous protein that is postulated to interact with it. In order to determine the role of protein-protein interaction in cardiac SR, we have made a comparative study of the rotational dynamics of the Ca-ATPase in cardiac and skeletal SR, using time-resolved phos phorescence anisotropy of the erythrosin-5-isothiocyanate-labeled enzymes. At 4°C, the phosphor escence anisotropy of both preparations is described by a three exponential function plus a constant, with two correlation times, ϕ_1 and ϕ_2, characteristic of the rotational motion of the monomer and a third tht is consistent with the rotation of an oligomer. The amplitudes corres ponding to ϕ_1 and ϕ_2 in cardiac and skeletal SR are identical within experimental error. The amplitude corresponding to ϕ_3 is lower in cardiac SR than in skeletal SR . The cardiac ATPase has a significantly higher residual anisotropy than the skeletal enzyme, r_∞/r_0 = 0.585 ± 0.037 and 0.227 ± 0.022 respectively. In order to determine the role of the lipid phase in restricting protein mobility in cardiac SR, we measured the fluorescence anisotropy of DPH in SR vesicles. The residual fluorescence anisotropy of DPH is significantly higher in cardiac SR, consistent with the higher cholesterol content in this preparation. The role of protein-protein interactions and lipid fluidity in modulating protein dynamics and enzymatic activity in the two tissues will be addressed.

M-Pos267 SODIUM-DEPENDENCE OF L-GLUTAMATE INFLUX IN BARNACLE MUSCLE. Lyle W. Horn, Dept. of Physiology, Temple Univ. School of Medicine, Philadelphia, PA 19140

L-Glutamate (GLU) influx was measured in internally dialyzed, metabolically inhibited, single fibers under zero trans (Na^+ and GLU) conditions at 10°C and constant membrane potential. GLU influx in normal artificial sea water (ASW) is a simple hyperbolic function of GLU concentration with a $K_{\frac{1}{2}}$ for GLU of 0.35 mM. Influx is a linear function of GLU concentration, up to 10 mM GLU, in 0 Na^+ 0 Ca^{2+} ASW. When influx is measured at 10 mM GLU and different Na^+ concentrations (2 to 435 mM) the Eadie-Hofstee plot of the leak-corrected data is linear, giving a $K_{\frac{1}{2}}$ for Na^+ of 98 mM. The corresponding Hill plot is also linear, with a slope of 1.02. Results are consistent with a Na^+-dependent GLU transporter which requires only one Na^+ ion for transport and functions as a bireactant system. Eadie-Hofstee plots for 2mM and 435 mM Na^+ ASW's are least consistent with a random binding process but are consistent with an ordered binding mechanism.

(Supported by NIH Grant No. NS-18868)

M-Pos268 **PROBING THE MECHANISM OF H+/LACTOSE SYMPORT BY SITE - DIRECTED MUTAGENESIS.** ***Paul D. Roepe* and H. Ronald Kaback, Dept. of Biochemistry, Roche Institute of Molecular Biology, Nutley, NJ 07110.***

The *lac* permease of *E. coli* catalyzes the coupled translocation of a single galactoside molecule with a single H^+ across the plasma membrane, and experiments utilizing site-directed mutagenesis demonstrate that Arg302 (putative helix IX), His322 (putative helix X) and Glu325 (putative helix X) play a critical role in the mechanism, possibly as components of a H^+ relay [Kaback, H. R. (1987) *Biochemistry 26*, 2071]. Recent experiments show that lactose exchange and substrate binding become highly pH dependent when Glu 325 is replaced with Asp, thereby providing a strong indication that protonation of Glu325 in the wild-type permease is essential for lactose exchange. In addition, the Tyr residues in the permease were replaced individually with Phe, and five of the mutations have a significant effect on permease activity. Two of the mutations (Y26F and Y336F) completely abolish all modes of activity and significantly raise the K_D for ligand, one (Y236F) appears to uncouple H^+ from lactose translocation, and two mutations (Y350F and Y382F) decrease turnover of the permease by 60% during active transport, but do not significantly effect equilibrium lactose exchange. Finally, three different five-residue sequences that exhibit homology to a sugar binding site in the crystal structure of a periplasmic sugar-binding protein [Quiocho, F.A. (1986) *Ann. Rev. Biochem. 55*, 287] were extensively mutagenized. Binding and transport experiments are consistent with the notion that two of these regions (R135-E139 and K335-S339) may be involved in substrate binding in the permease.

(* Supported by a Jane Coffin Childs Postdoctoral Fellowship).

M-Pos269 SIMULTANEOUS BIDIRECTIONAL MAGNESIUM ION FLUX MEASUREMENTS IN SINGLE BARNACLE MUSCLE CELLS BY MASS SPECTROMETRY. J. G. Montes*, R. A. Sjodin*, A. L. Yergey and N. E. Vieira. *Dept. of Biophysics, University of Maryland School of Medicine, Baltimore, MD, and Laboratory of Theoretical and Physical Biology, NICHD, National Institutes of Health, Bethesda, MD.

Stable isotopes of Mg were used to measure bidirectional magnesium ion fluxes in single barnacle giant muscle fibers immersed in Na-free, tris-substituted isosmotic media. Measurements were made using a novel approach that entailed thermal ionization mass spectrometry (TIMS) in conjunction with atomic absorption spectroscopy. Kinetic relations based on a first-order model were developed that permit the determination of unidirectional rate coefficients for Mg influx, k_i, and efflux, k_e, in the same experiment from knowledge of initial conditions and the initial and final ratios of $^{26}Mg/^{24}Mg$ and $^{25}Mg/^{24}Mg$ in ambient solutions: it is noteworthy that determination of such ratios inside the fibers was not required. The required ratios for ambient solutions were determined for three values of the external Mg ion concentration; 5 mM, 25 mM, and 60 mM. At the concentration $[Mg^{+2}]_o$ = 5 mM, k_i and k_e were about equal at a value of 0.01 min^{-1}. At the higher values of $[Mg^{+2}]_o$, the values of k_e increased with $[Mg^{+2}]_o$, suggesting possible saturation, while the values of k_i remained essentially constant. As could be expected on the basis of a constant k_i, the initial influx rate varied in direct linear proportion to $[Mg^{+2}]_o$, and was 11.8 pmole/cm^2sec when $[Mg^{+2}]_o$ was 5 mM; however, the initial efflux rate appeared to increase nonlinearly with $[Mg^{+2}]_o$, varying from 13.4 pmole/cm^2sec ($[Mg^{+2}]_o$ = 5 mM) to about 80 pmole/cm^2sec ($[Mg^{+2}]_o$ = 60 mM). The results are consistent with a model that assumes Mg influx to be mainly an electrodiffusive inward leak with P_{Mg} = 0.07 cm/sec and Mg efflux to be almost entirely by active transport processes. Where comparisons can be made, the rate coefficients determined from stable isotope measurements agree with those previously obtained using radioactive Mg.

M-Pos270 ENERGETICS OF ACTIVE TRANSPORT IN INVERTED MEMBRANE VESICLES. Mei H. Dung and Chang-Hwei Chen, Wadsworth Center for Laboratories and Research, New York State Department of Health, Albany, New York 12201

Employing microcalorimetry in combination with flow dialysis and oxygen uptake measurements, energetic parameters of the formation of a proton electrochemical potential ($\Delta\tilde{\mu}_{H^+}$) across inside-out (ISO) membranes were determined. ISO membranes prepared from Escherichia coli cells are inverted (interior positive and acidic) with respect to RSO membranes (interior negative and alkaline). The inside of ISO membranes exhibits a pH of 6.70 against 7.50 in the external medium, as the membranes are coupled with an electron donor (D-lactate). This pH difference corresponds to a proton gradient (ΔpH) of 46.4 mV. The electrical potential ($\Delta\Psi$) across ISO membranes is determined as 63.3 mV. The sum of the proton gradient and the electrical potential gives a $\Delta\tilde{\mu}_{H^+}$ of 110 mV. Microcalorimetric schemes have been employed to measure the heat change (ΔQ_m) associated with the formation of $\Delta\tilde{\mu}_{H^+}$ across membranes and thus confirm its formation from the thermochemical point of view. The determined enthalpy (ΔH_m), the free energy (ΔG_m) and the entropy (ΔS_m) changes were compared with those previously obtained in RSO membranes and reconstituted proteoliposomes. Identical positive signs for the energetic parameters in these membranes indicate that the characteristic of $\Delta\tilde{\mu}_{H^+}$ and the mechanism for its formation are analogous, regardless of the polarities across the membranes. The efficiency in the free energy transfer from the oxidation reaction to the formation of $\Delta\tilde{\mu}_{H^+}$ is essentially the same in both RSO and ISO membranes, while the enthalpy transfer is much lower in ISO membranes than in RSO membranes.

M-Pos271 Kinetics of Bumentanide-sensitive Cl influx. G.E. Breitwieser, Dept. of Physiology, Johns Hopkins University School of Medicine, Baltimore, MD 21205, J.M. Russell and A.A. Altamirano, Dept. of Physiology and Biophysics, University of Texas Medical Branch, Galveston, TX 77550.

The effects of varying the external concentrations of Na, K and Cl, and the internal concentrations of Cl and ATP on the bumentanide-sensitive (B-S) Cl influx were studied in internally dialyzed squid giant axons. B-S Cl influx increased as a saturable function as $\{K\}_o$ was varied over the range 0-100 mM, $K_{0.5}$ = 11 ± 3 mM, V_{max} = 64 ± 6 pmol/cm^2·sec, Hill coefficient (N) = 0.94 ± 0.2 (32 axons). The $\{Na\}_o$ dependence of B-S influx was determined in the presence of 100 mM $\{K\}_o$ (15 axons): $K_{0.5}$ = 46 ± 14 mM, V_{max} = 61 ± 7 pmol/cm^2·sec, N = 1.2 ± 0.3. The $\{Cl\}_o$ dependence of B-S Cl influx was examined at two $\{K\}_o$ concentrations: 10 mM (near $K_{0.5}$ for $\{K\}_o$) and 100 mM (approaching saturation of $\{K\}_o$). In the presence of 10 mM $\{K\}_o$, B-S Cl influx followed a sigmoidal relationship with $\{Cl\}_o$ (42 axons) with $K_{0.5}$ = 4900 ± 330 mM, V_{max} = 74 ± 42 pmol/cm^2·sec and N = 1.7 ± 0.6. When $\{K\}_o$ was 100 mM (30 axons), the $\{Cl\}_o$ dependence of B-S Cl influx had $K_{0.5}$ = 195 ± 20 mM, V_{max} = 82 ± 4 pmol/cm^2·sec and N = 2.2 ± 0.2. Two Cl_o replacements were used: no significant differences between the fluxes in the presence of gluconate or sulfamate were found. The effect on B-S Cl influx of increasing $\{Cl\}_i$ from 0-200 mM was examined in 36 axons. The $\{Cl\}_i$ inhibition was strongly sigmoidal, with $K_{0.5}$ = 90 mM ($\{K\}_o$ = 100 mM). B-S Cl influx was activated by $\{ATP\}_i$, with $K_{0.5}$ = 84 ± 20 μM, V_{max} = 33 ± 2 pmol/cm^2·sec and N = 1.1 ± 0.3 (41 axons; $\{Na\}_o$ = 425 mM, $\{K\}_o$ = 100 mM and $\{Cl\}_o$ = 561 mM). Supported by NIH NS-11946.

M-Pos272 SODIUM AND PHOSPHORUS MAGNETIC RESONANCE STUDIES OF THE ELECTRIC FISH NARCINE BRAZILIENSIS. R.G. Johnson, Jr. and H. Blum, HHMI, Depts of Med & Physiol, U of Penna, Philadelphia, Pennsylvania 19104.

In vivo studies of the electric organ of the marine elasmobranch Narcine braziliensis have been performed to evaluate the regulation of the Na^+, K^+-ATPase and its effect upon cellular bioenergetics. This unique organ is dependent on a purely glycolytic pathway with stored energy mainly in the form of the phosphogen phosphocreatine (PCr), and with the majority of its metabolic energy consumption due to the sodium pump. The large inward sodium conductance during depolarization of the electrocytes causes the Na^+, K^+-ATPase to pump significant quantities of sodium from the intracellular space after each discharge. The electric organ was discharged by direct electrical stimulation of the electric cortex. This caused immediate utilization of high energy phosphates, due to increased activity of the Na^+, K^+-ATPase, which we monitored in a nondestructive, noninvasive way with 31-P magnetic resonance spectroscopy (MRS). Studies of post-stimulation recovery versus depletion of PCr suggest that the maximum rate of ATP hydrolysis in the post-stimulated tissue in vivo is more than 2 orders of magnitude faster than the basal rate. Concurrent observation of 23-Na MRS after infusion of the shift reagent Dy(TTHA) allowed us to follow temporal changes in the sodium compartments. The intracellular sodium content is maintained at stable concentrations until full depletion of the high energy phosphate intermediates; during this stimulation the average Na^+ flux increases several orders of magnitude to 6 mM/min. After energy depletion large increases of intracellular sodium and commensurate decreases in extracellular sodium occur with continued organ discharge. These studies suggest that the control of the sodium pump is multifactorial and may not be entirely dependent on intracellular sodium concentration alone.

M-Pos273 **POSSIBLE IDENTIFICATION OF A cDNA CLONE FOR THE CARDIAC SARCOLEMMAL Na/Ca EXCHANGE PROTEIN.**

K.D. Philipson, S. Longoni, R. Ward, and B. Scott. Depts. of Medicine and Physiology and the Cardiovascular Research Laboratory, UCLA School of Medicine, Los Angeles, CA 90024-1760 and the Krannert Institute of Cardiology, Indiana Univ., School of Medicine, Indianapolis, IN 45202.

We have previously reported the isolation of the Na/Ca exchanger (MW=70 and 120 kDa) and the production of antibodies to these proteins (Biophys. J., 53,142a, 1988; Philipson et al., BBA, in press). We have now screened a dog ventricle cDNA λgt11 library with these antibodies and have found one positive clone. Antibodies eluted off of the fusion protein produced by this clone react with 70 and 120 kDa protein bands on Western blots. The cDNA insert is 3.2 kb in length and has two internal Eco R1 sites. Probes made from the cDNA insert react with 7 kb poly(A)$^+$RNA on a Northern blot. We are currently using cDNA from this clone in hybrid/selection experiments in conjunction with an oocyte expression system (Longoni et al., AJP, in press) to try to confirm that the clone represents the Na/Ca exchanger.

M-Pos274 INFLUENCE OF MEMBRANE POTENTIAL ON Ca-Ca EXCHANGE FROM NERVE MEMBRANE VESICLES.
Madalina Condrescu, Andrés Gerardi and Reinaldo DiPolo. Centro de Biofísica y Bioquímica, IVIC, Apdo. 21827, Caracas 1020A, Venezuela.
The concept of a Ca-Ca exchange operating through the Na-Ca exchanger has initially been proposed in cardiac muscle (Reuter and Seitz, 1967) and nerve cells (Baker and Blaustein, 1968) based on the existence of a Ca^{2+} efflux, activated by external calcium, in the absence of sodium. Recently, Allen and Baker (1986) have shown in giant axon that Ca-Ca exchange possesses, as Na-Ca exchange, a marked voltage sensibility. On the other hand, it has been reported in cardiac sarcolemma vesicles the existence of a Ca-Ca exchange activity which is stimulated by the presence of monovalent cations (Slaughter et al, 1983). However, the voltage dependence of Ca-Ca exchange has not been investigated yet in an isolated membrane system. In this work, we studied the effect of membrane potential on the squid optic nerve membrane Ca-Ca exchange activity. Vesicles were depolarized or hyperpolarized by using K^+-valinomycin in the presence of 200mM LiCl. This concentration of Li^+ was sufficient to saturate the exchanger's monovalent ion site of chemical activation. The results indicate that depolarization (26 mV, vesicle interior positive) depresses by about 40% the Ca-Ca exchange activity measured at 0mV (equal K^+ concentrations inside and outside the vesicles). On the other hand, hyperpolarization (26 mV, vesicle interior negative) increases Ca-Ca exchange activity by 100% approx. These observations suggest that the voltage dependence of Ca-Ca exchange observed in living cells has been maintained in the membrane vesicle preparation. (Supported by CONICIT, Proyecto S1-1934, NIH, 1R01 HL 39243-01 and TWAS RGBC 87-84).

M-Pos275 Na-Ca AND Na-Na EXCHANGE IN SQUID OPTIC NERVE VESICLES: IS TRANS-CALCIUM AN ESSENTIAL ACTIVATOR OF THE EXCHANGER? Madalina Condrescu, Andrés Gerardi and Reinaldo DiPolo, Centro de Biofísica y Bioquímica, Instituto Venezolano de Investigaciones Científicas, Apartado 21827, Caracas 1020A, Venezuela.
In squid axons, cardiac myocytes and barnacle muscle cells, reverse Na-Ca exchange (Na_i^+-Ca^{2+}) and Na-Na exchange (Na_i^+-Na^+) require the presence of micromolar Ca_i^{2+} (DiPolo and Beaugé 1986, DiPolo and Beaugé 1987, Kimura et al 1986, Rasgado-Flores and Blaustein 1987). This role of internal calcium first described in living cells has been explored in nerve membrane vesicles by investigating the effect on exchange activity (Na_i-Ca_o and Na_i-Na_o) of micromolar concentrations of intravesicular Ca^{2+}. In the presence of a Ca-chelating agent inside the vesicles (2mM EGTA or 10mM HEDTA) the results show: i) a basal level of Na-Ca exchange is observed, presumably due to the inside-out vesicle population and ii) no Na-Na exchange activity is detected in these conditions. In contrast, when Ca^{2+} is present within the vesicles (as Ca.EGTA or Ca.HEDTA) we obtain: i) a stimulation of the Na-Ca exchange activity with an apparent $K_{1/2}$ of 12μM and attaining saturation at 100μM Ca^{2+} and ii) Na-Na exchange activation. Thus, Na-Ca exchange activity in nerve membrane vesicles is stimulated by trans-Ca^{2+} while Na-Na exchange activity requires the presence of trans-Ca^{2+}. These findings suggest that the modulatory effect of internal Ca^{2+} on the Na-Ca exchanger has been preserved in the nerve membrane vesicles preparation. (Supported by CONICIT, S1-1934, NIH 1R01 HL 39243-01 and TWAS RGBC 87-84).

M-Pos276 CHARACTERIZATION OF "REVERSE MODE" Na/Mg EXCHANGE IN DIALYZED GIANT SQUID AXONS. H. Gonzalez-Serratos and H. Rasgado-Flores. Departments of Biophysics and Physiology, University of Maryland School of Medicine, Baltimore, MD 21201.

Active extrusion of Mg^{2+} must occur to account for the low intracellular concentration of this ion ($[Mg^{2+}]_i$). Since ^{28}Mg efflux from injected or dialyzed squid axons depends on the size of the Na gradient across the membrane, Mg^{2+} efflux must be driven by Na influx down its electrochemical gradient. However, at present, the stoichiometry and possible electrogenicity of Na/Mg exchange have not been established. A difficulty in these studies is the uncertainty in the value of $[Mg^{2+}]_i$ since this ion binds to membranes and numerous molecules. To avoid this problem we "reversed" the electrochemical Na gradient in dialyzed squid axons to characterize the "reverse mode" of Na/Mg exchange (Na efflux/Mg influx). Axons were dialyzed with solutions containing various Na_i (and ^{22}Na) in the presence of 0.1 mM ouabain and absence of Na_o (replaced by TRIS), and the efflux of ^{22}Na was measured as a function of external Mg (Mg_o). Reductions in Mg_o (replaced by Ba) produced reversible decreases in ^{22}Na efflux (accompanied by small depolarizations) while increases in external Ba (with constant Mg_o) produced no effect in ^{22}Na efflux. Amiloride inhibited this effect with $K_{0.5}$ = 2 mM. Mg_o-dependent Na efflux increased as a function of external Mg and internal Na. In the first case the relationship fitted a Michaelis-Menten kinetics relationship with half maximal Mg_o = 10.8 mM; in the second case the relationship fitted the Hill equation with a Hill coefficient of 2.2 (n = 6) with half maximal Na_i = 56 mM. Supported by NIH Grants NS17048 and AR39522.

M-Pos277 MULTIPLE SULFYDRYL RESIDUES ARE INVOLVED IN THE Na-INDUCED CONFORMATIONAL CHANGE OF THE INTESTINAL Na/GLUCOSE COTRANSPORTER. Brian E. Peerce and Rebecca D. Clarke. Department of Physiology and Biophysics, University of Texas Medical Branch, Galveston, TX 77550.

Sulfydryl residues have been reported to inhibit Na-dependent glucose uptake in intestinal brush border membranes (1). This inhibition appears to involve the Na-induced conformational change (2). To better understand the molecular mechanism of ion gradient driven cotransport and the role of sulfydryl residues in transport processes we have examined the effect of IAEDANS and ACRYLODAN on Na-dependent glucose uptake and Na-induced conformational change. Na-dependent glucose uptake was only slightly inhibited by IAEDANS, however ACRYLODAN inhibited 70% to 80% of the Na-dependent glucose uptake. Using the Na-induced quenching of tryptophan fluorescence as the measure of ion-induced cotransporter conformational changes and purified detergent soluble cotransporter, again only ACRYLODAN inhibited Na-induced tryptophan fluorescence quenching.

Two separate effects of ACRYLODAN on the Na-induced conformational change were noted. At short incubation times (<2 min) ACRYLODAN increased the apparent K_m for Na from 22 mM ± 3 mM to 50 mM ± 5 mM. This effect could be fit to a double exponential with rate constants of 0.38 min^{-1} and 0.06 min^{-1}. At higher ACRYLODAN (50 μM) concentrations the apparent Hill coefficient for Na increased from 1.1 to 2.5. The effect of ACRYLODAN on the apparent Hill coefficient was fit to three exponentials with rate constants of 0.43 min^{-1}, 0.04 min^{-1}, and 0.025 min^{-1}. We interpret these results as indicating that at least 3 classes of sulfydryl residues are involved in Na-induced conformational change of the Na/glucose cotransporter.

(1) Klip, A., S. Grinstein, and G. Semenza (1979) Biochim. Biophys. Acta 558:233.
(2) Peerce, B.E. and E.M. Wright (1984) J. Biol. Chem. 259:14105.

M-Pos278 CHLORIDE ACCUMULATION BY CHROMAFFIN VESICLES. Elizabeth A. Ries, Ward B. Wall, Peter Huettl and David Njus, Dept. of Biological Sciences, Wayne State Univ., Detroit MI 48202.

Like many secretory vesicles, the chromaffin vesicles of the adrenal medulla have an inwardly directed H^+-translocating ATPase which creates a membrane potential (interior positive). While this membrane potential should cause the vesicles to accumulate permeant anions such as chloride, Cl^- uptake does not lead to osmotic instability of the vesicles in vivo. To clarify the factors affecting Cl^- accumulation, we have studied Cl^- uptake and release in both intact chromaffin vesicles and resealed chromaffin-vesicle membranes ("ghosts"). Both accumulate $^{36}Cl^-$ over a period of about 15 min; the rate of Cl^- uptake indicates a Cl^- permeability coefficient of $\sim 2 \times 10^{-10}$ cm/sec at pH 7.0 and 30°C, a value comparable to the value for phospholipid bilayer membranes. The amount of Cl^- taken up is enhanced by ATP. Cl^- uptake is also proportional to but does not reach thermodynamic equilibrium with the Cl^- concentration of the medium. This $^{36}Cl^-$ accumulation is increased when the pH gradient is decreased by adding weak bases or by lowering the pH of the medium. Similar results are obtained using the quenching of 6-methoxy-N-(3-sulfopropyl)quinolinium fluorescence as an indicator of Cl^- uptake. This indicates that the pH gradient (inside acid) generated by the H^+-translocating ATPase may counter the stimulatory effect of the membrane potential. Thus, the H^+-translocating ATPase stimulates Cl^- uptake via the membrane potential and inhibits Cl^- uptake via the pH gradient. Since Cl^- influx tends to neutralize the membrane potential and to amplify the pH gradient, Cl^- accumulation should tend to be self-limiting. This work was supported by NIH Grant No. GM-30500 and by the American Heart Association.

M-Pos279 A SYMMETRIC MECHANISM FOR Na-Ca EXCHANGE. D.R. Lemieux, E.A. Johnson and J.M. Kootsey. National Biomedical Simulation Resource, Duke University, Medical Center, Durham, NC 27710.

Mechanisms for Na-Ca exchange have been described in which three Na^+ are exchanged for a single Ca^{++}, simultaneously (Johnson & Kootsey, J. Mem. Biol., 86:167-187, 1985) or consecutively (Lauger, J. Mem. Biol., 99:1-11, 1987). Although these mechanisms are consistent with a broad range of experimental observations of Na-Ca exchange, other results cannot be accounted for, e.g. Ca-Ca exchange in the equilibrium experiments of Slaughter et al. (J. Biol. Chem., 258:3183-3190, 1983). The discrepancy is an inherent property of both of the previous mechanisms. This paper describes a new symmetric mechanism; identical regions of the exchanger facing intracellular and extracellular space can bind either one Ca^{++}, three Na^+, or one monovalent cation other than Na^+. The 56 states of the exchanger are the minimum required by experimental observations under a variety of experimental conditions. The new mechanism not only accounts for all aspects of Ca-Ca exchange such as Ca-Ca exchange in the absence of monovalent cations, but also a broad range of experiments on Na-Ca exchange in squid giant axon, cardiac muscle, isolated sarcolemmal vesicles and retinal rod outer segments. The new mechanism surprisingly accounts for the puzzling experimental observation that Ca influx is dependent on intracellular Ca^{++} -- - the so called "essential activator" role of intracellular Ca^{++} (DiPolo & Beaugé, J. Gen. Physiol., 90:505-525, 1987).

M-Pos280 MEMBRANE LOCALIZATION OF Na/H EXCHANGER IN FROG SKELETAL MUSCLE. R. W. Putnam, Department of Physiology and Biophysics, Wright State University School of Medicine, Dayton, OH. 45401.

Frog skeletal muscle has two distinct membrane regions separating the cytoplasm from the external solution: the surface membrane (SM); and the transverse tubular membrane (TTM). The transport properties of these two membranes differ, but nothing is known about the distribution of membrane transport systems responsible for pH regulation in SM versus TTM. Glass pH-sensitive microelectrodes were used to study pH regulation in small bundles of semitendinosus muscle from Rana pipiens as previously described (Putnam et al., J. Physiol. (1986) 381:205-219). pH recovery from acidification induced after exposure to 30mM NH_4Cl (nominal absence of CO_2) is due entirely to Na/H exchange. The initial rate of this recovery in depolarized fibers is dependent on external buffering power, varying from 0.19 ± 0.07 pH unit/s in 5mM HEPES to 0.46 ± 0.11 pH unit/s in 50mM HEPES (both containing 50mM K, 100mM Cl). This suggests an effect on recovery from an external unstirred boundary layer. If Na/H exchangers reside on the TTM, the tubular lumen could contribute to this boundary layer. Recovery was thus studied in fiber bundles detubulated in 1.5M formamide (2.5mM K) (Argiro, J. Mus. Res. Cell Motil. (1981) 2:283-294). Compared to control cells, membrane capacitance was reduced in formamide-treated cells, from 7.6 ± 1.0 to 2.9 ± 0.2 $\mu F/cm^{-2}$, indicating that this treatment removed about 85% of the TTM. Preliminary studies of these detubulated fibers indicate that pH_i recovers from an NH_4Cl pulse (50mM K, 50mM HEPES) at a rate of about 0.7 pH unit/s. These data suggest that in frog skeletal muscle the Na/H exchanger largely resides on the surface membrane. [Supported by NIH Grant AR38881.]

M-Pos281 MYOCARDIAL GLUCOSE UTILIZATION: FAILURE OF ADENOSINE (ADO) TO ALTER IT AND INHIBITION BY N^6-(L-2-PHENYLISOPROPYL)-ADENOSINE (PIA). W.E. Dale[1], C.C. Hale[2], M.J. Rovetto[1] and H.D. Kim[3], Depts. of Physiol.[1], Vet. Biomed. Sci.[2], and Pharmacol.[3], Univ. MO-Columbia 65212.

ADO reportedly stimulates myocardial glucose uptake in vivo (Am. J. Physiol. 254:H970-H975, 1988). However, we found that endogenous ADO did not affect insulin stimulated, nor PIA inhibited, initial 3-O-methylglucose transport rates in isolated cardiocytes (FASEB J. 2:A1310, 1988). The present study was undertaken to determine if ADO altered glucose metabolism rather than transport. This was done by measuring the rate of ^3H_2O production from metabolism of ^{3}H-2-D-glucose in rat cardiac myocytes ([D-glucose]=11mM) following incubation (20 min) in PIA or ADO (concentration ranges were 20 nM to 1 mM for both) or insulin (8 pM to 1 μM). None of these factors significantly changed glycolytic flux. However, PIA inhibited D-glucose specific transport into both rat and bovine cardiac sarcolemmal (SL) vesicles (K_i=26 μM at [D-glucose]=5mM) whereas insulin (1 μM) had no effect. The mechanism of PIA inhibition of glucose transport was investigated by cytochalasin B (CB) binding to bovine SL vesicles. Between 0 and 100 μM, CB Bmax was unchanged (about 14 pmol/mg prot) whereas the K_D increased from 129 to 322 nM. Because ADO did not stimulate glycolysis in cells we studied its effects on perfused rat heart glucose metabolism. We found that ADO (1 or 100 μM) increased coronary flow but had no effect on glycolytic rates. Conclusions: (1) ADO does not effect glucose transport or glycolysis, (2) PIA decreases transport across the cell membrane, and (3) PIA inhibits glucose transport by binding to the glucose transport molecule. Supported by NIH-AM-3345, NIH-HL27336 and the E. Mallinckrodt Foundation.

M-Pos282 THE Ca PUMP MEDIATES Ca/2H EXCHANGE AT pHout = 6.3 IN RED CELLS. M. A. Milanick with the technical assistance of B.J. Wilson. Dept. of Physiology, Univ. of Missouri, Columbia, MO 65211.

Human red cells were loaded with ^{45}Ca (1 mM) using the ionophore A23187 and were subsequently washed to remove the ionophore. Cells were placed in an unbuffered medium containing DIDS to reduce the basal proton flux. The pH stat technique was used to add H to keep the pH-out fixed and thus determine the rate of H disappearance into the red cells. A La-sensitive H influx was observed in Ca loaded cells, but not in normal cells, cells loaded with Mg, or cells preloaded with vanadate and then loaded with Ca. La-sensitive H influx was also observed when Na instead of K was in the media. The effect of several concentrations of La on the rate of ^{45}Ca efflux and H influx was determined; the results, shown in the figure, indicate that the dose response curves for the two processes were very similar suggesting that the Ca pump mediates Ca/H exchange under these conditions. The stoichiometry ranged between 1.7 to 2.0 H/Ca. At pH 8, preliminary experiments suggest that there is no La-sensitive H influx. In the presence of 11 mM Ca-out, an increase in H from 1.5 nM to .15 μM stimulated Ca efflux 5 fold; in contrast, in the absence of Ca-out, a similar increase in H only slightly affected Ca efflux. These results are consistent with a model in which the Ca pump mediates Ca/2H exchange at high H-out and an uncoupled Ca efflux at low H-out. The rate of the two processes appears to be similar. Supported by NIH DK37512.

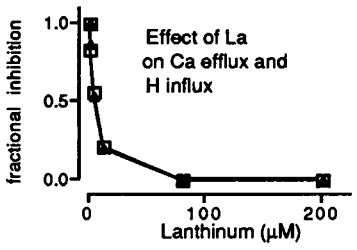

M-Pos283 LIGHT SCATTERING STUDIES OF BOVINE PROTEODERMATAN SULFATES: R. Gupta, L. Soby, A. M. Jamieson, J. Blackwell and L. Rosenberg, Department of Macromolecular Science, Case Western Reserve University, Cleveland, Ohio 44106 and the Orthopedic Research Labs, Montefiore Medical Center, Bronx, New York 10467.

Static and dynamic light scattering studies are reported of proteodermatan sulfates (PDS) derived from bovine fetal skin and calf articular cartilage. PDS species investigated included the PDS I and PDS II from calf articular cartilage, and the PDS II species from bovine fetal skin. These molecules were studied in 4M GdnHCl and in 0.15M NaCl. Parameters determined include weight-average molecular weights, z-average radii of gyration and hydrodynamic radii. In 4M GdnHCl, the results indicate that each species exists predominantly in the monomeric form. In 0.15M NaCl, a self association process occurs to form multimeric aggregates. Data will also be presented on the self-association behavior of the dermatan sulfate chains derived from PDS by digestion of the protein chains.

M-Pos284 SOLVENT EFFECTS ON CONFORMATION AND SELF-ASSOCIATION OF MUCIN GLYCOPROTEINS: A. Demers, B. K. Varma, A. M. Jamieson, J. Blackwell and N. Jentoft*, Departments of Macromolecular Science and Biochemistry*, Case Western Reserve University, Cleveland, Ohio 44106.

Static and dynamic light scattering studies are reported of Porcine Submaxillary Mucin (PSM), Canine Tracheal Mucin (CTM) and Human Tracheal Mucin (HTM), in three solvent systems, 6M Guanidimium Hydrochloride (GdnHCl), sodium chloride (0.05M-3M), and calcium chloride (0.05M-3M). These experiments yield structural information in the form of molecular weight, M_w, radius of gyration, $R_{g,z}$, hydrodynamic radius, R_h, and the longest intramolecular relaxation time, τ_1. The values of M_w, R_g, R_h, and τ_1 are all increased when comparing 0.15M NaCl versus 6M GdnHCl. Numerical analysis of these results indicates that the mucin chains undergo an end-to-end association in aqueous NaCl. In addition, it is evident that the conformation of the mucin peptide core is similar in 6M GdnHCl and in 0.15M NaCl. In aqueous $CaCl_2$, the M_w values are comparable to those in aqueous NaCl of equivalent ionic strength, however the values of R_g, R_h, and τ_1 decrease monotonically with increasing $CaCl_2$ concentration. The results indicate that, in $CaCl_2$, the mucin chains adopt a more compact configuration.

M-Pos285 CONFORMATIONAL STUDIES OF THE LEWIS BLOOD GROUP OLIGOSACCHARIDES BY NUCLEAR OVERHAUSER ENHANCEMENT IN NMR SPECTROSCOPY AND COMPUTER MODELING **Perseveranda Cagas, Zhen-yi Yan** and **C. Allen Bush** Dept. of Chemistry, Illinois Institute of Technology, Chicago, IL 60616 U.S.A.

The ^1H NMR spectra of the Lewis[a] pentasaccharide lacto-N- fucopentaose 2 (LNF-2) and of the Lewis[b] hexasaccharide lacto-N-difucohexaose 1 (LND-1) were completely assigned using phase sensitive 2-d DQF-COSY and HOHAHA spectroscopy in combination with ^1H detected 2-d ^1H-^{13}C correlation using the previously assigned ^{13}C spectra. In order to overcome difficulties in measuring nuclear Overhauser enhancements in molecules of this intermediate size range, NOESY experiments were carried out in D_2O and D_2O/DMSO mixtures at 5°C and at mixing times ranging from 250 to 900 ms, allowing observation and quantitation of negative NOE's at 500 MHz. The observation of small effects between ^1H on remotely connected residues in addition to substantial effects between ^1H on the same or directly bonded residues suggests the oligosaccharide may adopt a relatively rigid conformation. The observed NOE were interpreted with a complete spin relaxation matrix method in which theoretical 1-d and 2-d NOE peak intensities of computer-generated models were calculated by systematically varying the glycosidic dihedral angles. Comparison of the calculated NOE with experiment reveals that a single unique conformation fits the data and conformational energy calculations show a minimum energy conformation agreeing with the NOE result. The simplest interpretation of our results is that the Lewis blood group oligosaccharides have single rigid conformations. These results are similar to those previously found for blood group A and H oligosaccharides for which single conformations were found over a wide range of solvent and temperature conditions. We conclude that the conformations of blood group oligosaccharides are determined mainly by non-bonded interactions rather than electrostatic and hydrogen bonding effects which are important in peptides and nucleic acids.

M-Pos286 THE EFFECTS OF pH ON HYALURONATE AS OBSERVED BY COMBINED LIGHT SCATTERING TECHNIQUES. C. E. Reed, Li Xiao and W. F. Reed, Physics Department, Tulane University, New Orleans, La. 70118

Hyaluronate was observed over a wide pH range using total intensity and polarized and depolarized dynamic light scattering. Purified hyaluronate was prepared so as to yield solutions of low polydispersity in the range of 1.2 mg/ml and lower. Hyaluronate's polyelectrolyte behavior in the low and high pH range shows the effect of neutralizing the carboxyl groups and deprotonating hydroxyl groups, respectively. Kuhn segment length increases continuously from low to high pH, and reflects an increasingly stiff random-coil conformation. No evidence has yet been found for long range ordering, or its breakdown as ionic strength increases, as has been observed, for example, with poly-L-lysine. Association by entanglement, however, can occur at all but the highest pH values. The weak polyelectrolyte properties and high molecular weight of hyaluronate, compared to the other glycosaminoglycans (GAGs), are thought to be important in distinguishing hyaluronate from the other GAGs in its central role in proteoglycan aggregation, cell-cell interactions, and the maintenance of extra-cellular matrix swelling pressure and compressive stiffness.

(Supported by NSF grant DMB-8803760)

M-Pos287 DISACCHARIDE SOLUTION STRUCTURES BY OPTICAL ACTIVITY. Eugene S. Stevens and B. K. Sathyanarayana,† Department of Chemistry, State University of New York, Binghamton, New York 13901.

The problem of determining conformational preferences for oligosaccharides in solution is best approached by establishing, in increasing detail, the features of their potential energy surfaces as functions of the linkage dihedral angles ϕ and ψ. Here we apply a new semiempirical theory of saccharide optical activity to the disaccharides maltose and cellobiose. We relate results to calculated in vacuo potential surfaces and nmr measurements, in order to develop a picture of their potential surfaces in aqueous solution. The results confirm many of the previously emphasized conformational features, and indicate the likely role of "folded" conformations in providing stable turn geometries for the cellulose and amylose polymers.

†Present address: National Cancer Institute, Frederick Cancer Research Facility, Frederick, MD 21701.

M-Pos288 AXOBALL FORMATION IN SQUID GIANT AXON: THE VIDEO.

K.P. Tewari, P.G. Stein and H.M. Fishman, Department of Physiology and Biophysics, University of Texas Medical Branch, Galveston, Texas 77550.

As described in abstracts presented by us elsewhere at this meeting, injury to a squid giant axon in divalent cation-containing media causes the rapid formation of membranous balls within the axon. A videotape of this process, made using a Zeiss Axiovert microscope with differential interference contrast, will be shown illustrating the following features:

1) Time course of the process
2) Induction of ball formation and constriction of a cut end after addition of 10 mM/L Ca to the divalent-free ASW bathing a transected axon.
3) The accumulation and emergence of balls at a constricted, cut end.
4) Ball formation after nicking an axon in ASW.
3) The appearance of balls only along the sub-axolemmal surface.

We thank Dr. Roger T. Hanlon for cephalopod supply through NIH grant RR01024 and Philip Presley, David Floyd, and Zeiss for the use of equipment.
Aided by ONR contract N000-14-87-K0055.

M-Pos289 NEW VOLTAGE-SENSITIVE DYES FOR FAST OPTICAL MONITORING OF MEMBRANE POTENTIAL.

J.P. Wuskell[1], Z. Lojewska[1], L.M. Loew[1], J.-Y. Wu[2], L.B. Cohen[2], and H.P. Hopp[2].
[1]Dept. of Physiology, University of Connecticut Health Center, Farmington, CT 06032.
[2]Dept. of Physiology Yale University School of Medicine, New Haven, CT 06510 and the Marine Biological Laboratory, Woods Hole, MA 02543.

We have synthesized several styryl and oxonol dyes for use as optical indicators of membrane potential in situations where rapid response times (<1 msec) are required. These dyes have been screened using hemispherical bilayer model membranes and squid giant axons. Two new aminonaphthyl styryl dyes had relatively large signal-to-noise ratios in measurements from giant axons. One of these, a phosphonate, JPW1064, had a fractional fluorescence change ($\Delta F/F$) of 6×10^{-3}, that was larger by a factor of two than any previously tested dye. Several pyrazolone oxonol dyes were also synthesized and had relatively large absorption signals in measurements from giant axons. These dyes include bis[3-phenyl-1-(p-sulfophenyl)5-pyrazolone-(4)]pentamethine oxonol, JPW1034, which is identical to RGA509, the dye which gave the largest signals when tested on ganglia from the leech and was no longer available. Two new groups of molecules were also synthesized and tested, crown ethers and trinuclear cyanines, but thus far the signals obtained with these dyes have been small. (Supported by USPHS grants GM35063 and NS08437).

M-Pos290 VERSATILE FAST POTENTIOMETRIC MEMBRANE PROBES BASED ON THE 8-[2-AMINO-6-NAPHTHYL]VINYL-4-PYRIDINIUM CHROMOPHORE.

L.M. Loew[1], Z. Lojewska[1], D.L. Farkas[1], J.P. Wuskell[1], V. Montana[1], M.-D. Wei[1], L.B. Cohen[2], G. Salama[3], J.A. Dix[4], E.N. Fluhler[4]. [1]Physiology, U. Conn. Health Center, Farmington, CT 06032; [2]Physiology, Yale U. School of Medicine, New Haven, CT 06510; [3]Physiology, U. Pittsburgh School of Medicine, Pittsburgh, PA 15260; [4]Chemistry, SUNY at Binghamton, Binghamton, NY 13901.

The potenital-sensitive dye di-4-ANEPPS is an analogue of the styryl class with an aminonaphthyl ring in place of the usual aniline. It was first synthesized 4 years ago and has since proven itself to be a consistent and useful probe in a variety of applications. It has been characterized on the hemispherical bilayer model membrane and on the voltage-clamped squid axon. Binding and voltage sensitivity on lipid vesicle and red blood cell suspensions have also been studied. The probe allows mapping of electric field-induced membrane potential along the surface of single cells. In the perfused heart, it is as sensitive to cardiac action potentials as any dye that has been screened and has the additional advantages of very low toxicity and high stability and persistence (hours). In all systems where a comparison is possible (i.e. no extraneous background due to inactive stained membrane) the relative fluorescence response of the dye has been close to 10%/100mV for excitation at 546nm and emission at >590nm. Several variations on the di-4-ANEPPS structure with different charged sidechains have also been synthesized. (Supported by USPHS grants GM35063 and NS08437).

M-Pos291 INFLUENCE OF SODIUM-CALCIUM EXCHANGE ON PITUITARY CELL MEMBRANE CURRENTS. Stephen J. Korn and Richard Horn, Roche Inst. of Molec. Biol., Nutley, NJ 07110

Hormone secretion from anterior pituitary cells depends largely on the entry of extracellular Ca through voltage-activated Ca channels. Following entry, Ca activates Ca-dependent currents, which turn off as the Ca concentration near the cytoplasmic membrane surface decreases. We used the "perforated-patch" technique (Biophys. J. 53:360a, '88), which maintains endogenous Ca buffers, to investigate the influence of Na-Ca exchange on the duration of the Ca-dependent Cl current (I_{Cl}) in AtT-20 cells. To block Na-Ca exchange, TEA or TMA was substituted for external Na. We also examined the effect of blocking Na-Ca exchange on Ca current washout.

In whole-cell recordings, TEA or TMA substitution prolonged I_{Cl} in the absence of added internal Ca buffers. I_{Cl} was not prolonged by TEA substitution when activated in the presence of >200 μM $EGTA_i$. In perforated-patch recordings, I_{Cl} was also prolonged by block of Na-Ca exchange. In addition, other endogenous Ca removal mechanisms limited the duration of I_{Cl}. In whole-cell recordings, Ca current washout was dramatically accelerated by TEA substitution when EGTA was omitted from the cytoplasmic solution. This acceleration was prevented by addition of $EGTA_i$, and did not occur in perforated patch recordings.

M-Pos292 INTRACELLULAR FLUORIDE REDUCES THE LEAKAGE CONDUCTANCE IN DIALYSED ASCIDIAN OOCYTES BY FORMING PRECIPITATES IN THE MEMBRANE WITH EXTRACELLULAR CALCIUM.

Philippe Béhé & Luca Turin, UA 671 du CNRS, Station Marine, F-06230 Villefranche sur Mer, France*.

Foreign anions in high concentrations (> 100 mM) have long been used as components of perfusion and dialysis media, since their favourable effect on the leakage conductance was first described by Tasaki, Singer and Takenaka (J.Gen. Physiol. 48:1095 [1965]) . Noting that the two best anions, fluoride and phosphate, both form poorly soluble calcium salts, we hypothesized that precipitate formation between intracellular F or PO_4 and extracellular Ca might plug any "leakage channels" present in the membrane. This idea led to two predictions: 1) That another, unrelated precipitating ion pair (e.g. Co and ferricyanide) should be effective in reducing leakage conductance 2) That inverted dialysis, i.e exchanging extracellular for intracellular medium and vice versa should be possible.

We have tested these predictions on the dialysed oocyte of the ascidian Styela plicata. Our results show 1) That intracellular dialysis with 150 mM ferricyanide ions can maintain leakage conductance at fluoride levels provided precipitating cobalt ions are present in the extracellular medium. 2) That inverted dialysis is as effective as normal dialysis in maintaining leakage conductance low. 3) That the leakage conductance is in part composed of giant channels with a unit conductance of the order of 5000 pS. 4) That the F-sensitiveleakage conductance is not present in the native membrane but arises as a result of dialysis with fluoride . We conclude that dialysis with fluoride produces irreversible changes in the membrane, creating large leakage channels which then require a precipitating pair of ions on either side of the membrane to be kept in a nonconducting state.

*Supported by the CNRS and the Ministère de l'Education Nationale.

M-Pos293 SINGLE ION CHANNELS RECORDED FROM SQUID GFL NEURONS. Andres Oberhauser. Dept. of Physiology, Univ. of Pennsylvania, Philadelphia,PA 19104. (Intr. by Annemarie Weber).

We have used cells (1 to 6 weeks in culture) dissociated from the giant fiber lobe of the squid stellate ganglion to study the activity of single ion channels. One to 5 days old cells had roughly spherical shape and no processes. Using 400 NMG-Cl, 100 TEA-Cl in the pipette, Cl selective channels (Vrev= -30 mV) were observed in 3 of 20 patches. The conductance (γ) is 100 to 120 pS, and they open more frequently at hyperpolarizing potential (-60 mV). Calcium channels were studied by using 110 $CaCl_2$ in the pipette. The γ is 15 pS, are very selective for Ca (Vrev >100mV),the probability of opening (P_o) changes e-fold/10 mV and are not affected by nifendipine (10 uM) or Bay K8644 (1 uM) in the pipette. Two types of voltage-dependent K channels were observed. In inside-out patches (500 K in pipette, 440 K-ASW in bath) the first type had a γ of 50 pS, mean open time of 30ms at 20 mV and P_o=.6. The second channel had a γ of 80 pS, mean open time of 5ms at 20 mV and P_o=.2. The activity of both channels was inhibited by Ba in the bath solution (10 mM for complete block). Most of the 3-6 weeks old cells had processes with flaring ends that resemble growth cones, with long protuding microspikes. These cells had the same type of ion channels, regardless of the region of the cell (cell body or growth cones).

(Supported by a Grass Foundation Fellowship and NIH grant # NS 12543).

M-Pos294 WHOLE-CELL RECORDINGS FROM CULTURED GLOMUS CELLS OF THE RAT CAROTID BODY. A. Stea and C.A. Nurse. (Intr. by R.E. Garfield). Dept. of Biology, McMaster University, Hamilton, Ontario, L8S 4K1.

We are investigating the mechanisms of chemosensory transduction in the rat carotid body by use of dissociated cell cultures. Our initial focus has been on the physiological properties of the parenchymal glomus cells using the patch clamp technique and already we have characterized a large conductance chloride channel in inside-out patches of glomus cells (Soc. Neurosci. Abstr. 14: 643; submitted to AJP). We now extend these studies to whole-cell recordings from glomus cells in bathing solutions containing 140 mM NaCl, 2 mM $MgCl_2$, 1 mM $CaCl_2$, 10 mM glucose and 10 mM HEPES (pH 7.2); the pipettes contain typically 140 mM KCl, 10 mM HEPES (pH 7.2) and ca. 10^{-8} M free Ca^{2+}. Under voltage clamp, depolarizing steps from initial holding potentials between -60 and -80 mV to levels between -20 and 0 mV evoked voltage-dependent transient inward currents followed by delayed outward currents. With hyperpolarizing voltage steps the membrane behaved passively. The shape and time course of these voltage-gated currents resemble those in electrically-excitable cells and raise the possibility that glomus cells in the rat carotid body also display regenerative properties typical of neurons, as recently demonstrated in glomus cells of the rabbit carotid body (Neurosci. 29: 291-311). These voltage-gated inward and outward currents have been seen in 1-2 week-old cultures of glomus cells obtained from both newborn and older (> 30 days) rats, suggesting the corresponding ion channels appear early in development. The likely contribution of Na^+, K^+ and possibly Ca^{2+} ions to these voltage-gated currents is currently being investigated. Supported by the Heart and Stroke Foundation of Ontario.

M-Pos295 *OPTICAL AND ELECTRICAL MONITORING OF SIGNAL PROPAGATION IN AMPHIBIAN AND MAMMALIAN DEMYELINATED NERVE FIBERS.* Peter Shrager, Chaim Rubinstein, and J. Casey Donaher, Department of Physiology, University of Rochester Medical Center, Rochester, NY 14642.

Following demyelination, conduction in peripheral nerve fibers is first blocked, but is later restored. Central to an analysis of the recovery process is an evaluation of the relative importance of ionic channel redistributions as compared with remyelination. We have investigated this problem with three approaches: loose patch clamp, optical recording, and electron microscopy. In rat sciatic axons demyelinated by surgical injection of lysolecithin, voltage dependent Na and K channels could be demonstrated in internodal regions. Transient outward currents, indicative of regions of very high Na channel density just outside the patch zone, were detected only at paranodal sites. Peak internodal inward currents did not increase over the first week post-surgery, as the axons were progressively demyelinated. The sharp gradient in Na channel density seen at nodes was preserved over at least 36 days, indicating that lateral diffusion of these channels from the node may involve at most only a small fraction of the nodal channels. Schwann cells closely associated with newly forming nodes had no Na current. We conclude that in the rat, as found earlier in the frog, the normal internodal sodium channels may play an important role in the recovery process.

In *Xenopus* axons we are able to obtain optical records from normal nodes, demyelinated internodes, and nodes newly forming in regions that previously were internodal. At about 18 days post-injection the compound action potential shows that signals can propagate through the lesion in many fibers, but with slow conduction velocity. At this stage axons are undergoing ensheathment by proliferating Schwann cells. Since axons are heterogeneous with respect to the length of the demyelinated zone, we wished to know if only fibers with very short lesions were responsible for these electrical signals. Preliminary optical evidence suggests that at 18-22 days conduction through long (>1 mm) demyelinated segments can in fact occur. Measured conduction velocities in these regions are <1 m/sec. We are now preparing to examine these zones ultrastructurally to measure the extent of ensheathment and possible early remyelination. Supported by grants from the NIH (NS17965) and from the National Multiple Sclerosis Society.

M-Pos296 CARBACHOL-EVOKED CALCIUM-ACTIVATED K^+ CURRENTS IN ADHERED OR SUSPENDED HUMAN ASTROCYTOMA CELLS. Scott A. Oglesby & Barry S. Pallotta, Curriculum in Neurobiology and Department of Pharmacology, University of North Carolina, Chapel Hill, NC 27599

]321N1 human astrocytome cells respond to muscarinic agonists with an increase in intracellular $[Ca^{2+}]_i$ that activates single Ca^{2+}-activated K^+ channels (290 pS) recorded in cell-attached patch clamp configuration. Whether or not a cell responds to the muscarinic agonist carbachol depends on the length of time cells were allowed to adhere to coverslips.

Cells were suspended with trypsin or low-Ca^{2+} buffer and plated at low density onto plastic or glass coverslips. Cells challenged with carbachol (1-150 μM) 36 hr or more after plating showed a very low response rate (14%), and the increase in channel activity was totally dependent on extracellular Ca^{2+}. In contrast, cellsacutely plated for 15-120 min showed a very high response rate (94%). The initial large but transient increase in channel activity did not depend on extracellular Ca^{2+} while the secondary sustained increase in activity did depend on $[Ca^{2+}]_o$. Similar results were obtained with optical measurements (FACS) from single suspended cells loaded with Indo-1 AM. The response profile and $[Ca^{2+}]_o$-dependence were similar to that found in patch-clamp experiments with acutely plated cells: approx.90% of the cells showed a carbachol-evoked increase in the Indo-1 emission ratio.

M-Pos297 ALLOSTERIC MODULATION OF NMDA RECEPTOR DESENSITIZATION BY GLYCINE. M.L. Mayer, L. Vyklicky Jr. & J. Clements. Unit of Neurophysiology and Biophysics, LDN, NICHD, NIH, Bethesda MD 20892.

Glycine, at nM concentrations, strongly potentiates responses to NMDA in mammalian central neurons. On the basis of experiments on messenger RNA injected oocytes it has been suggested that glycine is a coagonist the presence of which is an absolute requirement for activation of ion channels linked to NMDA receptors. We have used a fast perfusion system (τ exchange ≈ 10 ms, measured by jumping [Na]o from 5 to 165 mM in the presence of kainic acid) to study the interaction between glycine and NMDA in cultures of mouse hippocampus. Our results show that as occupancy of the glycine binding site (Kd ≈ 250 nM) is reduced the response to NMDA (Kd with 3 μM glycine ≈ 30 μM, hill slope ≥ 1) shows strong desensitization. As a result glycine potentiation of responses to NMDA is much greater at steady state, than when measured before the onset of desensitization. We have found that even with glycine concentrations as low as 10 nM, substantial responses to NMDA can be evoked if measurements are made before the onset of desensitization. Our results are best interpreted using a nine state binding model, in which glycine increases the availability of resting desensitized NMDA receptors, and decreases NMDA-evoked desensitization be speeding up the rate constant for recovery from desensitization.

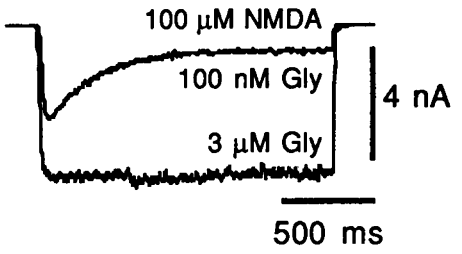

M-Pos298 CONTINUOUS LONG-TERM OPTICAL RECORDING FROM IDENTIFIED APLYSIA NEURONS IN CULTURE. T.D. Parsons, A.L. Obaid, D. Kleinfeld, and B.M. Salzberg. Univ. of Pennsylvania, Phila., PA 19104-6085 and AT & T Bell Labs., Murray Hill, NJ 07974.

We have used potentiometric probes and a photodiode array to obtain multiple-site optical recordings of synaptic interactions between identified invertebrate neurons in culture. In our previous work, we had maximized the optical S:N (50:1) by using a broadband (700 ± 25 nm) high intensity light source (~1.6 W/cm^2) and working in deoxygenated solutions to reduce phototoxicity. Our recording time was limited to ~20 sec by photobleaching of the dye. We now report that decreasing the light intensity by 99 % extended the recording times to at least 30 min in oxygenated ASW. The figure shows excerpts from a continuous optical record of evoked activity in an Aplysia LUQ cell stained with 0.2 mg/ml RH155. Measurement employed light from a tungsten-halogen source passed through an interference filter (710 ± 5 nm) and a 1.3 OD neutral density filter. The S:N is reduced, but permits easy identification of spikes. We hope to use long term optical recording to monitor electrical activity in small neuronal ensembles (see the two abstracts that follow). Supported by USPHS grant NS RO1 16824.

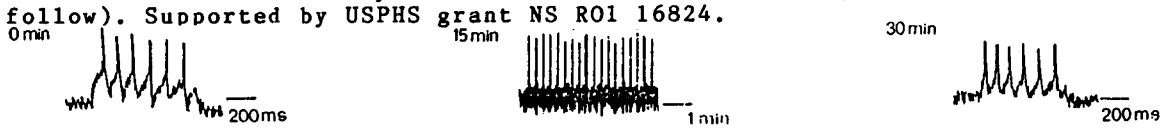

M-Pos299 R15 AND OTHER RHYTHMICALLY ACTIVE APLYSIA NEURONS EXHIBIT ENDOGENOUS BURSTING IN CULTURE: POSSIBLE ROLE AS ACTUATORS OF IN VITRO NEURONAL ENSEMBLES. A.L. Obaid, D. Kleinfeld, T.D. Parsons, G.F. Raccuia, and B.M. Salzberg, Univ. of Pennsylvania, Phila., PA 19104-6085 and AT & T Bell Labs., Murray Hill, NJ 07974.

R15, the "parabolic burster" (Strumwasser, F. In: Circadian Clocks, J. Aschoff, ed., North Holland, 1965) from the abdominal ganglion of Aplysia californica, is spontaneously active in situ, and the mechanisms underlying its behavior are located in the cell's soma. We have shown that R15, cultured in isolation, retains its characteristic bursting pattern (see Figure), and its exquisite sensitivity to modulation of its membrane potential. Although the burst parameters vary from cell to cell, a given R15 displays remarkable dynamic stability over periods of several hours. We have also observed bursting in neurons L10 and L4, but without the fixed firing pattern of the parabolic burster. We hope to employ such endogenously active cells as intrinsic stimulators within synaptically coupled neuronal ensembles. These networks might then be analyzed, non-invasively, using multiple site optical recording (see the two preceding abstracts). Supported by USPHS grant RO1 NS 16824.

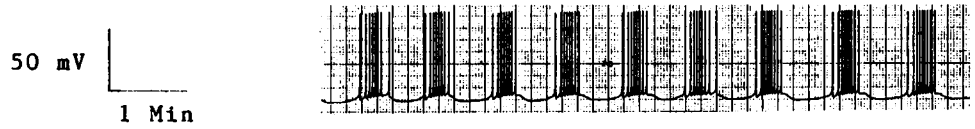

M-Pos300 NOVEL SYNAPTIC CONNECTIONS ARE FORMED AMONG IDENTIFIED APLYSIA NEURONS IN CULTURE. T.D. Parsons, G.F. Raccuia, B.M. Salzberg, D. Kleinfeld, Univ. of Pennsylvania, Phil., PA 19104-6085 and AT & T Bell Labs., Murray Hill, NJ 07974.

We have constructed ensembles of identified invertebrate neurons for the study of network phenomena in vitro. Our emphasis was on co-cultures containing the cholinergic interneuron, L10. In agreement with Camardo et al. (1983), we have have found that L10 reestablished characteristic chemical connections with many of its in vivo targets. However, we have also found that many of the same target cells (L7, L11, L12 and the LUQs), and at least one cell that is not an in vivo partner (L14), form strong chemical connections onto L10 in vitro. These novel connections are dual component IPSPs, whose fast phase is reversed by hyperpolarization and is blocked by d-Tubocurarine. The figure shows the connection from the gill motor neuron L7 to L10 (note the spontaneous PSP at the arrow). Our results suggest that restrictions imposed upon synaptic connectivity in the ganglion are relaxed during in vitro synaptogenesis.

Supported by USPHS grant RO1 NS 16824.

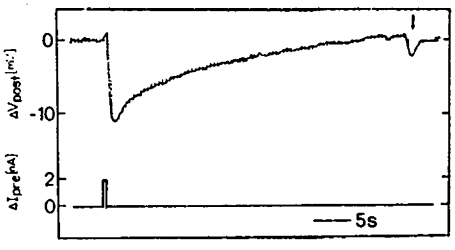

M-Pos301 AN IMPROVED TISSUE CULTURE SUBSTRATE FOR BOTH GROWTH AND ELECTROPHYSIOLOGICAL STUDIES OF MAMMALIAN SCHWANN CELLS. P.T. Hargittai, G.E. Groblewski & E.M. Lieberman, Dept. Physiology, Sch. Med., East Carolina U., Greenville, NC 27858.

An improved substrate suitable for growth and subsequent electrophysiological studies of mammalian Schwann cells in culture has been developed. The substrate was made from one layer of air dried rat tail collagen with an additional layer of the extracellular matrix (ECM) MATRIGEL™ prepared at various dilutions. A 1:5 dilution of the ECM ensures a high plating efficiency and stimulation of growth for a wide variety of cells including Schwann cells. These properties were demonstrated by a series of studies with primary and secondary Schwann cell cultures, measuring the effect of different substrates on their morphology and development. The resulting culture plate has excellent optical and mechanical properties which greatly facilitate microelectrode impalements and the use of voltage sensitive dyes for the study of the electrophysiological properties of single Schwann cells. Cells may also be grown on coverslips for use in cuvettes for fluorometry measurements. The membrane potential of cultured Schwann cells was monitored by fluorescence of the voltage-sensitive dye, Di-O-C(3). Fluorescence increased with increasing concentration of external K^+, as expected. The resting membrane potentials of young (<10 DIV) Schwann and dorsal root ganglion cells were -19.1±2.5 mV (n=7) and -55.0± 2.4 mV (n=27), respectively, as measured with conventional microelectrode techniques. Supported by Army Research Office Grant No. 27572-LS (to E.M.L.).

M-Pos302 DIFFERENTIAL EXPRESSION OF ION CHANNEL SUBTYPES CONTRIBUTES TO DIVERSITY OF ACTION POTENTIAL SHAPE IN VERTEBRATE SENSORY NEURONS. D.T. Campbell and L. Babeu, Hatfield Marine Science Center and College of Pharmacy, Oregon State University, Newport, OR 97365.

Ionic currents and action potentials were measured in frog DRG cells using the whole-cell patch clamp method. As previously found in garter snake (D.T. Campbell, *Biophys. J.*, 1988, 53: 15a), two Na channel subtypes are present in frog DRG cells: channels that inactivate rapidly and are blocked by TTX at nM concentrations, and channels that inactivate ~3 times slower which are very resistant to TTX. These subtypes are differentially distributed by cell size. In 18/18 cells with capacitance > 63 pF, block of Na current by 1 uM TTX averaged >99%. In 26 of 38 cells with capacitances < 63 pF an average of 39% of Na current remained unblocked in 1 uM TTX. In the remaining 12 small cells an average of > 99% of I_{Na} was blocked by 1 uM TTX. From kinetics, it appears that there are at least two subtypes of K channel in frog DRG cells, one activating ~2X faster than the other. The amount of I_K varies widely from cell to cell. In preliminary experiments, 10 of 10 cells smaller than 30 pF had relatively little I_K. Large I_K was observed in 6/10 cells with capacitance between 30 and 57 pF and in 3/3 cells larger than 57 pF. Action potentials measured under conditions that eliminated I_{Ca} were of three basic classes: short(1-2 ms duration)--TTX-blockable; long (5-10 ms), rounded-peak--TTX resistant; and long, sharp-peaked --TTX-resistant. In the last type, sharp peaks were eliminated by 1 uM TTX without blocking the action potential. These results suggest that without I_{Ca}, action potential shape in DRG cells depends on the amount and proportion of Na and K channel subtypes in the membrane. Thus, short duration action potentials may derive their rapid repolarization from both fast inactivation of TTX-sensitive Na channels and fast activation of large I_K. Longer action potentials may repolarize slowly, due both to slow inactivation of TTX-resistant I_{Na}, and to smaller more slowly activating I_K. Supported by USPHS (NS22577).

M-Pos303 CALYX, EN-PASSANT AND BOUTON-LIKE NEURON CONTACTS IN CHICK CILIARY GANGLION CULTURES AND THEIR CORRELATION WITH CALCIUM CURRENTS E.F Stanley. Laboratory of Biophysics, NINCDS NIH. Bethesda MD. 20892. (Spons. G. Ehrenstein).

Chick ciliary ganglion neurons *in vivo* form a remarkable calyx synapse in which the presynaptic nerve terminal envelopes the ciliary ganglion neuron cell body. The formation of calyxes and of other neuron-to-neuron contacts by ciliary ganglion neurons in culture has been explored in this study and these have been correlated with the presence of inward Ca currents. Individual cells were filled with the fluorescent due Lucifer yellow and a range of synapse-like structures were observed including boutons, en-passant contacts and occasional contacts in which the neuron completely enveloped a second cell. These calyx-like contacts occurred on the end of a neuronal process but more often were extensions of the neuron cell body itself forming a "proximal calyx" (PC). Ca currents were not observed in all cells. In most neurons without contacts with other cells or with processes making contacts distant from the cell body, Ca currents were absent. In neurons forming terminal-like contacts within a short (<50 μm) distance from the cell body, Ca spikes, rather than well clamped calcium currents were recorded. Most cells that formed PCs had well clamped inward Ca currents. The results indicate a correlation between Ca currents and the formation of presynaptic-like contacts and are consistent with the formation of calyx-type presynaptic structures in culture.

M-Pos304 REGULATION OF THE SECRETORY RESPONSE OF BOVINE CHROMAFFIN CELLS. G. Callewaert, R. Johnson & M. Morad. Univ. of Penn, Depts. of Physiology and Medicine, Philadelphia, PA

The secretory response of chromaffin cells to nicotine and high $[K^+]_o$ is transient and Ca^{2+}-dependent. We investigated possible mechanisms that underlie the transient nature of the secretory activity. Cultured bovine chromaffin cells were patch-clamped and secretion was induced using a fast perfusion system (10 ms). Rapid application of 60 uM nicotine induced an inward current which desensitized rapidly (fig.) (τ_f≅25 ms and τ_s=100-200 ms). Recovery from desensitization was slow (τ_{rec}=5-6 s). i_{Ca} activated by step depolarization from -90 mV diminished markedly on repetitive activation. Increasing the stimulation frequency from 0.05 to 1 Hz decreased i_{Ca} 5-fold. This decrease persisted for 10-30 s. i_{Ca} recorded in a cell within a cluster of chromaffin cells (but not in a single isolated cell) was strongly suppressed by inducing secretion with nicotine or K^+ (35.4 mM). Since the secretory vesicles of chromaffin cells contain catecholamines, ATP, enkephalins and high $[H^+]$ (pH 5.5), we examined the direct effect of these substances on i_{Ca}. Adrenaline (10 uM), ATP (10 mM), Met- or Leu-enkephalin (100 uM) failed to suppress i_{Ca}. However, step increases in $[H^+]_o$ strongly suppressed i_{Ca} and total catecholamine secretion. Our data suggests that the secretory response of chromaffin cells may be modulated by fast desensitization of the nicotinic receptor, and proton- and frequency-induced suppression of the Ca^{2+} channel. (Supported by HHMI and NIH #HL-16152).

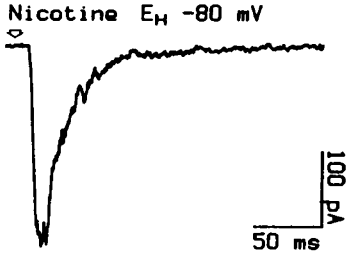

M-Pos305 **Reading a neural code** William Bialek, Fred Rieke, Rob de Ruyter van Steveninck,* and David Warland, *Departments of Physics and Biophysics, University of California, Berkeley, CA 94720. *Department of Biophysics, Rijksuniversiteit Groningen, The Netherlands.*

The "neural code" defines the representation of sensory information in patterns of neural activity. For spiking neurons it has been traditional to measure characteristics of this representation through repeated presentations of a limited class of stimuli. The goal of such experiments is often to make a model of the encoding dynamics which allows prediction of the cell's response to arbitrary stimuli. But the organism is not interested in predicting spike trains given a known signal input — on the contrary the organism would like to gain maximal information about an unknown signal by observations of the spike train. We present two strategies for characterizing the neural code from the organism's point of view, culminating in algorithms for stimulus reconstruction given a single sample of the spike train; as far as we know this is the first instance in which a direct "reading" of the neural code has been accomplished. These ideas are applied to the design and analysis of experiments on a movement sensitive cell in the visual system of the blowfly. Successful reconstructions will be illustrated and we will discuss the relation of reconstruction algorithms to models for neural computation.
Work supported in part by the National Science Foundation, the National Institutes of Health, and the Netherlands Organization for Scientific Research.

M-Pos306 **Non-Boltzmann dynamics in networks of spiking neurons** Michael Crair and William Bialek, *Departments of Physics and Biophysics, University of California, Berkeley, CA 94720.*

It is quite popular these days to model networks of neurons in a way which could reasonably lose any real biological relevance. Specifically, the import of action potentials as the mediator of interactions between neurons is usually glossed over or ignored, even though ample evidence exists to suggest that 'spikes' have a fundamental impact on network structure and function. We study a simple model in which trains of action potentials between neurons are specifically included, and find that they change basic properties of the networks.

A 'spiking' neuron receives its input from other neurons through its dendritic tree in the form of an electric signal, $V(t)$. $V(t)$ is a weighted sum of the post-synaptic potentials (PSP) generated by incoming spikes. Each PSP decays exponentialy with some characteristic time. The neuron generates spikes via an approximately Poisson process at a rate ($r(t)$) which is assumed to be a sigmoid function of $V(t)$. In the limit of large firing rate, this model is very similar to that of Little or Hopfield (1). We find however, that realistic firing rates alter the dynamics in a way that destroys the 'Boltzmann' property of the networks. That is, relative probabilities of different stable states of the network cannot be characterized by an energy function alone, because of non-zero probability currents. We analyze the dynamics in an attempt to reveal broader characteristics that would be useful in flushing out more robust properties of the system. An attempt is made to predict different regimes under which real networks of neurons behave.

1. See *Neurocomputing*, J. A. Anderson and E. Rosenfeld eds., MIT Press (1988).

Work supported in part by the National Science Foundation.

M-Pos307 **NOVEL SLOW EPSPs EVOKED BY CLIMBING AND PARALLEL FIBER ACTIVATION IN TURTLE CEREBELLAR PURKINJE CELLS.** L.J. Larson-Prior and N.T. Slater. Dept. of Physiology, Northwestern University Medical School, Chicago, IL 60611.

The two principal excitatory synaptic inputs to Purkinje cells in vertebrate cerebellum described to date are the climbing fiber (CF)-mediated complex spike and the parallel fiber (PF)-mediated fast EPSP. Both synaptic potentials are believed to be mediated by excitatory amino acid (EAA) receptors, the latter being of the "non-NMDA" type. In the present experiments, novel slow EPSPs have been observed following stimulation of both CFs and PFs in the isolated brainstem-cerebellum of the Painted turtle *Chrysemys picta*. This preparation is extremely resistant to anoxia, and thus stable intrasomatic and intradendritic recordings can be maintained in the cerebellum *in vitro* for 1 - 10 hrs. Stimuli were applied to the cerebellar peduncle (PD),inferior olive or the cerebellar molecular layer to activate CFs and PFs. Single PD stimuli evoked a CF complex spikefollowed by a late, slow EPSP (Fig 1A)which was associated with anincrease in membrane conductance, and was reversibly *abolished* by repetitive stimuli (Fig 1B). Single or brief (100 ms) trains of PF stimuli evoked a slow EPSP (Fig 1A) also associated with a conductance increase, which was *potentiated* by repetitive stimuli (not shown). The PD-evoked slow EPSP was evoked in an all-or-none fashion, whereas the amplitude of the PF-evoked slow EPSP was graded with increasing stimulus intensity. The amplitude of both slow EPSPs were enhanced by hyperpolarization (-65 to -110 mV). No interaction between the two synaptic potentials was observed, and both were blocked by broad spectrum EAA (*cis*-PDA, kynurenate) or selective "non-NMDA" antagonists (CNQX, DNQX), but not by the NMDA antagonists AP-5 and ketamine. These results provide evidence for novel slow EPSPs following activation of Purkinje cell afferents which may play a role in the plasticity of PF-mediated transmission in cerebellum observed following conjunctive stimulation of CFs and PFs. Supported by NIH Grant NS 25682.

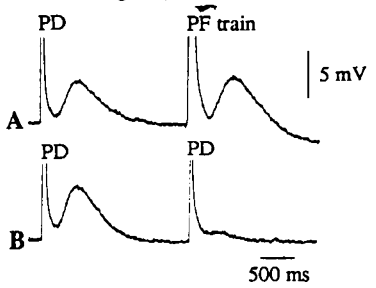

M-Pos308 **PROPERTIES OF AN L-AP4-SENSITIVE PARALLEL FIBER-EVOKED SLOW EPSP IN TURTLE CEREBELLAR PURKINJE CELLS.** N.T. Slater and L.J. Larson-Prior. Dept. of Physiology, Northwestern University Medical School, 303 E. Chicago Avenue, Chicago, IL 60611.

It has recently been demonstrated that slow EPSPs (sEPSPs) can be evoked by activation of the two principal excitatory synaptic inputs to turtle Purkinje cells, the climbing (CF)- and parallel (PF) fibers (Larson-Prior & Slater, 1989; this meeting). A single stimulus of the inferior olive or cerebellar penduncle (PD), or trains of 2-5 stimuli (20 ms intervals) of the cerebellar molecular layer, evokes CF-sEPSPs and PF-sEPSPs in the isolated turtle cerebellum or brainstem-cerebellum preparation *in vitro*. Application of the excitatory amino acid antagonist L-2-amino-4-phosphonobutyrate (L-AP4; 20-100 uM) selectively blocks the sEPSP evoked by PF stimulation, without significantly affecting other CF- or PF-evoked synaptic potentials. Both the CF- and PF-sEPSPs were reversibly blocked by low Cl- solutions. The PF-sEPSP was followed by a pronounced afterhyperpolarization (reversal potential = -90 mV). The PF-evoked sEPSP was exclusively activated by "on-beam" PF stimuli; summating fast EPSPs evoked by "off-beam" stimuli displayed no sEPSP. Furthermore, when stimulated near resting membrane potential, the PF-evoked sEPSP could readily trigger a number of cycles (2-5) of spontaneous burst discharges of the Purkinje cell. These data demonstrate the existence of a spatially segregated, pharmacologically distinct, sEPSP in turtle Purkinje cells triggered by brief trains of PFs. The lack of effect of L-AP4 on the fast PF-EPSP and the reversible blockade of the PF-sEPSP by L-AP4 and low Cl- solutions provides evidence that the PF-sEPSP could represent a N-acetylaspartylglutamate receptor-mediated slow synaptic potential which contributes to the synaptic drive for pacemaker activity in Purkinje cells. Supported by NS 25682 and NS 07140.

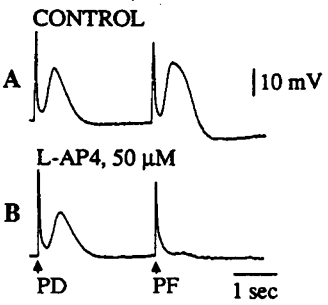

M-Pos309 NEUROMAGNETIC SOURCE LOCALIZATION OF COMPONENTS OF THE VISUAL EVOKED RESPONSE. John S. George, Cheryl J. Aine, and Edward R. Flynn. Neuromagnetism Laboratory. Los Alamos National Laboratory. M.S. M-881. Los Alamos, NM 87545

Scalp electrical potentials recorded during repetitive presentation of visual stimuli display a complex temporal waveform consisting of a series of negative and positive peaks referred to as "components". We have employed magnetic field mapping techniques to localize sources of neuromagnetic evoked response field distributions corresponding to electrical components. Measurements were made with a sensor array consisting of 7 SQUID-coupled second order gradiometers (an equilateral triangular grid) in an aluminum and Mu-metal shielded chamber designed for such experiments. Stimuli were sinusoidal intensity gratings subtending from 2-4 degrees of visual angle and were displayed for 100-400 msec. A series of neuromagnetic field maps were constructed from measurements at 6-12 array locations by sampling temporal waveforms at 10 msec intervals. Simultaneous potential measurements were obtained from 6-18 electrode locations. In contrast to potential distributions, evoked magnetic fields typically showed spatially constrained distributions with extrema of opposite polarity separated by a few centimeters. A simple current dipole model, fit using least squares procedures, often accounted for up to 90% of measured field variance. During some intervals, 2 dipole-like sources could be descriminated. Monte Carlo error analyses suggest that for large signals, source resolution on the order of 2 mm can be achieved, however, improved techniques for documenting sensor location with respect to the head must be employed to achieve this degree of absolute spatial accuracy. A coherent field distribution corresponding to the initial evoked potential component became apparent at ~90 msec poststimulus and was observed continuously through ~140 msec. The initial source of this activity was near the calcarine fissure (identified on magnetic resonance images) but the apparent location and orientation of the calculated equivalent dipole source systematically shifted with time. Computer models suggest that observed field patterns were more consistent with a single migrating source than with spatial summation of two discrete, stationary sources with differing timecourses.

M-Pos310 DEPENDENCE OF BLOOD-BRAIN BARRIER PERMEATION ON TREATMENT WITH n-HEXANE AND CYCLOHEXANE. Thomas R. Ward, Wendy L. Toler and Mark A. Spears (Intr. by John W. Allis). Health Effects Research Laboratory, U.S. Environmental Protection Agency, Research Triangle Park, North Carolina 27711

The blood-brain barrier (BBB) is a functional concept advanced to explain the restricted movement of many blood-borne substances into the central nervous system. The barrier has been identified as the endothelial cell layer of brain capillaries and is distinguished from most other capillaries by the presence of tight junctions between cells and low micropinocytotic activity. Because the BBB is essentially a membrane phenomenon known to be sensitive to surface active compounds (e.g. lysolecithin), it may be sensitive to aliphatic compounds that should concentrate within the membrane, potentially affecting membrane function. To test this hypothesis, rats were gavaged with 1 ml/kg body weight of either n-hexane or cyclohexane; then 2, 4 or 24 hrs later, the animals were injected with a radio-labled tracer (^{14}C sucrose). Twenty minutes after injection, the animals were sacrificed and permeation of tracer into eight brain regions was analyzed by calculating blood-to-brain transfer constants. This method factors in both total brain uptake of the tracer and total barrier exposure to the tracer during the twenty minute test period. No change in permeation was seen for either compound at any time. Why these compounds did not affect the BBB is unknown. However, due to the low aqueous solubility, these compounds may not have been transported well by the blood and perhaps reached the BBB only at very low levels. (This is an abstract of a proposed presentation and does not necessarily reflect EPA policy.)

M-Pos311 MEASUREMENT OF OXYGEN RELEASE FROM PS II USING TIME-RESOLVED MAGNETIC SUSCEPTIBILITY

John Philo and Peter Gast, Molecular and Cell Biology, U-125, University of Connecticut, Storrs, CT 06268

We will report measurements of the kinetics of oxygen production in PS II under flash illumination using time-resolved magnetic susceptibility to detect the S = 1 oxygen. These data are relevant to a recent controversy over the true rate at which oxygen appears after the $S_3 \rightarrow S_0$ transition. Using a low-voltage polarographic electrode, Plijter *et al.*[1] have reported that oxygen does not appear in solution until 30-150 ms after the third flash. They suggest that after the rapid water oxidation and reduction of the OEC, the product O_2 remains bound to the OEC and is slowly released.

Our magnetic technique provides an alternative approach which measures the appearance of normal triplet O_2, and is free of possible electrode artifacts. Supported by NIH HL-24644.

1. Plijter J.J., Aalbers, S.E., Barends, J.P.F., Vos, M.H. and v.Gorkom, H.J., *BBA*, in the press

M-Pos312 FTIR STUDIES OF THE $D^+Q_A^-$ AND $D^+Q_B^-$ STATES IN REACTION CENTERS FROM RB. SPHAEROIDES;* K.A. Bagley, E. Abresch, M.Y. Okamura, G. Feher; UCSD, La Jolla, CA 92093, and E. Nabedryk and J. Breton; C.E.N. Saclay, 91191 Gif-sur-Yvette cedex, France.

Fourier transform infrared (FTIR) difference spectroscopy(1) has been performed on reaction centers (RC's) from Rb. sphaeroides. We have obtained both the light-induced FTIR difference spectra between the charge separated state, $D^+Q_A^-$, and DQ_A (designated $D^+Q_A^-/DQ_A$) and between the charge separated state, $D^+Q_B^-$, and DQ_B ($D^+Q_B^-/DQ_B$). Several differences were found between these two difference spectra. The most striking of these is a negative band at ~1650 cm^{-1} in the $D^+Q_A^-/DQ_A$ spectrum that is absent in the $D^+Q_B^-/DQ_B$ spectrum. The absence of this band in the $D^+Q_B^-/DQ_B$ spectrum indicates that it arises from a change in a vibrational mode of the RC that is associated with the primary acceptor-protein complex; its frequency suggests that it arises from a carbonyl of either the quinone (Q_A) or the protein backbone. Preliminary FTIR difference spectra of RC's containing duroquinone (whose carbonyl stretching frequency is different from ubiquinone 50) in the Q_A site, do not show significant differences in the 1650 cm^{-1} band suggesting that this band probably does not arise from a change in a carbonyl vibration of the quinone, and therefore most probably originates from a change in a carbonyl vibration of the protein backbone. This effect could be due to a conformational change of the protein backbone near the Q_A pocket (e.g. the peptide carbonyl of Ala M260) when the electron is on Q_A. To help confirm this conclusion and to assist in the assignment of other bands that differ in the spectra, experiments on RC's, in which isotopically labelled (^{13}C or ^{18}O) ubiquinone 50 has been incorporated into the Q_A and Q_B sites, are in progress. *Work supported by NSF. (1)Mantele, W., Nabedryk, E., Tavitian, B.A., Kreutz, W. and Breton, J. (1985) FEBS 187, 227.

M-Pos313 TEMPERATURE AND FREE ENERGY DEPENDENCE OF ELECTRON TRANSFER KINETICS BETWEEN QUINONES BOUND AT THE Q_A AND Q_B SITES IN PHOTOSYNTHETIC REACTION CENTERS FROM RHODOBACTER SPHAEROIDES. Kathleen M. Giangiacomo and P.Leslie Dutton (Intr. by Takashi Yonetani), Dept. of Biochem. & Biophys., U. of Penn., Phila., PA

The free energy($-\Delta G^o$) dependence of electron transfer kinetics between Q_A and Q_B was determined in reaction centers from Rb. sphaeroides by replacing the native ubiquinone-10 at the Q_A site with lower potential quinones of known in situ $E_{1/2}$ values(1) and measuring the electron transfer from Q_A to a common quinone, DBMIB, at the Q_B site for which the in situ $E_{1/2}$ is also known. The results(see Figure) reveal that the rate of electron transfer from Q_A to Q_B(kab) is dependent on the $-\Delta G^o$. The activation energy(530meV) measured for electron transfer from Q_A to Q_B at a $-\Delta G^o$ of 70 meV(2) provides from Marcus theory a reorganization energy of 2eV and the fit shown to the data. A detailed analysis of the temperature dependence over a wider range of $-\Delta G^o$ values should facilitate the unambiguous determination of the reorganization energy for electron from Q_A to Q_B.(Supported by NSF DMB18433 and NIH GM27309.) (1)Gunner et al(1986) J. Phys. Chem, 90 3783-3795. (2) Mancino et al(1984) Biochem. Biophys. Acta, 764 46-54.

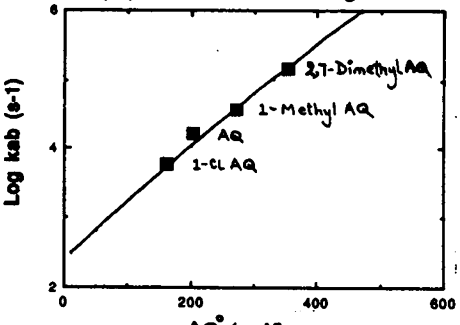

M-Pos314 PURIFICATION OF HIGHLY ACTIVE OXYGEN-EVOVING PHOTOSYSTEM II FROM CHLAMYDOMONAS REIHARDTII. Hyunsuk Shim, Jiancheng Cao, Govindjee and Peter G. Debrunner, Department of Physiology and Biophysics, University of Illinois at Urbana-Champaign, Urbana, IL 61801.

A method is described for the isolation and purification of an active, oxygen-evolving photosystem II from a green alga, Chlamydomonas reinhardtii. The isolation procedure is based on methods evolved for spinach (e.g. Berthold, et. al., FEBS Lett. 134, 231-234, 1981). The Chlamydomonas reinhardtii PSII preparations lack the PSI polypeptides and the PSI fluorescence emission (715 nm at 77K). Their maximum CHl a fluorescence yield is twice as large as that of thylakoids and they produce more thatn 650 μmol O_2/mg Chl per h and they show well-resolved S_2 state EPR multiline signal. We will report on the further purification of PSII particle which lack light-harvesting proteins and their characterization including electron paramagnetic resonance studies of the manganese complex in the oxygen-evolving center of PSII. Supported in part by NSF DMB87-16476 to PGD.

M-Pos315 **CHARACTERISATION OF THE INTERMEDIARY ELECTRON ACCEPTOR PHOTOREDUCTION IN D1/D2/CYTOCHROME B559 COMPLEX BY FTIR SPECTROSCOPY.** E. Barillot+, E. Nabedryk+, S. Andrianambinintsoa, W. Mäntele* and J.Breton+. +Service de Biophysique, CEN Saclay, 91191 Gif/Yvette cedex, France. *Institut für Biophysik der Universität Freiburg, D-7800 Freiburg, FRG.

Molecular changes associated with the photoreduction of the intermediary electron acceptor (H) in D1/D2/cytochrome b559 photosystem II reaction center (D1/D2 RC) were investigated by using FTIR difference spectroscopy. Upon photoaccumulation at 240K of reduced H in D1/D2 RC films, three negative carbonyl bands are observed at 1739 cm^{-1}, 1721 cm^{-1} and 1677 cm^{-1} in the light-minus-dark FTIR spectrum (see Fig.). Comparable signals have been reported for intact photosystem II (BBY) particles (Tavitian et al. 1986, FEBS Lett. 201, 151-157) and for Rp. viridis RC (Nabedryk et al. 1986, Photochem. Photobiol. 43, 461-465). These three bands are apparently specific for the H photoreduction in bacteria and plants which suggests that the bonding interactions of H with the protein might be comparable. The FTIR spectrum of the pheophytin a anion generated electrochemically in THF shows only two negative bands at 1742 cm^{-1} (predominantly 10a ester C=0) and 1706 cm^{-1} (9 keto C=0). The 1677 cm^{-1} band observed in vivo thus reflects an interacting 9 keto C=0 group in D1/D2 RC. As proposed for Rp. viridis RC, the 1721 cm^{-1} band in D1/D2 RC is tentatively assigned to a H-bonded 10a C=0 ester. However in contrast to Rp. viridis, no hydrogen-deuterium isotope effect is detected on the 1739 cm^{-1} band. Our data suggest that the interactions of the ester (most likely 10a) and 9 keto C=0 groups of H with the protein could be stronger in D1/D2 RC than in Rp. viridis RC.

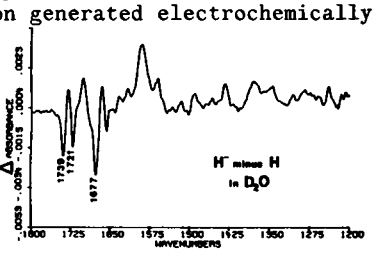

M-Pos316 CAROTENOID TO CHLOROPHYLL SINGLET ENERGY TRANSFER IN THE LIGHT-HARVESTING COMPLEX OF THE DIATOM PHAEODACTYLUM TRICORNUTUM. J. Trautman, A. Shreve, A.C. Albrecht and T.G. Owens. Chemistry Department and Section of Plant Biology, Cornell University.

We have measured the singlet excitation transfer time from the carotenoid fucoxanthin to chlorophyll a in the isolated light harvesting complex of the marine diatom P. tricornutum. The transfer time was found to be excitation wavelength dependent: for excitation on the low energy edge of the in vivo carotenoid absorption (540 nm) the transfer time was 1.4 ps.; for excitation wavelengths of 520 nm or lower, the time was 0.7 ps. These results will be discussed in terms of the Forster and Dexter transfer mechanisms and in light of our studies on the low lying electronic states of carotenoids.

M-Pos317 QUINONE ELECTROCHEMISTRY AND REACTION CENTER Q_A SITE AFFINITY ASSESSED IN A COMMON APROTIC SOLVENT SYSTEM. Kurt Warncke and P. Leslie Dutton, Intro. by Steven W. Meinhardt, Dept. of Biochem. and Biophys., Univ. of Penn., Philadelphia, PA 19104.

1-Chlorohexane is an aprotic solvent which supports measurement of both quinone electrochemical and quinone-RC Q_A site binding equilibria. Dissociation constants (K_D) were determined using RC from Rhodobacter sphaeroides R26 solubilized in inverted phospholipid/detergent micelles. Binding free energies ($\Delta G^0=RT\ln K_D$) for duroquinone (DQ), 2-methylthio-naphthoquinone (MTNQ) and anthraquinone (AQ) are -8.1, -8.8 and -6.4 Kcal/mole. In the same solvent, Em values for the Q/Q- couple were obtained by extrapolation of cyclic voltammetrically determined $E_{1/2}$ vs. mole fraction chlorohexane plots using methylene chloride/chlorohexane mixtures. $E_{1/2}$ values in chlorohexane of -830, -640 and -890 mV were obtained for DQ, MTNQ and AQ. The above values allow an estimation of ΔG^0 for Q^- when the in situ Em (Woodbury, et al., BBA 851, 6-22 (1986)) is also known via an equation derived from a Born cycle: $\Delta G^0(Q^-)=\Delta G^0(Q)-F(Em(\text{in situ}))+F(Em(\text{chlorohexane}))$. For DQ, MTNQ and AQ these values are -26.4, -22.8 and -21.8 Kcal/mole. A junction potential term is included in these values, but is expected to be insignificant relative to $\Delta G^0(Q^-)$. This work not only confirms the commonly held view that Q^- is bound much tighter than Q, but provides a quantitative means to evaluate the effects of structure and chemistry on each redox species individually. Supported by NSF grant DMB 85-18433.

M-Pos318 TEMPERATURE DEPENDENCE OF THE ELECTRON DONATION TO P^+ BY THE HIGH-POTENTIAL CYT-C IN RHODOPSEUDOMONAS VIRIDIS G. Neshich, D. DeVault, C. Wraight, Department of Physiology and Biophysics, University of Illinois, Urbana, IL 61801.

Bacterium R.VIRIDIS has four c-type cytochromes integrated to a single protein subunit of the reaction center complex[1]. Two of them are high redox midpoint potential hemes (Cyt-558; E_m=+350 mV) and the other two are low midpoint potential hemes (Cyt-553; E_m=0 mV)[2,3] The temperature dependence of the rate of oxidation of high-potential cytochrome following absorption of a short pulse of light from a ruby laser has been measured spectrophotometrically. At redox potential, E_h about 200 to 250 mV both high potential cytochromes are capable of donating an electron to the oxidized primary donor. Under these conditions the absorbance change observed at 554 nm is characterized by two-component exponential decays due to cytochrome oxidation. The fast phase is due to the electron transfer from the heme nearest to the P^+, while slow phase is explained in terms of electron sharing between the two high-potential hemes[2]. The half times were determined to be 1.65 ± 0.3 s and 0.14 ± 0.02 s for slow and fast phase, respectively, at 23°C and pH = 8.5. These values change as the temperature decreases so that at 77°K the half-times was determined to be 3.25 ± 0.2 ms and 0.28 ± 0.02 ms for slow and fast phase, respectively. In Figure 1. temperature dependence of rate constant for slow and fast phase is depicted. Activation energies were calculated to be 8.3 Kcal/Mol and 7.6 Kcal/mol for slow and fast phase, respectively. These values are higher then the one observed in Chromatium vinosum[4] where E_a = 4.2 Kcal/mol.

[1]Deisenhofer, J., et. al. 1984, J. Mol. Biol. 180, pp 385-398. [2]Shopes, R. et. al. Photosynthesis Research 1987, 12, 165-180, [3]Dracheva, et. al., FEBS lett. 1986, Vol. 205, No. 1 pp 41-46, [4]DeVault, 1984, Quantum-mechanical tunnelling in biological systems. Camb. U. Press.

M-Pos319 Expression and Preliminary Analysis of Site-Directed Mutant Reaction Centers of Rhodobacter sphaeroides. D. Gaul*, B. Brasher, K. Martin and C. Schenck, Dept. Biochemistry, Colorado State University, Fort Collins, CO 80523.

Site-directed mutations in both the pufL and pufM genes of R. sphaeroides have been constructed in coliphage M13. Mutant reaction center alleles were ligated into a broad host range puf expression plasmid, and shuttled into our previously characterized pufLMX deletion strain of R. sphaeroides. Expression of reaction center protein was achieved by plasmid complementation, and could be reversed by acridine orange curing.

Two residues, GluL104 and TyrM210, were chosen for mutagenesis. These residues are conserved in reaction centers from four species of purple bacteria, but do not obey the prosthetic group symmetry observed in the crystal structure. GluL104 is reported to hydrogen bond to the ring V keto group of the redox-active L-branch bacteriopheophytin, and TyrM210 occupies a position nestled in the triad of L-branch tetrapyrroles. Thus, these residues may play a role in determining the unidirectionality of electron flow through the reaction center.

GluL104->Val and TyrM210->Phe both produce thermostable mutant proteins, and are competent for photosynthetic growth. Mutant reaction centers have been purified and characterization by steady-state and kinetic spectroscopic techniques is in progress.

Supported by USDA and NIH. *National Science Foundation Plant Biology Postdoctoral Fellow

M-Pos320 PORPHYRIN DERIVATIVES AS PHOTOINDUCED MOLECULAR WIRES IN BILAYERS.

E.Bienvenue and P.Seta, Laboratoire de Physico-Chimie des Systèmes Polyphasés,CNRS,BP5051, 34033 Montpellier Cedex (France); B.Loock,P.Maillard and M.Momenteau, Institut Curie,Centre Universitaire, 91405 Orsay (France);Introduced by F.Heitz.

In order to model energy conversion in photosynthesis,we have synthesized new molecular assemblies: a covalently linked porphyrin cofacial trimer (trizinc derivative) and a basket-handled porphyrin-quinone.These compounds have been incorporated into bilayer lipid membranes separating two aqueous phases,a reducing one and an oxidizing one. Under continuous light excitation, a steady electrical current flows through the membrane.Such a system may be considered as an interesting model of the redox chains in the natural photosynthetic membranes.The experimental variations of the flux with some external physico-chemical parameters are accounted for by the proposed mechanism which relies on the ability of the molecular assemblies to act as electron wires.

M-Pos321 RESONANCE RAMAN STUDIES OF WILD TYPE AND GENETICALLY MODIFIED FORMS OF Rb. CAPSULATUS.

J. M. Peloquin[1], E. J. Bylina[2], D. C. Youvan[2] and D. F. Bocian[1], [1]Department of Chemistry, Carnegie Mellon University, Pittsburgh, PA 15213 and [2]Department of Chemistry, Massachusetts Institute of Technology, Cambridge, MA 02139.

The wild type and four genetically modified forms of the photosynthetic reaction center from Rhodobacter capsulatus have been examined by using resonance Raman spectroscopy. The modifications are of two types. The first involves substituting leucine and glutamine residues for the histidine residue (MH200) that ligates to the Mg ion of one of the special pair BCHls. The second modification involves substituting leucine and glutamine residues for the glutamic acid residue (LE104) hydrogen bonded to the C9-keto group of the active BPHEO. The vibrational data indicate that these genetic modifications affect only the pigment-protein interactions in the vicinity of the modification. Collectively, these data give new insight into the nature of pigment-protein interactions within the reaction center.

M-Pos322 KINETIC CORRELATION BETWEEN ELECTRON TRANSFER AND H^+-BINDING IN REACTION CENTERS OF PHOTOSYNTHETIC BACTERIA RB. SPHAEROIDES.

Péter Maróti and Colin A. Wraight, University of Illinois, Urbana, IL 61801.

Several previous observations have indicated that not only stoichiometric but also kinetic correlation exists between the electron transfer (ET) and proton binding (PB) in the quinone acceptor complex of reaction center: 1) the ET rate becomes limited by the PB with increasing pH and 2) a bound proton in the vicinity of the secondary quinone, Q_B, is required to stabilize the electron on Q_B. Experimental evidences will be presented for their common characteristics in rates and in their pH dependency. Both the ET and the PB kinetics show bi(or poly)-phasicity around pH=8, which merge to single component kinetics toward lower and higher pH values (see the figure for ET rates). The complex kinetics are related to the binding properties of the quinone in the Q_B binding domain. The kinetic correlation between ET and PB is explained by the model with two, independent protonatable groups in direct interaction with the acceptor quinones.

The work was supported by the NSF (DMB 86-17144).

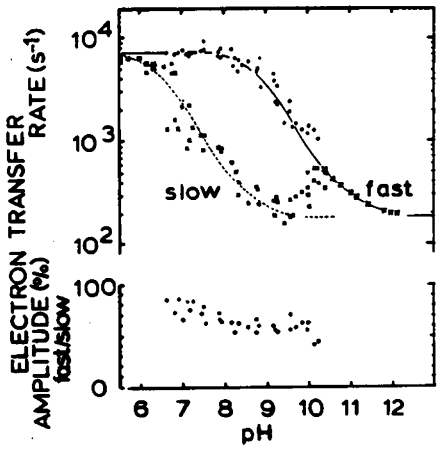

M-Pos323 **RESONANCE RAMAN INVESTIGATIONS OF CHLOROPHYLL a-BINDING PROTEINS AND SYNTHETIC COFACIAL PORPHYRINS.** *Julio C. de Paula[a], D.F. Ghanotakis[b], D.M. Demetriou[c], N.R. Bowlby[c], C.K. Chang[a,*], C.F. Yocum[c,*], and G.T. Babcock[a,*] - [a]Department of Chemistry, Michigan State University, E. Lansing, MI 48824; [b]Department of Chemistry, University of Crete, Iraklion, Crete, Greece; [c]Departments of Biology and Chemistry, The University of Michigan, Ann Arbor, MI 48109.*

The structures of the pigments bound to the D1-D2-cytochrome b_{559} complex and to the 47 kDa protein of plant photosystem II were investigated by resonance Raman (RR) spectroscopy. The RR spectra obtained with excitation in the Soret band of the chlorin macrocycles revealed that the chlorophyll molecules are five-coordinate in both the reaction center complex and in the 47 kDa protein. In general, the Raman frequencies for the C_9 keto groups are lower for pigments bound to the reaction center than for pigments bound to the 47 kDa protein. In the reaction center complex, there is clear evidence for a hydrogen-bonded C_9 keto group. Selective enhancement at 488 nm of the β-carotene modes afforded a RR spectrum that suggests an all-trans conformation for the molecule when bound to the reaction center complex. The RR technique can conceivably determine whether P680 is a monomer or dimer of chlorophylls. In an attempt to catalog "signature" RR bands for monomer and dimer structures, we have synthesized and characterized covalently-linked dimers of porphyrins. The inter-chromophore distance and slip angle were varied synthetically and the effects of these geometrical parameters on the optical and resonance Raman spectra of the porphyrin dimers were determined.

M-Pos324 FACTOR ANALYSIS OF THE NEAR-UV ABSORPTION SPECTRUM OF PLASTOCYANIN WITH MULTILINEAR MODELS. S. R. Durell, C.-H. Lee, R. T. Ross, & E. L. Gross, Biophysics Program and the Dept. of Biochemistry, Ohio State University, Columbus OH 43210

Bilinear, trilinear, and quadrilinear models of the near-UV absorption spectrum of plastocyanin are formed treating the absorption wavelength, plant species, oxidation state, and pH as variables. The application of trilinear and quadrilinear models is relatively unexplored; however, they have the advantage that they uniquely define the components and avoid the indeterminacy of bilinear models. The chemical-condition variables are found to interact, which contradicts the assumptions of the trilinear and quadrilinear models. However, the magnitude of these interactions is relatively small, so that the components are still accurately defined by these models. The results of the trilinear and quadrilinear models support the assumptions used to form the bilinear model. From analysis of the residuals of the models, it is determined that the absorption spectrum of plastocyanin is comprised of three components which respond independently to the variables. These components are the absorption of unperturbed tyrosine residues, perturbed tyrosine residues, and the reduced copper center. The shape of the spectrum of the perturbed tyrosine component suggests electronic coupling between transitions in the copper center and the perturbed tyrosine residues. The absorption of these perturbed tyrosines is pH dependent, and contributes to the net absorption increase of plastocyanin upon reduction of the copper center at pH 7.0.

M-Pos325 **ABSORPTION AND CIRCULAR DICHROIC SPECTRA OF SPINACH APO-PLASTOCYANIN.** **E.L. Gross, J.E. Draheim and G.P. Anderson, Dept. of Biochemistry, The Ohio State University, Columbus, Ohio, 43210 and Dept. of Chemistry, Adrian College, Adrian, MI, 49221.** **The near-UV absorption and circular dichroic (CD) spectra of plastocyanin (PC) vary in shape and magnitude depending on species, pH and oxidation state. One important question is whether these changes can be attributed to changes in transitions associated with the copper center as opposed to conformational changes in the protein portion of the molecule. To answer this question, we have studied the absorption and CD properties of apo-PC made by (1) dialysis vs. cyanide (CN-PC) and (2) by removal of Hg from Hg-PC using mercaptoethanol (M-PC). Near-UV absorption and CD spectra depended on the method of preparation. The near-UV absorption spectrum of CN-PC was almost identical to that of oxidized PC but the CD bands characteristic of oxidized PC were absent. M-PC was fractionated using ion exchange FPLC. The extinction of the major fraction of M-PC was greater than that for CN-PC at all wavelengths in the near-UV region and the 278 nm CD band was retained. Both forms of PC showed significant changes in the far-UV CD spectrum indicating changes in secondary structure. However, there was significant reconstitution with copper for M-PC. These results show that the conformation of apo-PC is variable depending on method of preparation.**

M-Pos326 ROLE OF AGGREGATION STATE IN DIRECTED ENERGY TRANSFER WITHIN THE B875 LIGHT-HARVESTING PIGMENT-PROTEIN COMPLEX OF *RHODOBACTER SPHAEROIDES*. Willem H.J. Westerhuis, Rolf Theiler and Robert A. Niederman. Department of Molecular Biology and Biochemistry, Rutgers University, Piscataway, NJ 08855-1059

A special bacteriochlorophyll *a* (BChl) species, designated as B896, which connects B875 with the reaction center BChl special pair, has been proposed on the basis of fluorescence polarization measurements in *R. sphaeroides*. In recent picosecond absorption recovery studies at 77 K, this long wavelength antenna component was found to be intrinsic to isolated B875 complexes. It was suggested that the highly ordered B896 BChls arise either from intrinsic asymmetry within minimal B875 units of 6-8 BChl molecules or from interactions between chromophores located on different units. Here, these possibilities have been tested by subjecting membranes of mutant strains M21, lacking the B800-850 antenna, and M2192, lacking both B800-850 and reaction centers, to lithium dodecyl sulfate-polyacrylamide gel electrophoresis at 4°C. In strain M21, this procedure yielded an apparent B875 minimal unit as well as a series of higher B875 oligomers. At 77 K, the absorption and emission maxima of the minimal unit and a highly aggregated B875 complex were observed at 882/900 nm and 885/902 nm, respectively, consistent with an increased B896 level in the higher oligomer. A similar red shift was observed in M2192 where the majority of the B875 formed large aggregates. Absorption spectra of M2192 membranes at 4 K revealed a long wavelength component at 897 nm, but significantly lower fluorescence polarization values were observed in comparison to M21 where the polarization rose to 0.42 in the red wing of the absorption band (Hunter, C.N. and van Grondelle, R. in Photosynthetic Light-Harvesting Systems, Scheer and Schneider, eds., de Gruyter, Berlin, p. 247-260, 1988). These differences were thought to arise from energy transfer among large numbers of B896 BChls which normally donate excitations to the reaction center. Surprisingly, the smallest units from the gel exhibited high polarization values ($p \geq 0.37$) which occurred across the major Q_y transitions. This suggests that the complexes from M2192 are not circularly degenerate and that the B875 and B896 BChls may be assembled differently than in the wild type or M21. [Supported by NSF/DMB85-12587]

M-Pos327 VIRTUAL INTERMEDIATES IN PHOTOSYNTHETIC ELECTRON TRANSFER Julian Joseph and William Bialek, *Departments of Physics and Biophysics, University of California, Berkeley, CA 94720*

There has recently been interest in the possibility of virtual intermediate states (in the sense of second-order perturbation theory) in photosynthetic electron transfer. Most of the discussion has been based on models with two electronic states (initial and final) in which any intermediate state simply generates an effective electronic matrix element evaluated at the classical 'transition state.' By doing a fully quantum-mechanical calculation of the electron transfer rate in a three-state system with few vibrational modes, we find that this picture is a good approximation when the reaction is coupled to only one mode with a frequency low compared to the redox potential (e.g. a protein breathing mode), but breaks down if the reaction is also coupled to a high frequency mode (e.g. carbonyl stretching in a quinone). One consequence of this is the impossibility of total destructive interference between direct hopping and the second-order path, implying the existence of a quantum-mechanical minimum for the reaction rate. We provide theoretical evidence for the possibility that significant interference occurs between these two paths in the $Q \rightarrow P$ recombination reaction, and thus that this reaction may approach the quantum limit. More generally, we try to give an intuitive discussion of the conditions for classical vs. quantum pictures of the transfer dynamics.

This work is supported in part by the the National Science Foundation.

M-Pos328 THE CREATION OF MONOLAYER LANGMUIR-BLODGETT CHROMATOPHORE MEMBRANES: IN VIVO FUNCTIONALITY, VECTORIAL ASYMMETRY AND FIELD SENSITIVITY OF QA TO QB ELECTRON TRANSFER. C.C Moser and P.L. Dutton, Dept. of Biochem. & Biophys., Univ. of Penna., PA.

We have made Langmuir-Blodgett (L-B) film monolayers from native biological membranes by spreading chromatophores of the photosynthetic bacterium Rhodopseudomonas capsulatus at the air-aqueous interface. Compression of the film and depostion of a single monolayer or a series of multilayers onto a transparent indium-tin-oxide electrode support followed by coating with an insulating polymer and evaporation of a second electrode creates a capacitor in which the partially dehydrated membrane demonstrates in vivo function, including light induced electron transfer from bacteriochlorophyll dimer to QA, QB, and Q pool. Indeed, antimycin sensitive cyt b reduction is visible. The monolayer capacitors are highly ordered and vectorial, as demonstrated by conspicuous spectral dichroism and by the large flash induced currents observed in direct voltage clamp measurements. Both the sign of the flash induced current and the observation that cyt c2 is not present kinetically or spectrally, strongly suggests that spread chromatophores fuse with the air-aqueous interface such that the chromatophore contents, including the soluble cyt c2, are released and diluted into the L-B aqueous subphase. The direct electrical measurements reveal a surprising sensitivity of the amplitude of the reverse current of charge recombination following a flash to modest applied fields (3 volts across the capacitor eliminates the net reverse current) which we interprete as a modulation of the QA to QB electron transfer by means of the mildly electrogenic protonation reaction. We believe these powerful techniques will find broad application to native membranes in general.

M-Pos329 QUADRATIC CAROTENOID BANDSHIFT IN CHROMATOPHORE MONOLAYERS

C.C Moser and P.L. Dutton, Intr. by D.E. Robertson, Dept. of Biochem. & Biophys., Univ. of Penna., PA.

We believe that we have shown the theoretically anticipated, but here-to-fore unobserved quadratic electric field dependence of the bandshift of the bulk carotenoid in the chromatophore memebrane. Chromatophores from Rps. capsulatus have been spread on a Langmuir-Blodgett trough and deposited on a transparent electrode as a monolayer or multilayer film. The film was covered with a polymer and a second electrode was evaporated to create a capacitor containing the mono- or multilayer. Spectral dichroism and direct electrical measurements of the flash activated film indicate a high degree of sample orientation. When an external electric field is imposed across the sample capactitor, a carotenoid bandshift is observed. The dominant bandshift appears to represent the response of the carotenoid that is dominant in the total absorption spectrum and shows a clear quadratic dependence on field, in contrast to the linear field response frequently reported in the literature and traditionally relied upon for calibration of transmembrane electric field strength. We compare the electric field induced spectral response of the chromatophore monolayers with monolayers of isolated antennae--carotenoid complex.

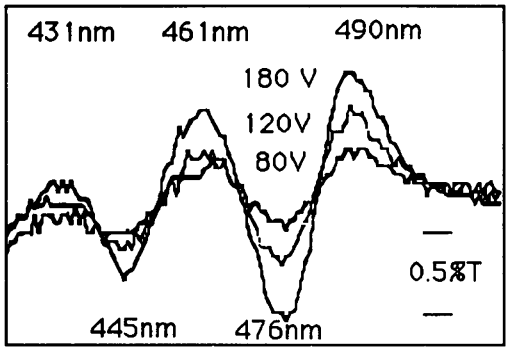

M-Pos330 THE ACTIVATION OF THE CHLOROPLAST ATP-ASE MEASURED BY THE ELECTROCHROMIC CHANGE IN INTACT PLANTS USING A HIGHLY SENSITIVE PORTABLE KINETIC SPECTROPHOTOMETER. David M. Kramer and Antony R. Crofts. Department of Physiology and Biophysics, University of Illinois, 407 S. Goodwin, Urbana, IL 61801.

A completely portable, highly sensitive (noise levels less than 10^{-5} A) double flash kinetic spectrophotometer for the measurement of light-induced absorbance changes in intact leaves is described. This instrument was used to study the activation of the ATP-ase in leaves of intact Cucumber plants. The flux through the ATP-ase was measured by using the decay of the electrochromic shift at 515 nm (a linear indicator of the electrical potential across the thylakoid membrane) as an indicator of the flux of potential across the thylakoid membrane. Plots of the rate of decay of the electrochromic shift against its amplitude were used to determine the threshold for activation of the ATP-ase. A fast phase of decay of the electrochromic shift was found above a certain threshold amplitude in control leaves. This fast phase was eliminated after treatment of the leaves with dicyclohexylcarbodiimide (DCCD), indicating that it was associated with flux through the active ATP-ase. The threshold amplitude of the electrochromic shift was lower in light-adapted leaves than in dark-adapted leaves indicating a lower threshold amplitude for the activation of the ATP-ase. The lowering of the threshold amplitude by light-adaption was eliminated by treatment of the leaves with methyl viologen, which blocks electron flow to the thioredoxin system. These results are interpreted in terms of a model presented by Junesch and Graber (Biochim.Biophys.Acta. 893, 275-288) to explain results from isolated systems. The reoxidation kinetics of the γ-subunit of the ATP-ase were followed by observing the extent of the slow decay phase of electrochromic shift. These kinetics showed a lag time which was dependent on the amount of light adaptation, and a recovery which did not appear to be dependent on the amount of light adaptation. The kinetics are interpreted in terms of a model consisting of a large redox buffering pool with a midpoint potential somewhat lower than that of the sulfhydryl groups of the γ-subunit of the ATP-ase, in equilibrium with a smaller pool equipotential with the γ-subunit sulfhydryls. Some possible characteristics of this pool are discussed.

M-Pos331 LONG-RANGE CHIRAL DOMAINS IN THYLAKOID MEMBRANES OF GRANAL CHLOROPLASTS REVEALED BY DIFFERENTIAL POLARIZATION IMAGING

Laura Finzi and *Carlos Bustamante*, Department of Chemistry, University of New Mexico, Albuquerque, NM 87131, *Gyozo Garab*, Hungarian Academy of Science, Szeged, Hungary

The existence of long-range chiral organizations in the pigment-protein complexes in mature granal chloroplasts has been established by means of Differential Polarization Imaging. The chloroplasts were imaged in two different orientations: edge on and face up, so as to render the data interpretable and reproducible. Circular dichroism images are obtained which space-resolve the chirality of individual chloroplasts and depict the spatial distribution of localized domains with large optical activity. The size of these domains is comparable to the size of the grana which could host them. Circular dichroism spectra were also recorded at each domain location and show very large ellipticities that seem to indicate that macroscopic measurements may underestimate the chirality at the microscopic level and also that the bands at 665 and 695 nm observed in CD spectra of chloroplast suspensions are not due to an excitonic effect, but have distinct structural and spatial origins. Finally, chiral regions displaying preferential scattering of circularly polarized light were differentiated from those displaying preferential absorbance, using wavelengths outside the absorption bands. The physiological significance of these domains of large chirality is discussed.

M-Pos332 RED LIGHT STIMULATES ION CHANNEL ACTIVITY IN MOUGEOTIA. R. R. Lew[1], B. Serlin[2] and C. L. Schauf[1]. (1) Department of Biology, Indiana University - Purdue University, Indianapolis, Indiana and (2) Department of Biology, DePauw University, Greencastle, Indiana.

The alga Mougeotia has a large single chloroplast whose positioning relative to a light source is regulated by red light/far-red light: thus it is phytochrome-mediated (W. Haupt, Ann. Rev. Plant Physiol. 33: 205-233, 1982), apparently via changes in cytosolic calcium (B. Serlin and S. J. Roux. Proc. Natl. Acad. Sci. 81: 6368-6372, 1984). We are examining red light/far-red light effects on ion channel activity in Mougeotia protoplasts to test the possibility that phytochrome causes changes in cytosolic calcium levels by activating Ca^{++} channels in the plasma membrane.

We find that red light activates two separate channels. At 0 mV the amplitude of these channels were 0.8 and 2.2 pA respectively, with single channel conductances estimated to be about 10 pS and 50 pS. Mean open times varied from 5 to 300 msec. Red light increased both the frequency of channel opening and the duration of openings. There was a two minute lag between the onset of red light irradiation and the observed increase in channel activity. The increase in channel activity persisted for about five minutes following return to the dark. Far-red light had no effect once the channels were activated. Red light/far-red light reversibility, selectivity, and mechanisms of channel activation are currently being investigated.

(Supported by NSF grants BNS 87-15847 and DCB 87-15558 to C. L. Schauf and by a grant to B. Serlin from the William and Flora Hewlett Foundation Grant of Research Corporation).

M-Pos333 LOW TEMPERATURE KINETICS OF CYTOCHROME C OXIDASE AND CARBON MONOOXIDE AFTER Y-IRRADIATION.
Ayene, I. Dept. Biochem.Biophys, University of Pennsylvania, Phila., PA 19104

EXAFS study of cytochrome c oxidase at room temperature leads to an altered edge feature of copper which subsequent workers identified with reduction to copper (1). The first on-line optical monitoring of cytochrome oxidase at room temperature showed the kinetics of reduction during irradiation and reoxidation after irradiation (2). Hence, the present study was carried out to quantitate both spectroscopically and polarographically the radio-biological damage and its significance in EXAFS. Experiments were also carried out to protect the samples against irradiation by radio-protectants.

Reduction of cytochrome c oxidase by dithionite and CO binding to cytochrome a_3 are affected proportionately whereas the electron transfer from cytochrome c is damaged independent of heme damage. Further, the radiation dose needed to alter the heme environment is many fold more (15,000 Gy) than it is needed to impair the cytochrome c binding (1000 Gy). The unaltered low temperature CO kinetics and the relatively low decrease of total heme and cytochrome a_3 concentration indicates that under the protein damage leading to the impairment of cytochrome c binding is predominant.

Of the various radio-protectants screened, cystamine was found to reduce the protein damage of cytochrome c oxidase without altering the activity and the spectral characteristics of the enzyme.

The significance of radiation damage and the chemical radio-protection of the sample in the study of EXAFS will be discussed in light of the present studies.

(1) Hu VW, Chan SI, Brown GS (1977) PNAS USA 74:3821-5; (2) Powers L, Blumberg WE, Ching Y, et al (1979) Biophys J. 25:43. SUPPORTED IN PART BY: NIH Grant GM 31992.

M-Pos334 THE EFFECT OF HYPERTHERMIA ON COLONY-STIMULATING FACTOR PRODUCTION BY THE LUNG
Goliaei, B., Rajabi, H., and Rabbani, A., Inst. Biochem. Biophys., Univ of Tehran, Tehran, IRAN

We have studied the effect of in-vitro administration of hyperthermia on colony-stimulating factor (CSF) production by the rat lung. CSF was prepared by incubating finely minced rat lung tissue in serum-free Dulbecco's MEM for 48 hrs. The CSF activity was assayed by colony formation of mouse bone marrow cells in semi-solid agar medium in the presence of CSF. Hyperthermia was administered by heating the minced lung tissues in a water bath in the range of 40-46°C for various period of time. Hyperthermia treatment reduced the CSF production by the lung in a dose dependent manner. Survival curves were generated by plotting the log of the ratio of the activity of heat treated samples to controls versus the duration of heating for each temperature. The survival curves were logarithmic for all temperatures tested. Low temperature survival curves had an initial shoulder and a logarithmic phase. The extent of the initial shoulder decreased as the temperature increased, but the slope of the logarithmic phase increased with incresing the temperature. The Arrhenius analysis of surviving curves indicated a biphasic heat inactivation pattern. The initial phase including the temperature range of 40-43°C had a low activation energy of 67K Cal/mole, while the final phase including the temperature range of 44-46°C had a high activation energy of 327K Cal/mole. The results suggest at least two different mechanisms of hyperthermic inactivation of CSF production by the lung. The low temperature hyperthermia (40-43°C) behaving like low LET radiation and the high temperature hyperthermia (44-46°C) behaving like high LET radiation.

M-Pos335 THEORETICAL AND EXPERIMENTAL BASES OF A MODEL TO EXPLAIN THE TOXIC & PROTECTIVE MECHANISMS OF ETHANOL (EtOH) & ACETALDEHYDE (AlCHO) AND IONIZING RADIATION (I.R.).
Losada, A. & Egaña, E. University of Chile; Faculty of Medicine - Institute of Experimental Medicine - Laboratory of Neurochemistry - Santiago 7 - Chile.

Our Institute has previously communicated the radioprotection action (R.P.) of EtOH & AlCHO in rats. A scavenger effect (S.E.) has been proposed as explanation (Egaña et al. 1980-86). It accepts DNA is the main target radiation molecule & presume the S.E. of EtOH & AlCHO, stimulation of repair & remodelation of DNA. We don't have a theoretical model to explain such effect. Both I.R. and EtOH & AlCHO oxidation produce free radicals. Survival postexposure got in our experiments could be interpretated as a remaining of information ability inside the cell. Contrary, radiosensibility (cell necrosis) signifies lost of current information between nucleus & cytoplasm within vital tissue & their basic information. Besides DNA damage, energy production is broken in mitochondrial transfer of $\bar{e}$, H^+, cations channels (Egaña et al. 1980-88). Material & Methods. Adult ♂ & ♀ Wistar rat. Exposure: doses rate 1,000 R whole body gamma (^{60}Co). EtOH rats: submitted to free ethanol selection; AlCHO rats 200mg/Kg rat/24 h. R.P.: days of survival after exposure, dose-rat, repeated every 60 days up to death. CNS' DNA, RNA & protein were measured days before death. Comments: 1. Noticeable is the coexistence of both EtOH & AlCHO R.P. & production of free radicals. 2. I.R. produce i) DNA damage (& consequently DNA, RNAs & protein function). ii) Intra & extracellular fluid desarrangement conduces to loss of cell & tissue basic energy relationship, affecting DNA repairing. We assume EtOH & AlCHO R.P. could explain as adaptative process to free radicals produced by the EtOH & AlCHO oxidation, protecting DNA to I.R. free radicals.

M-Pos336 THE EFFECT OF AN INTERSTRAND PSORALEN CROSSLINK ON THE IN VITRO STRAND EXCHANGE REACTION OF E. COLI REC A PROTEIN. S. L. Shaner, M. Munn and C. M. Radding, Depts. of Human Genetics and Therapeutic Radiology, Yale University, New Haven, CT 06510.

The E. coli recA protein is essential for general genetic recombination, recombinational DNA repair, and mutagenesis. One standard model system which has been used to investigate the molecular mechanism of strand exchange in vitro is a "three-stranded" system in which linear duplex M13 DNA is paired with single-stranded (ss) viral M13 DNA. We have placed a single interstrand psoralen crosslink at position 1906 on the linear duplex M13 DNA and have investigated the effect of this lesion upon the recA protein-promoted strand exchange reaction. These experiments should clarify certain molecular aspects of the recA protein-dependence of the in vivo mechanism for repair of interstrand crosslinks in E.coli and should also differentiate between the two extreme molecular mechanisms which have been proposed to explain how recA protein-promoted strand exchange might occur between two parental duplexes which have come into homologous alignment. Under reaction conditions in which heteroduplex formation goes to completion between ssDNA and homologous linear duplex DNA with no interstrand crosslink, we observe that heteroduplex formation with the linear crosslinked DNA does not go to completion. The nature of this block to completion of strand exchange will be discussed.

M-Pos337 A STOCHASTIC MODEL FOR LOW DOSE LOW LET IRRADIATION-INDUCED ONCOGENIC TRANSFORMATION OF MAMMALIAN CELLS. Mary N. Stamatiadou, Institute of Biology, NRC "Demokritos", Aghia Paraskevi, Athens, Greece.

Interaction of ionizing radiation with atoms generally involves collisions with orbital electrons, with ensuing ionization and excitation which eventually may lead to a disruption of the organizational and structural patterns that hold together a host of basic cellular functions. A hit cell may thus be permanently damaged or altered, depending on the interplay of numerous factors, dominant among which are the magnitude and the rate of radiation dose. The length of the time interval between two consecutive radiation pulses is of importance in that it is considered to have a positive influence on the probability that the cell will be able to optimally react against the primary physical and biochemical effects of the radiation absorption event. Results obtained with low LET-irradiated mammalian cells have indicated that for most radiobiological endpoints, including cell killing and oncogenic transformation, dose fractionation and protraction lead to a substantial reduction in the measured consequences of a given dose, within a wide dose range; however, at very low doses, fractionation enhances low LET radiation-induced transformation. A theoretical model of dose-effect relationship is thus suggested, which includes consideration of the enhancement in transformation which occurs with split-dose exposure to low doses, in conjuction with the question of a threshold dose below which no radiation-induced effect occurs.

M-Pos338 THE PICOSECOND MULTI-HARMONIC FOURIER (MHF) FLUOROMETER - AN INSTRUMENT FOR COLLECTING PHASE/MODULATION LIFETIME DATA SIMULTANEOUSLY AT MANY FREQUENCIES OF EXCITATION.
GEORGE W. MITCHELL, INTR. BY RICHARD D. SPENCER

The use of pulsed lasers and synchrotrons as light sources for frequency domain fluorescence lifetime measurements has become an established technique. In these instruments, the sample is excited simultaneously at a base frequency and all integer harmonics of that frequency. Cross-Correlation detection is typically used to isolate the sample response at the single frequency of excitation.

Once harmonic response methodology is introduced into the instrumental design and analytical considerations, however, an entire new realm of performance and capabilities emerges. Furthermore, it is possible to extend multi-harmonic operation to CW light sources and to the detection of the fluorescent signal. The use of the full capabilities of multi-harmonic technology allows construction of a picosecond multi-harmonic fourier (MHF) fluorometer which can collect phase and modulation values simultaneously at many frequencies. Most importantly, multi-harmonic detection recovers much of the information which single frequency correlation methods discard. One major benefit is that acquisition times for multi-frequency data are dramatically reduced. Secondly, the acquisition is so fast that the picosecond MHF spectrofluorometer can be used for kinetic studies.

This paper, therefore, will present a new instrument technology and actual data demonstrating capability to resolve single and multicomponent fluorescent lifetimes, and polarization decay rates in a single shot. This advancement means that full frequency response curves for picosecond fluorescence analysis can be obtained instrumentally in acquistion times of seconds rather than hours. Furthermore, kinetic studies utilizing fluorescence lifetimes are now possible with multi-frequency analysis.

M-Pos339 SPATIALLY-RESOLVED ANISOTROPY IMAGES OF FLUORESCENT PROBES INCORPORATED INTO LIVING CELLS.
James A. Dix and A.S. Verkman, Cardiovascular Research Institute, UCSF, CA 94143.

Steady-state fluorescence anisotropy (r) gives information about molecular motion of fluorescent probes and hence the effective local "microviscosity". This methodology has been restricted to bulk, spatially-averaged measurements of r. We have extended these measurements by using an epifluorescence microscope, equipped with excitation and emission polarizers, and an image analysis system to resolve spatially r of fluorescent probes incorporated into cultured cells. To obtain accurate r values, images obtained with parallel and perpendicular polarizer orientations were corrected individually for nonuniform sensitivity of the intensifier/camera system, nonlinearities in intensifier gain, background fluorescence, histogram clipping, and polarization artifacts of the optical system. r for glycogen scattering solutions was >0.98. An anisotropy image of three capillary tubes filled with fluorescein in solutions of varying viscosity gave r values within 5% of those measured in a fluorimeter. r for TMA-DPH incorporated into the plasma membrane of MDCK cells was in the range of 0.28-0.32, and decreased by 10% upon treatment with 10 mM hexanol. Simultaneous labelling of MDCK cells with TMA-DPH and the cytoplasmic marker, ANTS, showed that adjacent structures having different r are well-resolved. Treatment of MDCK cells with the intracellular pH-probe, BCECF, gave distinct fluorescence from two areas, one in cytoplasm and one at the cell periphery. r of cytoplasmic BCECF was 0.12 and uniform, corresponding to cytoplasmic viscosity of 5 cP, while r for BCECF near the plasma membrane was 0.02. The low r region represents aqueous BCECF trapped beneath the tight junctions. The data firmly establish a new methodology to measure spatially-resolved fluorescence anisotropy which should prove useful in probing intracellular fluidity and the role of fluidity in cell signalling.

M-Pos340 EFFECTS OF SPECIFIC MOLECULAR INTERACTIONS ON TRYPTOPHAN SIDECHAIN FLUORESCENCE DECAYS IN NONPOLAR SOLVENTS. Iain Johnson and Bruce Hudson. Department of Chemistry, University of Oregon, Eugene, OR 97403.

The fluorescence decay behavior of indole and 3-methylindole in nonpolar solvents containing small amounts (typically 10mM) of polar additives has been investigated. This type of system is more representative of the generally hydrophobic tryptophan environments of proteins than the aqueous solvents usually used in model photophysical studies. The initially exponential fluorescence decay of 3-methylindole in cyclohexane is perturbed by addition of alcohols (e.g. 1-butanol) resulting in the appearance of a second component with a negative amplitude and an overall decrease in the decay rate. This effect is attributable to excited state dipolar relaxation within an indole/alcohol complex. The existence of such specific complexes has previously been inferred from steady-state fluorescence measurements by R. Lumry and co-workers. Nonexponential fluorescence decay can also result from transient quenching interactions. Quenching by amino acid sidechain model species such as ethyl methyl sulfide (for methionine) is examined in this context. The relationship of these effects to tryptophan fluorescence decay behavior in proteins will be discussed.

M-Pos341 PARALLEL WAVELENGTH ACQUISITION OF FLUORESCENCE DECAY WITH PICOSECOND RESOLUTIONS USING AN OPTICAL MULTICHANNEL ANALYZER. Brett Feddersen, Martin vandeVen and Enrico Gratton. Department of Physics, Laboratory for Fluorescence Dynamics, UIUC, 1110 W. Green, Urbana, IL 61801

Frequency domain fluorometry provides an alternative method for the recording of fluorescence decay kinetics. The time resolution and the fast measurement of lifetime values are major advantages of this method. There are several systems, both clinical and biological, where there is a lifetime change across the emission band. These systems include heterogeneous ground-state systems, where species emit at different wavelengths; excited-state reactions, with products emitting at different parts of the spectrum; and dipolar relaxation processes, where the emission spectra change with time. To fully characterize the decay of these systems, it is necessary to collect the emission decay at several wavelengths. Generally this process is obtained by successive measurements using a monochrometer or a series of bandpass filters. For steady-state spectra, optical multichannel analyzers are available, which can collect the entire emission spectra at once. By gating of the image intensifier, used with some of these analyzers, it is possible to obtain time windows of the order of a few nanoseconds. This time resolution is inadequate for most of the fluorescence substances. We have developed a new method based on frequency domain fluorometry which extends the time resolution of an OMA to the picosecond region. The entire emission decay is collected in a few seconds and the lifetime information across the entire emission band is analyzed at once. Some examples of the application of this new technique will be presented. Supported by NIH grant RR03155.

M-Pos342 PADE-LAPLACE METHOD FOR THE ANALYSIS OF TIME-RESOLVED FLUORESCENCE DECAY CURVES. Željko Bajzer, Andrew C. Myers, Joe C. Sharp, John F. Hedstrom, and Franklyn G. Prendergast, Mayo Foundation, Rochester, MN 55905.

The Pade-Laplace method (PLM) has been modified to recover the lifetimes, fractions and number of components of multicomponent systems from time-resolved fluorescence decay data. The PLM was originally developed to detect the number of components and to extract the parameters of multi-exponential functions [E. Yeramian and P. Claverie, Nature 236(1987)169]. We recently developed a frequency domain version which has been applied to phase/modulation measurements of fluorescence decay [Ž. Bajzer, A. C. Myers, S. S. Sedarous, and F. G. Prendergast - subm. to Biophys. J.]. This poster describes a new algorithm which includes the effects of the impulse response function. The deconvolution of the decay function from impulse response is an automatic consequence of the Laplace transformation of the observed signal. We first showed the effectiveness of this method by use of simulations; for example, a four component system with lifetimes 6,4,1,0,2(ns) in fractional amounts of 0.3,0.3,0.2,0.2 respectively, with Poisson noise (1000 channels, 2.8ps/ch., 24000 counts at peak) and actual system response profile was recovered as 6.6,4.1, 1.0,0.19(ns) in fractions of 0.23,0.38,0.20,0.20. The recoveries of the parameters of experimental data on known mixtures of fluorophores and the analysis of tryptophan fluorescence in Scorpion Neurotoxin and other proteins will be presented. Supported by GM 34847.

M-Pos343 **A 6 GHz FREQUENCY-DOMAIN FLUOROMETER.** Gabor Laczko and Joseph R. Lakowicz, University of Maryland, Department of Biochemistry, Baltimore, MD 21201.

We constructed a frequency-domain fluorometer capable of routine measurements to 6 GHz. The modulated excitation is provided by the harmonic content of a cavity-dumped ps laser. The detector is a high speed microchannel plate PMT. The instrument was tested using the time delay of 25 ps provided by a glass etalon, which yielded a measured delay of 26 ± 2 ps from 200 MHz to 7.5 GHz. We also measured the frequency response of fluorophores with decay times ranging from 50 to 800 ps. These data did not reveal any systematic errors over the frequency range from 50 MHz to 6 GHz. We will describe the use of this instrument for measurements of other picosecond processes including rotational diffusion.

M-Pos344 METHOD FOR MEASURING INTRACELLULAR CALCIUM IN WHOLE HEART PREPARATIONS USING FURA-2. D Rigney, D Klein, Y Kihara, J Morgan, J Wei & W Grossman. Dept. of Medicine, Cardiovascular Division, Beth Israel Hospital and Harvard Medical School, 330 Brookline Avenue, Boston MA 02215

In some applications, Fura-2 (J Biol Chem 260:3440) is the preferred fluorescent dye for measuring intracellular calcium (Ca). Fura has been considered unsuitable for measuring rapidly changing Ca signals (such as those occurring during each beat of a heart's contraction) because its use would require simultaneous fluorescence measurement at two excitation wavelengths. We show that such measurements may in fact be made from perfused fura-loaded ferret whole heart preparations. Our method involves simultaneous fiber-optic illumination at two excitation wavelengths (periodically interrupted at different frequencies > 1KHz), fluorescence detection by a single PMT, lock-in amplification at the two chopping frequencies, and ratiometry. The time-varying Ca signal obtained by our method resembles those that may be obtained by other methods (J Gen Physiol 92:47a, PNAS 84:7793). To show that the observed Ca oscillations are not simply motion artifact, we used different concentrations of BDM to vary contractile vs Ca oscillation. Since Ca oscillation may persist even when the heart's movement is depressed, we conclude that our measurements do in fact reflect the myocytes' intracellular Ca concentration.
Supported by HL01611, HL31117, DA05171, Mass Heart Fellowship, & Jpn Fnd Metab &Dis.

M-Pos345 MULTILINEAR ANALYSIS OF BIOMOLECULAR FLUORESCENCE.

Robert T. Ross, Choon-Hwan Lee, and Sue E. Leurgans, Department of Biochemistry, Biophysics Program, and Department of Statistics, The Ohio State University, Columbus OH 43210.

Fluorescence from biological molecules can be a sensitive measure of their immediate environment, of their distance from other molecules or phases, and of excitation transfer. However, in many circumstances a single specimen contains multiple components with overlapping spectra, components which cannot be physically separated without great effort or without seriously altering important properties of the native specimen. Fortunately, fluorescence data is particularly susceptible to mathematical analysis. The intensity of fluorescence from a chromophore can be a linear function of up to five of its properties: excitation spectrum, emission spectrum, concentration, fluorescence quantum yield, and decay kinetics. The resulting multilinear models are a class of nonlinear models with unusually tractable structure. Some statistical methods and algorithms for analysing multilinear data have been developed, primarily for exploratory analyses by psychometricians and social scientists; however, modifications are required to apply them to spectroscopic data. We have used these methods to resolve a test system composed of a mixture of rhodamine dyes; chlorophyll-protein complexes in pea thylakoids; and phycocyanin, allophycocyanin, and chlorophyll in cyanobacteria. Work on intrinsic protein fluorescence is in progress.

M-Pos346 CONCENTRATIONS AND FLUORESCENT YIELDS OF DISTINCT CHEMICAL COMPONENTS IN MIXTURES MEASURED BY HIGH ORDER AUTOCORRELATION IN FLUORESCENCE CORRELATION SPECTROSCOPY. Arthur G. Palmer III and Nancy L. Thompson, Department of Chemistry, University of North Carolina at Chapel Hill, Chapel Hill, NC 27599-3290

Clustering of ligand-receptor complexes on cell surfaces is thought to be an initial event in cellular responses to a variety of ligands, but few techniques exist that can detect and characterize submicroscopic clusters of membrane-bound proteins in viable cell membranes. High order autocorrelation in fluorescence correlation spectroscopy has been developed to investigate polydispersity or aggregation of fluorescent species in solution or on surfaces. Presented are theoretical and experimental methods for obtaining the high order fluorescence fluctuation autocorrelation functions from the experimentally accessible photoelectron fluctuation autocorrelation functions and for obtaining parameters, called relative norms, that depend on the spatial optical intensity profile of the experimental apparatus and are required for quantitative analyses of the autocorrelation functions. Methods for detecting polydispersity or aggregation and for determining the concentrations and relative fluorescence yields of distinct fluorescent species or aggregates of different sizes from a series of high order autocorrelation functions are outlined and applied to well-defined mixtures of fluorescent molecules. The results show that polydispersity or aggregation can be detected for a range of mixture compositions, and that, in certain cases, absolute concentrations and relative fluorescence yields of the components can be determined as well. This work was supported by NIH Grant GM-37145 and NSF Grant DCB-8552986.

M-Pos347 3D MICROTUBULE DISTRIBUTION IN SINGLE CELLS DETERMINED BY 3D IMAGE RESTORATION OF OPTICAL SECTIONS Walter A. Carrington, Kevin E. Fogarty, & Fredric S. Fay. Dept. of Physiology, University of Massachusetts Medical Center, Worcester, MA 01655.

The 3D distribution of microtubules in a single cell can now be examined in the digital imaging microscope by using fluorescently labelled tubulin. The digital imaging microscope consists of a conventional epi-fluorescence microscope interfaced to a microcomputer which controls focus to 25nm resolution, wavelength of excitation or emission, and duration of illumination. Images formed by the microscope are recorded by a CCD camera cooled to -80 °C whose output is stored digitally. 3-D images of fluorescent probe distribution are obtained by recording a series of optical sections at 0.25 - 0.5μm intervals through focus. The distortion of this 3-D set by the optical system, which is especially severe along the optical axis, is characterized by the point spread function, which has been empirically determined by acquiring a series of optical sections of a known object. This optical distortion and blurring can be substantially diminished by deconvolution using an L^2 regularization method for image restoration that incorporates a non-negativity constraint. This non-negativity constraint is especially effective in images of structures such as microtubules, where the fluorescent dye occupies a small fraction of the cells volume. The resulting images have significantly improved contrast and resolution. Details of the structure of the microtubule organizing center are revealed that are not visible in the unprocessed image. Supported by NIH HL14523.